Aus dem Institut für Virologie
des Fachbereichs Veterinärmedizin
der Freien Universität Berlin

Equine Herpesvirus Type 1 (EHV-1) pUL56 Promotes Dynamin-dependent Endocytosis and Cooperates with pUL43 for Downregulation of Cell Surface MHC class I

Inaugural-Dissertation
zur Erlangung des akademischen Doktorgrades
***philosophiae doctor* (Ph.D.)**
in "Biomedical Sciences"
an der Freien Universität Berlin

vorgelegt von

Teng Huang

aus Pingxiang, Volksrepublik China

Berlin 2015

Journal-Nr.: 3806

Gedruckt mit Genehmigung des Fachbereichs Veterinärmedizin

der Freien Universität Berlin

Dekan:	Univ.-Prof. Dr. Jürgen Zentek
Erster Gutachter:	Univ.-Prof. Dr. Nikolaus Osterrieder
Zweiter Gutachter:	Univ.-Prof. Dr. Salah Amasheh
Dritter Gutachter:	Prof. Dr. Robert Klopfleisch

Deskriptoren (nach CAB-Thesaurus):
Equid herpesvirus 1, major histocompatibility complex, immune evasion, endocytosis, inhibitors, bacterial artificial chromosomes, identification, surface proteins, inactivation, localization

Tag der Promotion: 10.07.2015

Bibliografische Information der *Deutschen Nationalbibliothek*
Die Deutsche Nationalbibliothek verzeichnet diese Publikation in der Deutschen Nationalbibliografie; detaillierte bibliografische Daten sind im Internet über <http://dnb.ddb.de> abrufbar.

ISBN: 978-3-86387-617-3
Zugl.: Berlin, Freie Univ., Diss., 2015
Dissertation, Freie Universität Berlin
D 188

Choriner Str. 85 - 10119 Berlin
verlag@menschundbuch.de – www.menschundbuch.de

Table of Contents

List of Figures

List of Tables

Abbreviations

Aa	Amino acid
ADCC	Antibody dependent cell-mediated cytotoxicity
ATP	Adenosine triphosphate
β2M	β2-microglobulin
BAC	Bacterial artificial chromosome
Bp	Base pair
BHV-1	Bovine herpesvirus type 1
CBS	Citrate buffered saline
CD46	Cluster of differentiation 46
CIE	Clathrin-independent endocytosis
CME	Clathrin-mediated endocytosis
CTL	Cytotoxic T lyphocyte
DN	Dominant negative
DNA	Deoxyribonucleic acid
EGFP	Enhanced green fluorescence protein
EHV-1	Equine herpesvirus type 1
EHV-4	Equine herpesvirus type 4
EMEM	Earle’s minimum essential medium
ER	Endoplasmatic retriculum
ESCRT	Endosomal sorting complex required for transport
FACS	Fluorescence-activated cell sorting
FCS	Fetal calf serum
gM	Glycoprotein M
HA	Hemagglutinin
HCMV	Human cytomegalovirus
HEK	Human embryonic kidney 293 cells
h p.i.	Hour post infection
HSV-1	Herpes simplex virus 1
HSV-2	Herpes simplex virus 2
IE	Immediate early
IFA	Indirect immunofluorescence assay
IgG	Immunoglobulin G
IR	Internal repeat
kDa	Kilodalton
KSHV	Kaposi’s sarcoma-associated herpesvirus
MAb	Monoclonal antibody
MCMV	Murine cytomegalovirus
MDV	Marek's disease virus
MFI	Mean fluorescence intensity
MHC-I	Major histocompatibility class I

MOI	Multiplicity of infection
mRNA	messenger RNA
Nedd4	Neuronal precursor cell-expressed, developmentally downregulated 4
NK	Natural killer
ORF	Open reading frame
PAA	Phosphonoacetic acid
PAb	Polyclonal antibody
PAGE	Polyacrylamide gel electrophoresis
PBS	Phosphate-buffered saline
PEI	Polyethylenimine
PFU	Plaque forming unit
PRV	Pseudorabies virus
PVDF	Polyvinylidene fluoride
RFLP	Restriction fragment length polymorphism
RIPA	Radioimmunoprecipitation assay
RK13	Rabbit kidney cells
RT	Room temperature
RT-PCR	Reverse transcription-polymerase chain reaction
SDS	Sodium dodecyl sulfate
TAP	Transporter associated with antigen processing
TMD	Transmembrane domain
TR	Terminal repeat
UL	Unique long
US	Unique short
VZV	Varicella-zoster virus

CHAPTER 1

Introduction

1.1 Biology of EHV-1

Herpesviridae constitutes a large family of enveloped viruses that are characterized by doubled-stranded DNA genomes of considerable size and complexity. Infection of herpesvirus occurs in almost all groups of vertebrate animals, including mammals, birds, reptiles and fishes (Burrows, 1977). During the co-evolution history, herpesviruses have become naturally adapted to the host immune system and established pathogenesis dedicated to a specific host, although species jumping may sporadically be found. Conventionally, members of the *Herpesviridae* family are further classified into three subfamilies, namely, *Alpha-*, *Beta-*, *Gammaherepesvirinae*, according to their phylogenetic relationship and biological properties (Gable et al., 2014).

Hitherto, more than 120 distinct herpesviral species have been isolated and identified. Nine of these viruses are officially recognized as equine herpesviruses (Paillot et al., 2008). Among them, equine herpesvirus type 1 (EHV-1) and the closely related virus EHV-4 are intensively studied. EHV-1 and EHV-4 were previously thought to be the same pathogen that causes respiratory disease in horses and discrimination of these 2 viruses remained impossible prior to 1981 (Patel and Heldens, 2005). EHV-1 is more aggressive than EHV-4. EHV-1 infection is not only restricted to the upper respiratory tract but also spreads to the placenta or the trigeminal ganglion, resulting in miscarriage, neonatal death or severe myeloencephalitis (Dunowska, 2014). The prevalence of diseases associated with EHV-1 infection has attracted substantial attention from the horse industry worldwide and veterinary virologists. The following review of literature will briefly summarize the basic knowledge about EHV-1 and recent progress that helps us better understand how EHV-1 and other alphaherpesviruses interact with host immune system.

1.1.1 Genomic organization and virus structure

EHV-1 is classified as a member of the subfamily *Alphaherpesviridae*. The complete genome of EHV-1had been sequenced and annotated only after those of varicella-zoster virus (VZV) and herpes simplex virus type 1 (HSV-1), both of which are allocated to the same subfamily (Telford et al., 1992). The EHV-1 genomic DNA with a size of approximately 150 kbp is packaged into an icosahedral nucleocapsid (Allen and Bryans, 1986). Until now, at least 80 open reading frames (ORFs) plus some non-coding RNAs have been predicted within this linear double-stranded DNA genome (Dunowska, 2014). A majority of these ORFs are

compactly distributed throughout the unique long (U_L) and the unique short (U_S) regions. These unique sequences of different length are each flanked by inverted repeats, designated as internal repeat (IR) and terminal repeat (TR) regions, respectively, in which 4 copies of ORFs are located (Patel and Heldens, 2005). Overlapping of genes may occur in several loci, but each gene in general is transcriptionally regulated by separate promoters (Weir, 2001). Introns are rarely found in the entire collection of putative ORFs, with the exception of ORF64 that encodes alternative transcript variants (Harty et al., 1989).

Similar to other herpesviruses, the pattern of EHV-1 gene expression is roughly divided into three distinct but optimally coordinated stages: immediate early (IE), early (E) and late (L) time courses during cytolytic infection. Alternatively, the Greek letters α, β and γ can be used to name the corresponding process (Weir, 2001). Upon virus entry, expression of IE genes first occurs independently of *de novo* protein synthesis. IE gene products function as *trans*-activators of the promoters that initiate the expression of early genes or regulate the transcription of late genes. Because IE genes are the essential regulators directing the replication cycle, only a limited number of them have been identified. As for HSV-1, 5 genes are grouped into the IE category, including *ICP0*, *ICP4*, *ICP22*, *ICP27* and *ICP47* (Roizman and Knipe, 2001). In contrast, EHV-1 has a single IE gene, which is located in the IR region and therefore designated as *IR1* gene (Smith et al., 1994). This EHV-1 IE gene product is predicted to be an ICP4 homologue (Garko-Buczynski et al., 1998). ICP0, ICP22 and ICP27 homologues are also present in EHV-1, but they are expressed with early kinetics and facilitate virus replication later (Kim et al., 2001). Chemical inhibitors, such as cycloheximide (CHX) and phosphonoacetic acid (PAA), are commonly used as a powerful tool to determine the expression pattern of a specific gene after herpesvirus infection. In the presence of CHX, only mRNA transcripts of IE genes are synthesized, allowing detection of IE proteins but not the others (Fenwick and Clark, 1983). When infected cell culture is treated with PAA, production of viral dsDNA will be inhibited, resulting in considerable loss of structural proteins for virus assembly, e.g., a series of glycoproteins (Honess and Watson, 1977). HSV-1 represents a paradigm for the subfamily *Alphaherpesvirinae*, and phylogenic analyses reveal that EHV-1 and HSV-1 resemble in the gross arrangement and molecular structures of their homologues. This feature is also known as co-linearity. Although most genes are supposed to be functional analogues due to evolutionary conservation, there are 5 ORFs (2, 3, 34, 59 and 67) exclusive to EHV-1, whose homologues do not exist in HSV-1 (Telford et al., 1998).

The structure of EHV-1 virion is rather complex, which is composed of numerous viral gene products with incorporation of various host cellular proteins. The morphology of a typical virus particle is delineated by three major subunits: nucleocapsid, tegument and envelope (Fig. 1.1).

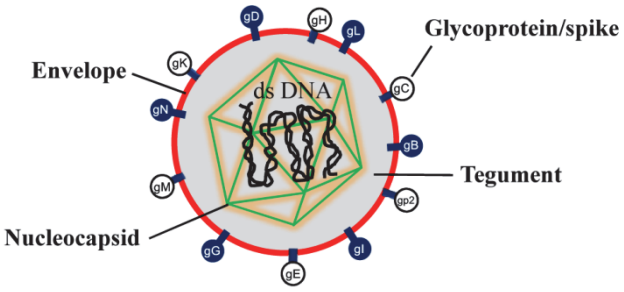

Figure 1.1 Schematic illustration of EHV-1 architecture. A representative particle of EHV-1 contains three distinct components: nucleocapsid, tegument and envelope. The entire viral genome is condensed in a nucleoccapsid. 12 glycoproteins are embedded into the lipid bilayer envelope that surrounds the tegument. The diameter of EHV-1 virion is approximately 150 nm.

The nucleocapsid consists of six proteins, which are components for 162 capsomers surrounding the entire EHV-1 genome (Perdue et al., 1974). The tegument represents an amorphous matrix between the nucleocapsid and the envelope. It is filled with multiple viral proteins and enzymes that facilitate viral replication. The envelope is a lipid bilayer on which 11 viral glycoproteins are presented, including gB, gC, gD, gE, gG, gH, gI, gK, gL, gM and gN) (Paillot et al., 2008). These glycoproteins share considerable homology with the counterparts of HSV-1 and therefore are named accordingly. During the lytic infection cycle, these glycoproteins play important roles in virus adsorption, penetration, and cell-to-cell spread (Mettenleiter, 2002). Apart from the 11 conserved homologues, EHV-1 encodes another distinct glycoprotein, known as gp2, which is also found in EHV-4 and AHV-3 (asinine herpesvirus type 3) but absent from the majority of alphaherpesviruses (von Einem et al., 2004). In general, the abundant capacity of the EHV-1 genome lays a foundation to optimize expression of numerous proteins involved in virus replication, latency, pathogenesis and immune modulation in the host.

1.1.2 Lytic infection

Naturally, EHV-1 infection is solely confined to horse populations, but a variety of non-equine mammalian cell lines, including rabbit kidney (RK13), Chinese hamster ovary (CHO), HEK293 and HeLa cells, etc. (Azab and Osterrieder, 2012), have been used to prepare virus stocks and study certain steps of EHV-1 replication cycle. Instead of horses, small laboratory animals, such as mice and hamsters, are susceptible to EHV-1 challenge infections and serve as models to evaluate the pathogenicity and immune responses to field isolates or engineered mutants (Stokes et al., 1989; Van de Walle et al., 2008). There are two avenues for establishment of EHV-1 infection *in vitro*, namely, direct exposure and transmission between infected cells. The lytic infection period of alphaherpesviruses is characterized by rapid production of progeny virus and arbitrarily divided into several

dynamic stages that include attachment, penetration, viral DNA transcription and translation, virion assembly and egress (Mettenleiter et al., 2009). Similar to other herpesviruses, envelope glycoproteins are required for EHV-1 entry into the host and permissive cells (Csellner et al., 2000). Attachment of the virus particles to cells is mediated by glycoprotein C (gC) (Osterrieder, 1999). With the assistance of gB, gD and presumably gH/gL complex, a fusion process occurs at the interface between the envelope and the plasma membrane, leading to the virus uptake under neutral pH conditions (Azab and Osterrieder, 2012). Alternatively, the virus opts for a non-classical endocytic pathway to cross the cell surface (Azab et al., 2013). Once the penetration completed, release of viral subunits, such as the nucleocapsid and tegument proteins, takes place in the cytoplasm where the components of cytoskeleton network, particularly microtubules, serve as vehicles responsible for transport of nucleocapsids to the periphery of nucleus (Frampton et al., 2010). When the nucleocapsid is close to the outer nuclear membrane, the viral DNA is released and enters into the nucleus through the nuclear pore complex (NPC) with the empty shell left outside. Prior to the synthesis of EHV-1 genomic DNA, expression of the single IE gene (*ORF64*) is induced by a *trans*-activator VP16 (von Einem et al., 2006). This IE gene product is a potent regulator that dictates the transcription of early genes, which encode proteins and enzymes essential for viral DNA replication. After the capsid proteins and certain glycoproteins are expressed, the newly synthesized viral DNA is filled into the interior of capsid. The resulting nucleocapsid undergoes two rounds of envelopment and acquires processed glycoproteins during migration through the Golgi apparatus (Leuzinger et al., 2005). Along the secretory pathway, the mature infectious particles are conveyed to the inner layer of the plasma membrane. Ultimately, exocytosis of vesicles occurs at the cell surface, resulting in budding of progeny virus or invasive fusion with neighboring cells (Mettenleiter, 2004).

1.1.3 Latent infection

Apart from cell lysis caused by primary infection, herpesviruses are notorious for their potential to maintain life-long infection in the hosts. Although the hallmark of latency is not clinically apparent in healthy individuals due to repression of viral DNA replication, the dormant virus might be reactivated and become infectious from time to time (Kinchington et al., 2012). Before the target tissues can be transformed into the reservoir for silent virus, EHV-1 at least has to overcome the physical barrier such as respiratory mucosa and placenta. When EHV-1 invades a horse by inhalation route, the acute infection causes damage of the upper respiratory tract and allows virus to access the blood and lymphatic vessels, in which leukocytes are infected, leading to circulation of EHV-1 throughout the internal organs. Finally, the spread of EHV-1 extends to the central nervous system (CNS) by severe cell-associated viremia (Patel and Heldens, 2005). This process is believed to be an essential

step for latency establishment, but the primary locations for maintenance of persistent infection remain largely ambiguous. It has been shown that latency of EHV-1 is detectable in various cell populations and tissues, including peripheral blood mononuclear cells (PBMCs) (Baxi et al., 1996), $CD5^+CD8^+$ T lymphocytes (Smith et al., 1998), lymph nodes (Allen, 2006) and trigeminal ganglia (Slater et al., 1994). In clinical practice, the potential threat of latently infected leukocytes cannot be underestimated, as the fetus originated from EHV-1 infected mare likely carries the latent virus in its blood and therefore might become an additional source of EHV-1 transmission (Lunn et al., 2009). By far, there is no effective treatment to completely eliminate EHV-1 from the infected animals. This can be partly explained by the development of EHV-1 latency, which is not an immediate and isolated event but a complicated battle between the virus and the horse immune system.

In the stage of latent infection, a majority of viral genes are not expressed and virus shedding is switched off as well, whereas synthesis of regulatory RNAs is not affected. These RNAs are mainly transcribed from the *ORF64* gene (Pusterla et al., 2009), which also encodes the only IE protein for EHV-1. Unlike the essential role of the IE protein in virus replication, it remains uncertain whether the latency-associated transcripts (LATs) produced by alternative splicing of the *ORF64* gene directly contribute to EHV-1 latent infection. In the case of HSV-1, LATs are thought to be microRNAs that originate from a common primary transcript (Umbach et al., 2008). They enhance the status of latency by inhibiting neuronal apoptosis but cannot determine the establishment of latency, as abrogation of LATs fails to prevent the reactivation of silent virus (Perng et al., 2000). This evidence also indicates the complexity of genetic factors that lead to persistent infection with herpesviruses. As for the EHV-1 *ORF64* gene, it will be interesting to characterize the potential species of LATs involved in the development of latency. Overall, the lesson from latency emphasizes the importance of daily management, because recurrence of EHV-1 infection depends on the conditions of host immune system. In this sense, any factors related to immunity, e.g., age, stress, pregnancy and nutrition, etc., might give rise to different outcomes of a latent infection, ranging from being asymptomatic to severely ill. Thus measures to avoid immunosuppression should be in place for the control of virus recrudescence in latently infected horses.

1.2 Immunity to EHV-1

In vertebrates, the fundamental arms to fight the invading pathogens include innate and adaptive immunity (Clark and Kupper, 2005). Young horses with premature immune system are susceptible to primary EHV-1 infection. The presence of virus is first recognized by innate immune sensors, which initiate the synthesis of type I interferons (IFNs) and a variety of cytokines. After a few weeks, symptoms caused by the acute infection are subdued owing to

the activity of host antiviral effectors and the end of inflammation. In addition, dendritic cells (DCs) and other professional antigen-presenting cells (APCs) are primed by capturing viral antigenic peptides. As a consequence, activation of APCs promotes the differentiation and proliferation of naïve T and B cells, which constitute the effective components of adaptive immunity targeting EHV-1. However, duration of the adaptive immunity against EHV-1 challenge is short-lived and variable usually within 4 to 8 months followed by primary infection (Paillot et al., 2008).

1.2.1 Innate immune responses

Antiviral innate immunity represents the first line of defense that controls herpesvirus infection by release of type I IFNs and recruitment of natural killer (NK) cells (Platanias, 2005). To invade and manipulate the host cells, herpesviruses require a series of functional components (e.g., glycoproteins and nucleic acids) that are essential for their life cycle. These molecular structures are collectively deemed as pathogen-associated molecular patterns (PAMPs). Conceptually, sensing of PAMPs by pattern recognition receptors (PRRs) initiates a signaling cascade, which eventually enhances host resistance to another imminent infection (Kawai and Akira, 2011). Until now, there are two predominant signaling networks to detect the presence of HSV-1 and/or -2, including (i) Toll-like receptors (TLRs), for example, cell surface TLR1-TLR2 heterodimer that recognizes envelope glycoproteins, plus TLR3, TLR7 and TLR9 that sense viral nucleic acids in endosomes (reviewed in Paludan et al., 2011); (ii) Cytosolic nucleic acid receptors, such as RNA polymerase III, RIG-I-like receptors (RLRs) and the recently identified cyclic GMP-AMP synthase (cGAS), which detect various forms of viral DNA and RNA intermediates (reviewed in Wu and Chen, 2014). Recognition of viral nucleic acids by TLRs, RLRs or cGAS causes the induction of type I IFN synthesis and the production of numerous pro-inflammatory cytokines. In particular, type I IFNs play a central role in activation of the signaling pathways that trigger the expression of Mx proteins, PKR (Protein kinase RNA-activated) and OAS (2′-5′-oligoadenylate synthase). These effector molecules confer antiviral effects and protect cells from viral infections (Ivashkiv and Donlin, 2014).

In response to the early infection of EHV-1, type I IFNs are released into nasal discharge and serum (Edington et al., 1989); however, the mechanisms on how EHV-1 triggers innate immune responses remain poorly understood. Recently, equine respiratory epithelial cells were used as a model to investigate the innate immune responses to EHV-1 (Soboll Hussey et al., 2014a). At 24 h after EHV-1 inoculation, the mRNA levels of TLR3 and TLR9 as well as cytokines (TNF-α, IFN-α, IL-1 and IL-6) were elevated. Moreover, the pUL56 homologue of EHV-1 seems to be involved in modulation of cytokine expression (IFN-α and IL-10) (Soboll

Hussey et al., 2014b). These findings demonstrate the interaction between EHV-1 and the horse innate immune system and will be valuable resource for further understanding the importance of antiviral innate immunity in horses. It is foreseeable that the signaling pathways of RLRs and cGAS would become promising aspects in the study of horse innate immune responses, as their homologues are evolutionarily conserved in vertebrates.

1.2.2 Adaptive immune responses

A broad range of adaptive immune responses to EHV-1 can be elicited by both natural infection and vaccination. EHV-1 specific T and B cell populations are proliferated after the viral antigens are processed and presented by the APCs residing in NALT (nasal associated lymphoid tissue) and MALT (mucosal associated lymphoid tissue) (Paillot et al., 2008). Subsequently, the blood and lymphatic vessels facilitate the circulation of these immune cells throughout the entire body, leading to systemic immune responses that require the involvement of antibodies and cytotoxic T lymphocytes (CTLs). Approximately two weeks following EHV-1 infection, virus neutralizing (VN) and complement fixing (CF) antibodies, which constitute the humoral immune responses, are detectable in the sera. In contrast to the CF antibodies, the VN antibodies have relatively longer duration of activity (Thomson et al., 1976). Epitopes for VN antibodies are primarily found on glycoproteins, such as gB, gC, gD, gH as well as the unique gp2 (Crabb et al., 1991). Humoral immunity to EHV-1 is notoriously short-lived (usually less than 1 year), and thus its role in the control of virus shedding and recurrence seems inconsistent. Virus-specific IgA secreted from the local mucosal tissue proves to be effective in reducing virus shedding after a secondary infection; however, the antiviral effects of circulating antibodies, e.g., IgGa, IgGb, IgGc and IgG (T), are not clearly defined. In some studies, no correlation was reported between the serum VN antibody titers and protection against infection (Patel et al., 2003), but the VN antibodies in nasopharyngeal secretion are sufficient to inhibit EHV-1 shedding (Hannant et al., 1993). Although the humoral immunity generates plenty of antibodies that neutralize the release of EHV-1 during the lytic infection stage, these antibodies do not have significant effect on preventing horses from abortion and neurological disorder caused by cell-associated viremia.

Virus-specific cellular immunity plays a crucial role in restricting the systemic dissemination of herpesvirus, particularly when the circulating VN antibodies fail to block the virus that survives in the cytosol and transmits from cell to cell. In response to intracellular EHV-1 infection, production of IFNγ by effector cells is increased, which boosts the activation of CTLs by modulating viral antigen presentation and development of T helper 1 (Th1) lymphocytes (Paillot et al., 2005). CTLs precisely destruct the infected cells by recognizing the viral peptides that are associated with the MHC class I (MHC-I) molecules on the cell

surface. Mechanistically, this killing process depends on the perforin and granzymes released from the CTLs. These two types of cytotoxic proteins trigger programmed cell death by disrupting the integrity of the plasma membrane and cellular DNA, which ultimately leads to the burst of target cells and rapid engulfment of cellular debris by phagocytes. Alternatively, apoptosis mediated by CTLs may occur through the Fas/FasL signaling pathway, which requires neither perforin nor granzymes (Barry and Bleackley, 2002). During cell-associated viremia, the importance of CTLs in defending against EHV-1 infection is manifested by the increased percentage of specific lymphoblasts in the peripheral blood; for instance, pregnant mares with higher frequency of EHV-1 specific memory CTLs have been shown to be more resistant to abortion following experimental infection (Kydd et al., 2003). Moreover, the lifetime of EHV-1 specific CTLs is more durable than that of serum antibodies and can still be detected after infection for one year (Allen et al., 1995). Because of its efficiency in controlling the spread of virus between cells, enhancement of EHV-1 specific CTL activity and frequency is considered an ideal solution to restrain cell-associated viremia, which poses threats to the reproductive and central nervous systems of the infected horses. To understand the development of cellular immunity that targets the circulating EHV-1, research efforts need to focus on the viral proteins that elicit potent cellular immune responses as well as the genetic resources of equine MHC-I. It has been known that only a small number of viral proteins contain the epitopes relevant to CTL priming. These epitopes can be found on glycoproteins (e.g., gC, gD, gI and gL) and the single IE gene product (ICP4 encoded by *ORF64* gene). The capability of glycoproteins to induce CTL response varies greatly from individuals (Allen et al., 1995), while effector CTLs isolated from ponies with the equine leukocyte antigen A3 haplotype (located in the B2 allele) can be constantly induced by transfecting DCs with ICP4 (Soboll et al., 2003). These findings suggest that the epitopes for CTL activation are closely associated with specific haplotypes of equine MHC-I. It remains elusive whether other haplotypes are involved in presentation of the viral IE protein and which haplotypes target the epitopes derived from glycoproteins. If these concerns are properly addressed in the future, vaccination against viremia caused by EHV-1 infection will become more effective.

1.3 Immune evasion strategies of EHV-1 and other alphaherpesviruses

As with other herpesviruses, EHV-1 is refractory to elimination by the host immune system and imposes persistent harassment to the horses that had been previously exposed to primary infection. Although our knowledge about how EHV-1 overcomes the host defense network remains rather limited, extensive studies based on HSV and other closely related alphaherpesviruses might provide useful lessons to reflect on the possible mechanisms that allow EHV-1 to evade innate and adaptive immune responses.

1.3.1 Resistance to innate immunity

It is not surprising that the innate immune system encounters defeat in clearance of aggressive pathogens such as herpesviruses, which are composed of numerous viral proteins that interfere with cellular signaling pathways. The general mechanisms that herpesviruses have evolved to antagonize innate immunity include evasion of recognition by PRRs, attenuation of type I IFN signaling and inhibition of autophagy (Paludan et al., 2011). There are several well-described viral proteins that facilitate HSV to evade innate immune responses, including vhs, ICP0, ICP27 and ICP34.5. Their roles can be independently linked to one aspect of the evasion strategies or collaborate with each other to repress the innate defense as a whole. According to phylogenic analyses, vhs homologues are conserved in all members of the *Alphaherpesvirinae* subfamily with RNA endonuclease activity, which induces random cleavage of cellular mRNA following virus infection (Smiley, 2004). As a result, the vhs protein has been recognized as an unbiased modulator designed by alphaherpesviruses. On the one hand, vhs is able to substantially block the action of TLR3 and RLRs presumably by degrading mRNA transcripts encoding these nucleic acid sensors or by impairing viral RNA intermediates required for this process (Cotter et al., 2010). On the other hand, vhs contributes to reducing the production of IFNs and interfering with the downstream JAK/STAT signaling events (Yokota et al., 2004). Currently for EHV-1, little is known about whether its vhs homologue (encoded by *ORF41* gene) plays a role in regulating IFN response, and it is of interest to compare the immunomodulatory scope of different vhs proteins by replacing one with another in the context of recombinant virus.

ICP0 and ICP27 are two representative viral proteins that antagonize expression of type I IFNs and IFN-stimulated signaling pathways. The ICP0 homologues are present in most alphaherpesviruses and commonly known as viral E3 ubiquitin ligases, as they contain a consensus RING (Really Interesting New Gene) finger domain that mediates the binding of ubiquitin molecules to substrates (Everett et al., 2010). In the case of HSV-1, ICP0 blocks the activation of interferon regulatory factors IRF3 and IRF7, thereby inhibiting the synthesis of type I IFNs (Lin et al., 2004). The mechanism of ICP0 depends on preventing the translocation of IRF3 into the nucleus but seems not linked to the proteasomal degradation induced by its E3 ubiquitin ligase activity (Paladino et al., 2010). With respect to ICP27, it primarily acts on the JAK/STAT pathway that requires the stimulation by type I IFNs. In detail, ICP27 is able to downregulate the levels of phosphorylated STAT-1 protein, which leads to the reduction of STAT-1 dimers accumulated in the nucleus and consequently represses the antiviral effects (Johnson et al., 2008). Until now, the roles of EHV-1 ICP0 and ICP27 as *trans*-activators have been documented (Bowles et al., 1997; Zhao et al., 1995), but their involvement in modulation of IFN signaling pathway still needs to be confirmed.

Autophagy is an ancient catabolic process for eukaryotic organisms to selectively dispose of cellular waste and maintain homeostasis; however, it has recently emerged as a potential platform manipulated by herpesviruses for innate immune evasion (Williams and Taylor, 2012). The HSV-1 ICP34.5 was first identified as a viral inhibitor that disrupts the degradation of virions mediated by the autophagic pathway in a PKR-dependent manner (Talloczy et al., 2006). Later, it was further revealed that ICP34.5 binds to Beclin-1, a chaperone crucial for autophagosome formation. This interaction inhibits the normal function of autophagy and leads to severe encephalitis in infected mice (Orvedahl et al., 2007). These studies highlight that manipulation of autophagy benefits HSV-1 not only for replication in permissive cells but also for neural invasion. Although there is no ICP34.5 homologue present in EHV-1, it remains worthwhile to explore whether autophagy is undermined during the innate immune response to EHV-1 infection.

1.3.2 Resistance to adaptive immunity

Compared to the scarce understanding of innate immune responses against EHV-1 infection, more and more studies have shown that EHV-1 is equipped with various countermeasures to circumvent the line of adaptive immune defense, ranging from humoral and cell-mediated immunity. To minimize the direct exposure of viral antigen to specific antibody, EHV-1 has developed two putative approaches. First, the viral envelope proteins, which are recognized by neutralizing antibodies, cannot be detected on the cell surface of PBMCs during cell-associated viremia (van der Meulen et al., 2006). This strategy renders EHV-1-infected cells invisible to antibody-dependent cell-mediated cytotoxicity (ADCC) and accelerates the systemic dissemination of virus via blood circulation. Second, formation of gE-gI heterodimer might confer EHV-1 additional resistance to antibody and/or complement-mediated apoptosis. Although this assumption has not been tested by experiments related to EHV-1, the gE-gI complex from pseudorabies virus (PRV), which is phylogenetically close to EHV-1, has been reported to bind the Fc domain of immunoglobulin G (IgG), thereby protecting the infected cells from destruction by humoral immune response (Favoreel et al., 1997; Van de Walle et al., 2003).

The CTL-mediated immunity is thought to be a major player in eliminating the cells subjected to herpesvirus infection (Borysiewicz and Sissons, 1994). Thus it is not surprising that evasion from recognition by CTLs is favored by many different herpesviruses. To block the danger signals that trigger recruitment of CTLs to the infection site, herpesviruses have to weaken the antigen presentation pathway mediated by MHC-I. Prior to interaction with T cell receptor (TCR), MHC-I complex needs to be processed by several critical steps, which involves uptake of antigenic peptides in the endoplasmic reticulum (ER) lumen, modifications

in the Golgi apparatus and ultimately stable retention on the cell surface (Neefjes et al., 2011). As a consequence, herpesviruses exploit a variety of inhibitors that target each checkpoint during MHC-I antigen presentation. Since the discovery of HSV-1 ICP47 as a viral regulatory protein for peptide loading (Fruh et al., 1995), the topic on how herpesvirus interferes with the expression of cell surface MHC-I continues to attract attention, and several novel proteins responsible for MHC-I downregulation have been identified (summarized in Table 1.1). As these viral gene products are derived from different species, it is reasoned that their molecular mechanisms are distinct. For example, the pUL49.5 homologues are present in most members of the genus *Varicellovirus*, including EHV-1, EHV-4, PRV, bovine herpesvirus type 1 (BoHV-1) and varicella-zoster virus (VZV), which have been shown to shut off peptide transport. However, they use different measures to inhibit the activity of TAP (transporter associated with antigen processing) and in general lead to the reduction of mature MHC-I presented on the cell surface. BoHV-1 pUL49.5 induces degradation of TAP in a proteasome-dependent manner (Koppers-Lalic et al., 2005), while pUL49.5 homologues of PRV, EHV-1 and EHV-4 disable the function of TAP by obstructing the supply of ATP (Koppers-Lalic et al., 2008). On top of pUL49.5, an early protein encoded by EHV-1, namely pUL56, has recently been shown to induce MHC-I downregulation in the context of viral infection (Ma et al., 2012). Unlike the ER-resident pUL49.5, pUL56 is predominantly located to the Golgi compartment, indicating that the potential mechanism of pUL56 might be different from that of pUL49.5 (Said et al., 2012). Given that endocytosis could be an important factor contributing to reduction of cell surface MHC-I molecules during EHV-1 infection (Rappocciolo et al., 2003), it is reasonable to evaluate the possible association between pUL56 and MHC-I downregulation mediated by endocytic pathways.

Table 1.1 List of MHC-I inhibitors encoded by herpesviruses

Subfamily	Modulator	Mechanism	Virus	References
Alphaherpesvirinae	ICP47	Inhibtion of peptide binding to the TAP	HSV-1	Fruh et al., 1995
	pUL49.5	Inducing TAP degradation or sequesting ATP from TAP	VZV, EHV-1, EHV-4, PRV, BoHV-1, MDV	Koppers-Lalic et al., 2005 Koppers-Lalic et al., 2008 Jarosinski et al., 2010
	pUL56	Enhancement of dynamin-mediated endocytosis	EHV-1, EHV-4	Work in this thesis; Ma et al., 2012; Said et al., 2012
	pUL43	Cooperation with EHV-1 pUL56	EHV-1	Work in this thesis
	US3	MHC-I maturation delayed by the kinase activity	VZV, PRV, HSV-1	Eisfeld et al., 2007 Deruelle et al., 2009 Imai et al., 2013
Betaherpesvirinae	EBNA1	Inhibition of proteasomal processing	EBV	Levitskaya et al., 1995
	BNLF2a	Blocking peptide transport	EBV	Horst et al., 2009
	US2, US11	Proteasomal degradation of nascent MHC-I in ER	HCMV	Barel et al., 2006
	US3	Inhibition of tapsin activity	HCMV	Park et al., 2004
	US6	Inhibition of ATP binding and hydrolysis	HCMV	Hewitt et al., 2001 Kyritsis et al., 2001
	gp48	Diversion of MHC-I to lysosomal degradation	MCMV	Reusch et al., 1999
Gammaherpesvirinae	K3, K5	Ubiquitination, endocytosis and lysosomal degradtion	KSHV	Coscoy et al., 2000 Coscoy et al., 2001
	mK3	Ubiquitination and ER-associated degradtion of MHC-I	MHV-68	Boname et al., 2001

1.4 Outline of the thesis

This cumulative dissertation is made up of two studies, which explored the involvement of two viral proteins in modulating the antigen presentation by MHC-I. Pioneering studies have suggested that MHC-I downregulation might be caused by enhanced endocysosis and that EHV-1 pUL56 is responsible for significant downregulation of MHC-I. Therefore, the first part of this thesis aimed to experimentally verify the correlation between pUL56 expression and MHC-I reduction through endocytosis. To seek the possible endocytic pathway involved, a series of specific chemical inhibitors were used in combination with dominant negative mutants. To confirm the multiple roles of pUL56 in immune modulation, other cell surface markers such as CD46 and CD63 were also analyzed.

In the second part, a library of EHV-1 mutants was created and screened to search for an elusive protein that cooperates with pUL56 for MHC-I downregulation. One viral mutant out of 26 was found to be capable of inducing considerable decrease of MHC-I expression at the cell surface. This newly identified viral protein belongs to a pUL43 homologue that prevails in the *Alphaherpesvirinae* subfamily. Since the functions of EHV-1 pUL43 are poorly understood, a characterization study of pUL43 was performed, including expression profiling, growth properties and subcellular localization. Interestingly, the cooperative role of pUL43 and pUL56 in MHC-I downregulation was investigated under uninfected conditions.

References

Allen, G., Yeargan, M., Costa, L.R., Cross, R., 1995, Major histocompatibility complex class I-restricted cytotoxic T-lymphocyte responses in horses infected with equine herpesvirus 1. J Virol 69, 606-612.

Allen, G.P., 2006, Antemortem detection of latent infection with neuropathogenic strains of equine herpesvirus-1 in horses. Am J Vet Res 67, 1401-1405.

Allen, G.P., Bryans, J.T., 1986, Molecular epizootiology, pathogenesis, and prophylaxis of equine herpesvirus-1 infections. Prog Vet Microbiol Immunol 2, 78-144.

Azab, W., Lehmann, M.J., Osterrieder, N., 2013, Glycoprotein H and alpha4beta1 integrins determine the entry pathway of alphaherpesviruses. J Virol 87, 5937-5948.

Azab, W., Osterrieder, N., 2012, Glycoproteins D of equine herpesvirus type 1 (EHV-1) and EHV-4 determine cellular tropism independently of integrins. J Virol 86, 2031-2044.

Barel, M.T., Pizzato, N., Le Bouteiller, P., Wiertz, E.J., Lenfant, F., 2006, Subtle sequence variation among MHC class I locus products greatly influences sensitivity to HCMV US2- and US11-mediated degradation. Int Immunol 18, 173-182.

Barry, M., Bleackley, R.C., 2002, Cytotoxic T lymphocytes: all roads lead to death. Nat Rev Immunol 2, 401-409.

Baxi, M.K., Borchers, K., Bartels, T., Schellenbach, A., Baxi, S., Field, H.J., 1996, Molecular studies of the acute infection, latency and reactivation of equine herpesvirus-1 (EHV-1) in the mouse model. Virus Res 40, 33-45.

Boname, J.M., Stevenson, P.G., 2001, MHC class I ubiquitination by a viral PHD/LAP finger protein. Immunity 15, 627-636.

Borysiewicz, L.K., Sissons, J.G., 1994, Cytotoxic T cells and human herpes virus infections. Curr Top Microbiol Immunol 189, 123-150.

Bowles, D.E., Holden, V.R., Zhao, Y., O'Callaghan, D.J., 1997, The ICP0 protein of equine herpesvirus 1 is an early protein that independently transactivates expression of all classes of viral promoters. J Virol 71, 4904-4914.

Burrows, R., 1977, Herpes virus infections of animals--a brief review. J Antimicrob Chemother 3 Suppl A, 9-14.

Clark, R., Kupper, T., 2005, Old meets new: the interaction between innate and adaptive immunity. J Invest Dermatol 125, 629-637.

Coscoy, L., Ganem, D., 2000, Kaposi's sarcoma-associated herpesvirus encodes two proteins that block cell surface display of MHC class I chains by enhancing their endocytosis. Proc Natl Acad Sci U S A 97, 8051-8056.

Coscoy, L., Sanchez, D.J., Ganem, D., 2001, A novel class of herpesvirus-encoded membrane-bound E3 ubiquitin ligases regulates endocytosis of proteins involved in immune recognition. J Cell Biol 155, 1265-1273.

Cotter, C.R., Nguyen, M.L., Yount, J.S., Lopez, C.B., Blaho, J.A., Moran, T.M., 2010, The virion host shut-off (vhs) protein blocks a TLR-independent pathway of herpes simplex virus type 1 recognition in human and mouse dendritic cells. PLoS One 5, e8684.

Crabb, B.S., Allen, G.P., Studdert, M.J., 1991, Characterization of the major glycoproteins of equine herpesviruses 4 and 1 and asinine herpesvirus 3 using monoclonal antibodies. J Gen Virol 72 (Pt 9), 2075-2082.

Csellner, H., Walker, C., Wellington, J.E., McLure, L.E., Love, D.N., Whalley, J.M., 2000, EHV-1 glycoprotein D (EHV-1 gD) is required for virus entry and cell-cell fusion, and an EHV-1 gD deletion mutant induces a protective immune response in mice. Arch Virol 145, 2371-2385.

Deruelle, M.J., Van den Broeke, C., Nauwynck, H.J., Mettenleiter, T.C., Favoreel, H.W., 2009, Pseudorabies virus US3- and UL49.5-dependent and -independent downregulation of MHC I cell surface expression in different cell types. Virology 395, 172-181.

Doll, E.R., Crowe, M.E., Bryans, J.T., Mc, C.W., 1955, Infection immunity in equine virus abortion. Cornell Vet 45, 387-410.

Dunowska, M., 2014, A review of equid herpesvirus 1 for the veterinary practitioner. Part A: clinical presentation, diagnosis and treatment. N Z Vet J 62, 171-178.

Edington, N., Bridges, C.G., Griffiths, L., 1989, Equine interferons following exposure to equid herpesvirus-1 or -4. J Interferon Res 9, 389-392.

Eisfeld, A.J., Yee, M.B., Erazo, A., Abendroth, A., Kinchington, P.R., 2007, Downregulation of class I major histocompatibility complex surface expression by varicella-zoster virus involves open reading frame 66 protein kinase-dependent and -independent mechanisms. J Virol 81, 9034-9049.

Everett, R.D., Boutell, C., McNair, C., Grant, L., Orr, A., 2010, Comparison of the biological and biochemical activities of several members of the alphaherpesvirus ICP0 family of proteins. J Virol 84, 3476-3487.

Favoreel, H.W., Nauwynck, H.J., Van Oostveldt, P., Mettenleiter, T.C., Pensaert, M.B., 1997, Antibody-induced and cytoskeleton-mediated redistribution and shedding of viral glycoproteins, expressed on pseudorabies virus-infected cells. J Virol 71, 8254-8261.

Fenwick, M.L., Clark, J., 1983, The effect of cycloheximide on the accumulation and stability of functional alpha-mRNA in cells infected with herpes simplex virus. J Gen Virol 64 (Pt 9), 1955-1963.

Frampton, A.R., Jr., Uchida, H., von Einem, J., Goins, W.F., Grandi, P., Cohen, J.B., Osterrieder, N., Glorioso, J.C., 2010, Equine herpesvirus type 1 (EHV-1) utilizes microtubules, dynein, and ROCK1 to productively infect cells. Vet Microbiol 141, 12-21.

Fruh, K., Ahn, K., Djaballah, H., Sempe, P., van Endert, P.M., Tampe, R., Peterson, P.A., Yang, Y., 1995, A viral inhibitor of peptide transporters for antigen presentation. Nature 375, 415-418.

Gable, J.E., Acker, T.M., Craik, C.S., 2014, Current and Potential Treatments for Ubiquitous but Neglected Herpesvirus Infections. Chem Rev.

Garko-Buczynski, K.A., Smith, R.H., Kim, S.K., O'Callaghan, D.J., 1998, Complementation of a replication-defective mutant of equine herpesvirus type 1 by a cell line expressing the immediate-early protein. Virology 248, 83-94.

Hannant, D., Jessett, D.M., O'Neill, T., Dolby, C.A., Cook, R.F., Mumford, J.A., 1993, Responses of ponies to equid herpesvirus-1 ISCOM vaccination and challenge with virus of the homologous strain. Res Vet Sci 54, 299-305.

Harty, R.N., Colle, C.F., Grundy, F.J., O'Callaghan, D.J., 1989, Mapping the termini and intron of the spliced immediate-early transcript of equine herpesvirus 1. J Virol 63, 5101-5110.

Hewitt, E.W., Gupta, S.S., Lehner, P.J., 2001, The human cytomegalovirus gene product US6 inhibits ATP binding by TAP. EMBO J 20, 387-396.

Honess, R.W., Watson, D.H., 1977, Herpes simplex virus resistance and sensitivity to phosphonoacetic acid. J Virol 21, 584-600.

Horst, D., van Leeuwen, D., Croft, N.P., Garstka, M.A., Hislop, A.D., Kremmer, E., Rickinson, A.B., Wiertz, E.J., Ressing, M.E., 2009, Specific targeting of the EBV lytic phase protein BNLF2a to the transporter associated with antigen processing results in impairment of HLA class I-restricted antigen presentation. J Immunol 182, 2313-2324.

Imai, T., Koyanagi, N., Ogawa, R., Shindo, K., Suenaga, T., Sato, A., Arii, J., Kato, A., Kiyono, H., Arase, H., Kawaguchi, Y., 2013, Us3 kinase encoded by herpes simplex virus 1 mediates downregulation of cell surface major histocompatibility complex class I and evasion of CD8+ T cells. PLoS One 8, e72050.

Ivashkiv, L.B., Donlin, L.T., 2014, Regulation of type I interferon responses. Nat Rev Immunol 14, 36-49.

Jarosinski, K.W., Hunt, H.D., Osterrieder, N., 2010, Down-regulation of MHC class I by the Marek's disease virus (MDV) UL49.5 gene product mildly affects virulence in a haplotype-specific fashion. Virology 405, 457-463.

Johnson, K.E., Song, B., Knipe, D.M., 2008, Role for herpes simplex virus 1 ICP27 in the inhibition of type I interferon signaling. Virology 374, 487-494.

Kawai, T., Akira, S., 2011, Toll-like receptors and their crosstalk with other innate receptors in infection and immunity. Immunity 34, 637-650.

Kim, S.K., Buczynski, K.A., Caughman, G.B., O'Callaghan, D.J., 2001, The equine herpesvirus 1 immediate-early protein interacts with EAP, a nucleolar-ribosomal protein. Virology 279, 173-184.

Kinchington, P.R., Leger, A.J., Guedon, J.M., Hendricks, R.L., 2012, Herpes simplex virus and varicella zoster virus, the house guests who never leave. Herpesviridae 3, 5.

Koppers-Lalic, D., Reits, E.A., Ressing, M.E., Lipinska, A.D., Abele, R., Koch, J., Marcondes Rezende, M., Admiraal, P., van Leeuwen, D., Bienkowska-Szewczyk, K., Mettenleiter, T.C., Rijsewijk, F.A., Tampe, R., Neefjes, J., Wiertz, E.J., 2005, Varicelloviruses avoid T cell recognition by UL49.5-mediated inactivation of the transporter associated with antigen processing. Proc Natl Acad Sci U S A 102, 5144-5149.

Koppers-Lalic, D., Verweij, M.C., Lipinska, A.D., Wang, Y., Quinten, E., Reits, E.A., Koch, J., Loch, S., Marcondes Rezende, M., Daus, F., Bienkowska-Szewczyk, K., Osterrieder, N., Mettenleiter, T.C., Heemskerk, M.H., Tampe, R., Neefjes, J.J., Chowdhury, S.I., Ressing, M.E., Rijsewijk, F.A., Wiertz, E.J., 2008, Varicellovirus UL 49.5 proteins differentially affect the function of the transporter associated with antigen processing, TAP. PLoS Pathog 4, e1000080.

Kydd, J.H., Wattrang, E., Hannant, D., 2003, Pre-infection frequencies of equine herpesvirus-1 specific, cytotoxic T lymphocytes correlate with protection against abortion following experimental infection of pregnant mares. Vet Immunol Immunopathol 96, 207-217.

Kyritsis, C., Gorbulev, S., Hutschenreiter, S., Pawlitschko, K., Abele, R., Tampe, R., 2001, Molecular mechanism and structural aspects of transporter associated with antigen processing inhibition by the cytomegalovirus protein US6. J Biol Chem 276, 48031-48039.

Leuzinger, H., Ziegler, U., Schraner, E.M., Fraefel, C., Glauser, D.L., Heid, I., Ackermann, M., Mueller, M., Wild, P., 2005, Herpes simplex virus 1 envelopment follows two diverse pathways. J Virol 79, 13047-13059.

Levitskaya, J., Coram, M., Levitsky, V., Imreh, S., Steigerwald-Mullen, P.M., Klein, G., Kurilla, M.G., Masucci, M.G., 1995, Inhibition of antigen processing by the internal repeat region of the Epstein-Barr virus nuclear antigen-1. Nature 375, 685-688.

Lin, R., Noyce, R.S., Collins, S.E., Everett, R.D., Mossman, K.L., 2004, The herpes simplex virus ICP0 RING finger domain inhibits IRF3- and IRF7-mediated activation of interferon-stimulated genes. J Virol 78, 1675-1684.

Lunn, D.P., Davis-Poynter, N., Flaminio, M.J., Horohov, D.W., Osterrieder, K., Pusterla, N., Townsend, H.G., 2009, Equine herpesvirus-1 consensus statement. J Vet Intern Med 23, 450-461.

Ma, G., Feineis, S., Osterrieder, N., Van de Walle, G.R., 2012, Identification and characterization of equine herpesvirus type 1 pUL56 and its role in virus-induced downregulation of major histocompatibility complex class I. J Virol 86, 3554-3563.

Mettenleiter, T.C., 2002, Herpesvirus assembly and egress. J Virol 76, 1537-1547.

Mettenleiter, T.C., 2004, Budding events in herpesvirus morphogenesis. Virus Res 106, 167-180.

Mettenleiter, T.C., Klupp, B.G., Granzow, H., 2009, Herpesvirus assembly: an update. Virus Res 143, 222-234.

Neefjes, J., Jongsma, M.L., Paul, P., Bakke, O., 2011, Towards a systems understanding of MHC class I and MHC class II antigen presentation. Nat Rev Immunol 11, 823-836.

Orvedahl, A., Alexander, D., Talloczy, Z., Sun, Q., Wei, Y., Zhang, W., Burns, D., Leib, D.A., Levine, B., 2007, HSV-1 ICP34.5 confers neurovirulence by targeting the Beclin 1 autophagy protein. Cell Host Microbe 1, 23-35.

Osterrieder, N., 1999, Construction and characterization of an equine herpesvirus 1 glycoprotein C negative mutant. Virus Res 59, 165-177.

Paillot, R., Daly, J.M., Juillard, V., Minke, J.M., Hannant, D., Kydd, J.H., 2005, Equine interferon gamma synthesis in lymphocytes after in vivo infection and in vitro stimulation with EHV-1. Vaccine 23, 4541-4551.

Paillot, R., Case, R., Ross, J., Newton, R., Nugent, J., 2008, Equine Herpes Virus-1: Virus, Immunity and Vaccines. Open Vet Sci J 2, 68-91.

Paladino, P., Collins, S.E., Mossman, K.L., 2010, Cellular localization of the herpes simplex virus ICP0 protein dictates its ability to block IRF3-mediated innate immune responses. PLoS One

5, e10428.

Paludan, S.R., Bowie, A.G., Horan, K.A., Fitzgerald, K.A., 2011, Recognition of herpesviruses by the innate immune system. Nat Rev Immunol 11, 143-154.

Park, B., Kim, Y., Shin, J., Lee, S., Cho, K., Fruh, K., Ahn, K., 2004, Human cytomegalovirus inhibits tapasin-dependent peptide loading and optimization of the MHC class I peptide cargo for immune evasion. Immunity 20, 71-85.

Patel, J.R., Foldi, J., Bateman, H., Williams, J., Didlick, S., Stark, R., 2003, Equid herpesvirus (EHV-1) live vaccine strain C147: efficacy against respiratory diseases following EHV types 1 and 4 challenges. Vet Microbiol 92, 1-17.

Patel, J.R., Heldens, J., 2005, Equine herpesviruses 1 (EHV-1) and 4 (EHV-4)--epidemiology, disease and immunoprophylaxis: a brief review. Vet J 170, 14-23.

Perdue, M.L., Kemp, M.C., Randall, C.C., O'Callaghan, D.J., 1974, Studies of the molecular anatomy of the L-M cell strain of equine herpes virus type 1: proteins of the nucleocapsid and intact virion. Virology 59, 201-216.

Perng, G.C., Jones, C., Ciacci-Zanella, J., Stone, M., Henderson, G., Yukht, A., Slanina, S.M., Hofman, F.M., Ghiasi, H., Nesburn, A.B., Wechsler, S.L., 2000, Virus-induced neuronal apoptosis blocked by the herpes simplex virus latency-associated transcript. Science 287, 1500-1503.

Platanias, L.C., 2005, Mechanisms of type-I- and type-II-interferon-mediated signalling. Nat Rev Immunol 5, 375-386.

Pusterla, N., Wilson, W.D., Mapes, S., Finno, C., Isbell, D., Arthur, R.M., Ferraro, G.L., 2009, Characterization of viral loads, strain and state of equine herpesvirus-1 using real-time PCR in horses following natural exposure at a racetrack in California. Vet J 179, 230-239.

Rappocciolo, G., Birch, J., Ellis, S.A., 2003, Down-regulation of MHC class I expression by equine herpesvirus-1. J Gen Virol 84, 293-300.

Reusch, U., Muranyi, W., Lucin, P., Burgert, H.G., Hengel, H., Koszinowski, U.H., 1999, A cytomegalovirus glycoprotein re-routes MHC class I complexes to lysosomes for degradation. EMBO J 18, 1081-1091.

Roizman, B., Knipe, D. M., 2001, Herpes simplex viruses and their replication, p. 2399-2459. In P. M. Howley and D. M. Knipe (ed.), Virology, 4th ed. Lippincott-Raven, Philadelphia, Pa.

Said, A., Azab, W., Damiani, A., Osterrieder, N., 2012, Equine herpesvirus type 4 UL56 and UL49.5 proteins downregulate cell surface major histocompatibility complex class I expression independently of each other. J Virol 86, 8059-8071.

Slater, J.D., Borchers, K., Thackray, A.M., Field, H.J., 1994, The trigeminal ganglion is a location for equine herpesvirus 1 latency and reactivation in the horse. J Gen Virol 75 (Pt 8), 2007-2016.

Smiley, J.R., 2004, Herpes simplex virus virion host shutoff protein: immune evasion mediated by a viral RNase? J Virol 78, 1063-1068.

Smith, D.J., Iqbal, J., Purewal, A., Hamblin, A.S., Edington, N., 1998, In vitro reactivation of latent equid herpesvirus-1 from CD5+/CD8+ leukocytes indirectly by IL-2 or chorionic gonadotrophin. J Gen Virol 79 (Pt 12), 2997-3004.

Smith, R.H., Zhao, Y., O'Callaghan, D.J., 1994, The equine herpesvirus type 1 immediate-early gene product contains an acidic transcriptional activation domain. Virology 202, 760-770.

Soboll, G., Whalley, J.M., Koen, M.T., Allen, G.P., Fraser, D.G., Macklin, M.D., Swain, W.F., Lunn, D.P., 2003, Identification of equine herpesvirus-1 antigens recognized by cytotoxic T lymphocytes. J Gen Virol 84, 2625-2634.

Soboll Hussey, G., Ashton, L.V., Quintana, A.M., Lunn, D.P., Goehring, L.S., Annis, K., Landolt, G., 2014a, Innate immune responses of airway epithelial cells to infection with equine herpesvirus-1. Vet Microbiol 170, 28-38.

Soboll Hussey, G., Ashton, L.V., Quintana, A.M., Van de Walle, G.R., Osterrieder, N., Lunn, D.P., 2014b, Equine herpesvirus type 1 pUL56 modulates innate responses of airway epithelial cells. Virology 464-465, 76-86.

Stokes, A., Allen, G.P., Pullen, L.A., Murray, P.K., 1989, A hamster model of equine herpesvirus type 1 (EHV-1) infection; passive protection by monoclonal antibodies to EHV-1 glycoproteins 13, 14 and 17/18. J Gen Virol 70 (Pt 5), 1173-1183.

Talloczy, Z., Virgin, H.W.t., Levine, B., 2006, PKR-dependent autophagic degradation of herpes simplex virus type 1. Autophagy 2, 24-29.

Telford, E.A., Watson, M.S., McBride, K., Davison, A.J., 1992, The DNA sequence of equine herpesvirus-1. Virology 189, 304-316.

Telford, E.A., Watson, M.S., Perry, J., Cullinane, A.A., Davison, A.J., 1998, The DNA sequence of equine herpesvirus-4. J Gen Virol 79 (Pt 5), 1197-1203.

Thomson, G.R., Mumford, J.A., Campbell, J., Griffiths, L., Clapham, P., 1976, Serological detection of equid herpesvirus 1 infections of the respiratory tract. Equine Vet J 8, 58-65.

Umbach, J.L., Kramer, M.F., Jurak, I., Karnowski, H.W., Coen, D.M., Cullen, B.R., 2008, MicroRNAs expressed by herpes simplex virus 1 during latent infection regulate viral mRNAs. Nature 454, 780-783.

Van de Walle, G.R., Favoreel, H.W., Nauwynck, H.J., Pensaert, M.B., 2003, Antibody-induced internalization of viral glycoproteins and gE-gI Fc receptor activity protect pseudorabies virus-infected monocytes from efficient complement-mediated lysis. J Gen Virol 84, 939-948.

Van de Walle, G.R., Sakamoto, K., Osterrieder, N., 2008, CCL3 and viral chemokine-binding protein gg modulate pulmonary inflammation and virus replication during equine herpesvirus 1 infection. J Virol 82, 1714-1722.

van der Meulen, K., Caij, B., Pensaert, M., Nauwynck, H., 2006, Absence of viral envelope proteins in equine herpesvirus 1-infected blood mononuclear cells during cell-associated viremia. Vet Microbiol 113, 265-273.

von Einem, J., Schumacher, D., O'Callaghan, D.J., Osterrieder, N., 2006, The alpha-TIF (VP16) homologue (ETIF) of equine herpesvirus 1 is essential for secondary envelopment and virus egress. J Virol 80, 2609-2620.

von Einem, J., Wellington, J., Whalley, J.M., Osterrieder, K., O'Callaghan, D.J., Osterrieder, N., 2004, The truncated form of glycoprotein gp2 of equine herpesvirus 1 (EHV-1) vaccine strain KyA is not functionally equivalent to full-length gp2 encoded by EHV-1 wild-type strain RacL11. J Virol 78, 3003-3013.

Weir, J.P., 2001, Regulation of herpes simplex virus gene expression. Gene 271, 117-130.

Williams, L.R., Taylor, G.S., 2012, Autophagy and immunity - insights from human herpesviruses. Front Immunol 3, 170.

Wu, J., Chen, Z.J., 2014, Innate immune sensing and signaling of cytosolic nucleic acids. Annu Rev Immunol 32, 461-488.

Yokota, S., Yokosawa, N., Okabayashi, T., Suzutani, T., Miura, S., Jimbow, K., Fujii, N., 2004, Induction of suppressor of cytokine signaling-3 by herpes simplex virus type 1 contributes to inhibition of the interferon signaling pathway. J Virol 78, 6282-6286.

Zhao, Y., Holden, V.R., Smith, R.H., O'Callaghan, D.J., 1995, Regulatory function of the equine herpesvirus 1 ICP27 gene product. J Virol 69, 2786-2793.

CHAPTER 2

Major histocompatibility complex class I downregulation induced by equine herpesvirus type 1 pUL56 is through dynamin-dependent endocytosis

Teng Huang[a], Maik J. Lehmann[b], Abdelrahman Said[a,c], Guanggang Ma[a,] Nikolaus Osterrieder[a]

[a] Institut für Virologie, Freie Universität Berlin, Zentrum für Infektionsmedizin - Robert von Ostertag-Haus, 14163 Berlin, Germany; [b] Department of Molecular Parasitology, Humboldt University, 10115 Berlin, Germany; [c] Parasitology and Animal Diseases Department, National Research Center, Dokki, Giza, Egypt

 [Journal of Virology, 2014, 88:12802-12815. doi: 10.1128/JVI.02079-14].

2.1 Summary

Equine herpesvirus type 1 (EHV-1) downregulates cell surface expression of major histocompatibility complex class I (MHC-I) in infected cells. We have previously shown that pUL56 encoded by the EHV-1 *ORF1* gene regulates the process (G. Ma, S. Feineis, N. Osterrieder, and G. R. Van de Walle, J. Virol. 86:3554-3563, 2012, doi:10.1128/JVI.06994-11). Here, we report that cell surface MHC-I in EHV-1-infected cells is internalized and degraded in the lysosomal compartment in a pUL56-dependent fashion. pUL56-induced MHC-I endocytosis required dynamin and tyrosine kinase but was independent of clathrin and caveolin-1, the main constituents of clathrin- and raft/caveolae-mediated endocytosis pathways, respectively. Downregulation of cell surface MHC-I was significantly inhibited by the ubiquitin-activating enzyme E1 inhibitor PYR41, indicating that ubiquitination is essential for the process. Finally, we show that downregulation is not specific for MHC-I and that other molecules, including CD46 and CD63, are also removed from the cell surface in a pUL56-dependent fashion.

2.2 Introduction

To achieve productive infection in host cells, viruses have evolved strategies to evade the recognition by the host immune system. Immunity mediated by cytotoxic $CD8^+$ T lymphocytes (CTLs) is of critical importance in the defense against cell-associated pathogens (Wong and Pamer, 2003). CTLs interact with major histocompatibility complex class I (MHC-I), onto which antigenic peptides are loaded in the endoplasmic reticulum (ER). MHC-I molecules mature while trafficking through the ER and Golgi network before they

eventually reach the cell surface (Peaper and Cresswell, 2008). Presentation of antigenic peptides derived from viruses and other nonself proteins results in specific sensing by CTLs and ultimate elimination of (infected) cells displaying such peptides. However, a number of viral proteins target the MHC-I antigen presentation pathway, resulting in the downregulation of cell surface MHC-I and immune evasion (Fruh et al., 1999; Lilley and Ploegh, 2005).

The adenovirus E3-19K was the first identified viral protein shown to block antigen presentation by MHC-I (Burgert and Kvist, 1985). Later, a number of MHC-I downregulators in the *Herpesviridae* were identified, with ICP47 of herpes simplex virus type 1 (HSV-1) being the first. ICP47 is a cytoplasmic protein that prevents transport of proteasome-generated peptides into the ER through irreversible blockade of the transporter associated with antigen processing (TAP) (Fruh et al., 1995; Hill et al., 1995). Other alphaherpesviruses also encode proteins that reduce the expression of surface MHC-I. Recently, the central role of pUL49.5 in interfering with MHC-I assembly and transport was characterized for pseudorabies virus (PRV), bovine herpesvirus type 1 (BHV-1) and equine herpesvirus type 1 (EHV-1) and type 4 (EHV-4). This ER-resident membrane protein also inhibits TAP activity and delays maturation of MHC-I, because in the absence of antigenic peptides, the tri-molecular complex (MHC-I heavy chain, β2-miroglobulin and peptide) cannot be properly assembled (Koppers-Lalic et al., 2005; Koppers-Lalic et al., 2008).

As a member of the genus *Varicellovirus*, EHV-1 is an important pathogen that threatens horse populations worldwide. EHV-1 infection is characterized by upper respiratory disease, neurological disorders and abortion in pregnant mares (Ma et al., 2013). It has been known that CTL-based immunity confers protection against EHV-1-induced abortion in mares (Kydd et al., 2003). However, EHV-1 subverts this host defense mechanism by reducing cell surface MHC-I, which may provide an explanation why vaccination has failed to provide satisfactory protection against infection and also clinical disease. Studies have shown that MHC-I downregulation caused by EHV-1 might be associated with endocytosis and mediated by the expression of an early viral gene(s) (Rappocciolo et al., 2003). Recently, we identified pUL56 of EHV-1 as an early viral protein that plays a dominant role in this process (Ma et al., 2012). A similar function of the pUL56 homologue of EHV-4 was also reported (Said et al., 2012), suggesting that MHC-I downregulation caused by pUL56 might be evolutionarily conserved in the genus. However, the mechanism of pUL56 in downregulating cell surface MHC-I remains unknown.

In the present study, we explored the mechanism underlining pUL56-induced MHC-I downregulation in more detail. Our findings can be summarized as follows: (i) cell surface MHC-I is degraded mainly in the lysosomal compartment of infected cells; (ii) relocation of

surface MHC-I to lysosomes coincides with the expression of pUL56; (iii) internalization of cell surface MHC-I is dependent on dynamin but does not occur through clathrin- or caveolae-dependent endocytosis; (iv) pUL56-induced MHC-I downregulation requires tyrosine kinase and ubiquitination; (v) the immune cell surface markers CD46 and CD63 are additional targets of pUL56 for degradation. We therefore propose that pUL56 induces degradation of cell surface immune molecules in lysosomes through dynamin-mediated endocytosis in which ubiquitination plays a critical role.

2.3 Materials and methods

2.3.1 Cells and viruses

Rabbit kidney (RK13) cells and human HeLa cells were maintained in Earle's minimum essential medium (EMEM) supplemented with 10% heat-inactivated fetal bovine serum (FBS, Biochrom AG), 100 U/ml penicillin and 0.1 mg/ml streptomycin (1% Pen/Strep, Sigma). The equine skin fibroblast cell line NBL6 (ATCC) was maintained in Iscove's modified Dulbecco's medium (Invitrogen) supplemented with 10% FBS, 1% non-essential amino acids (Biochrom AG), and 1% Pen/Strep. RK13 cells were used to propagate and titrate all the viruses in this study.

EHV-1 strain Ab4, constructed previously as a bacterial artificial chromosomes (BAC) by insertion of a mini-F sequence in place of the gp2-encoding gene 71 (Goodman et al., 2007), and mutants derived thereof were used in this study. The pAb4 BAC was maintained in *Escherichia coli* GS1783 (a gift from Greg Smith, Northwestern University, Chicago, IL) and BAC-reconstituted viruses vAb4G and its *ORF1* deletion mutant, vAb4GΔ1, were described previously (Ma et al., 2012). vAb4G and vAb4GΔ1 both express enhanced green fluorescent protein (EGFP) and allow rapid identification of virus-infected cells. Based on vAb4G and vAb4GΔ1, vAb4 and vAb4Δ1 were generated, in which mini-F sequences containing *egfp* genes were removed and expression of gp2 was restored (Ma et al., 2012).

To generate Ab4-dsRed2, *egfp* in the mini-F vector sequence of pAb4 was replaced with the *dsRed2* gene using two-step Red-mediated recombination (Tischer et al., 2006). Briefly, a kanamycin resistance gene (*kan*) with an I-*Sce*I restriction site upstream was amplified using primer pair dsRed2-kan Fw/Rv (Table 2.1) and cloned into the *Bst*XI site within the *dsRed2* gene present in plasmid pdsRed2-N1 (Clontech). Using primers dsRed2-ep Fw/Rv (Table 2.1), the entire cassette was amplified by PCR, and the product was electroporated into GS1783 cells harboring pAb4. After the first Red recombination, kanamycin-resistant colonies were screened by restriction fragment analysis. In the second round of Red recombination, the *kan* gene was excised and the resolved clones were analyzed by PCR, sequencing and restriction

fragment analysis. The final construct was transfected into RK13 cells to obtain the recombinant virus Ab4-dsRed2.

2.3.2 Antibodies

Anti-MHC class I monoclonal antibody (MAb) H58A (mouse anti-human MHC class I MAb) was purchased from VMRD. Rabbit anti-EHV-1 pUL56 polyclonal antibodies (PAbs) were designed and produced by GenScript Corporation (NJ, USA) (Ma et al., 2012). Rabbit antiserum for EHV-1 IR6 was prepared in previous study (O'Callaghan et al., 1994). A β-actin (13E5) rabbit MAb was obtained from Cell Signaling Technologies. Rabbit PAbs against the hemagglutinin (HA) epitope, LAMP-1 and caveolin-1 were obtained from Abcam. Mouse anti-human CD46 and CD63 MAbs were from BioLegend. Mouse anti-human CD58, CD59, and CD95 MAbs were purchased from Genway Biotech. Alexa Fluor 647-conjugated goat anti-mouse IgG, Alexa Fluor 488-conjugated goat anti-rabbit IgG, and Alexa Fluor 568-conjugated goat anti-mouse IgG were from Invitrogen, while horseradish peroxidase (HRP)-labeled goat anti-rabbit IgG was from Southern Biotech.

Table 2.1 Oligonucleotides used for plasmid construction

Primer name	Sequence (5'-3') [a]
DsRed2-kan Fw	ATCGTACCCATCTACATGGCCAAGAAGCCCGTGC**TAGGGATA ACAGGGTAATCGAT**
DsRed2-kan Rv	AAGCTGTCCATGTAGATGGACTTGAACTCCA**CCACCAGTGT TACAACCAATTAACC**
DsRed2-ep Fw	TAGTGAACCGTCAGATCCGCTAGCGCTACCGGTCGCCACC ATGGCCTCCTCCGAGAACGT
DsRed2-ep Rv	GTAAAACCTCTACAAATGTGGTATGGCTGATTATGATCAG CTACAGGAACAGGTGGTGGC
Cav1 Fw	GATCAAGCTTATGTCTGGGGGCAAATACGT
Cav1 Rv	CGCGGATCCCG*AGCGTAGTCTGGGACGTCGTATGGGTA*TATTTC TTTCTGCAGGTTGA
Cav1Y14F Fw	GATCAAGCTTCGATGTCTGGGGGCAAATACGTGGACTCCGAG GGACATCTC***TTC***ACGGTTCCCATCCGGGAACA

[a] Underlined letters indicate restriction sites; bold letters indicate annealing sequences targeting kanamycin; italic letters indicate HA tag sequences; bold italic letters indicate the point mutation corresponding to the 14th amino acid residue of caveolin-1.

2.3.3 Pharmacological inhibitors and flow cytometry

All pharmacological inhibitors used in this study were purchased from Sigma and dissolved in either water or DMSO depending on the drug and the recommendation of the supplier. The drug concentrations used were 5 μM lactacystin, 150 μM chloroquine, 10 mM ammonium

chloride (NH_4Cl), 0.1 to 2 μM bafilomycin A1, 2 to 80 μM dynasore, 0.5 to 10 μg/ml chlorpromazine, 2 to 50 μg/ml genistein, 1 to 5 μg/ml filipin, 2 and 20 μg/ml nystatin, 10 and 20 mM methyl-β-cyclodextrin (MβCD), 5 μM and 10 μM PYR41. Pitstop2 was dissolved in DMSO and used at 5 μM and 10 μM, and Pitstop2-Neg (10 μM) was used as a negative control (Pitstop2 and Pitstop2-Neg were kindly provided by Volker Haucke, MDC Berlin-Buch, Germany) (von Kleist et al., 2011). The biological functions of each inhibitor are summarized in Table 2.2. To examine the effect of drugs on MHC-I surface expression after EHV-1 infection, NBL6 cells were infected with vAb4G at a multiplicity of infection (MOI) of 5. After 2 h of incubation, virus was removed, and fresh medium containing different concentrations of drugs was added. After 4 h of inhibition, cells were trypsinized and washed twice with 1X phosphate-buffered saline (PBS) containing 2.5% FBS. Cell surface MHC-I was stained with H58A MAb (1/100), followed by incubation with Alexa Fluor 647-conjugated goat anti-mouse IgG (1/500), and analyzed immediately using a FACSCalibur flow cytometer (Becton-Dickinson). For each sample, at least 10,000 cells were recorded. To stain both cell surface and intracellular MHC-I (total MHC-I), cells were fixed in 3.5% paraformaldehyde (PFA) for 10 min before incubation with antibodies in buffer containing 0.02% saponin (Sigma). Cell death was examined in parallel by staining the cells with propidium iodide (PI). When samples were analyzed in a three-color detection mode, compensation between two contiguous channels was adjusted to subtract the spillover background, as the manufacturer's instructions suggest (BD Biosciences). MHC-I levels are presented as mean fluorescence intensities unless stated otherwise. At least three independent experiments were performed for each treatment condition

Table 2.2 Summary of inhibitors and their effects on recovery of MHC-I

Inhibitor	Targeted pathway	Concen(s)	Specificity	Recovery of MHC-I[a]
Lactacystin	*Proteasome*[b]	5 μM	Inhibition of proteasome activities by modifying threonine residual	-
	Endocytosis[b]			
Chloroquine	Lysosome	150 μM	Induction of lysosomotropic pH elevation to prevent subsequent fusion of endosomes	++
Ammonium chloride	Lysosome	10 mM	Neutralizing the low pH step required for the progression of lysosome	++
Bafilomycin A1	Lysosome	0.1, 0.5, 2 μM	Potent inhibition of acidification by blocking vacuolar proton pump	+
Dynasore	Dynamin-mediated	2, 20, 80 μM	Interference with the GTPase activity of the dynamin family	+
Chlorpromazine	Clathrin-mediated	0.5, 2, 10 μg/ml	Reshuffling of clathrin and its adaptor protein in the endocytic route	-
Pitstop2	Clathrin-mediated	5, 10 μM	Reversible competition for the clathrin-box binding site in terminal domain	-
Genistein	Clathrin-independent	2, 10, 50 μg/ml	Tyrosin-kinase inhibitor that disrupts the actin network of endocytic site	+
Filipin	Clathrin-independent	1, 2, 3, 5 μg/ml	Selectively bound to constitutive cholesterol in caveolae structure	+
Nystatin	Caveolae-mediated	2, 20 μg/ml	Sequestration of sterol embeded in lipid bilayers	-
Methyl-β-cyclodextrin	Caveolae-mediated	10, 20 mM	Perturbation of lipid raft synthesis essential for caveolin-dependent endocytosis	-
PYR41	*Ubiquitination*[b]	5, 10 μM	Inhibition of ubiquitination by targeting ubiquitin-activating enzyme (E1)	+

[a] -, no significant effect; +, significant effect; ++, very significant effect. [b] Italics indicate pathways versus individual mechanisms.

.

2.3.4 Internalization assay

To determine the dynamics of MHC-I on cell surface, antibody-based surface labeling was performed as described elsewhere (Coscoy and Ganem, 2000). Briefly, mock- or virus-infected cells were incubated on ice with excess amounts (100 μg/ml) of MAb CZ3 (kindly provided by Douglas F. Antczak, Cornell University, USA). After 30 min of gentle rocking, cells were washed with ice-cold PBS three times to remove unbound MAb, and the incubation temperature was shifted to 37^{o}C. At different time points, cells were returned to 4^{o}C and harvested. Following incubation with Alexa Fluor 647-conjugated goat anti-mouse IgG (1/500) for 30 min, cells were analyzed by flow cytometry.

2.3.5 Dominant-negative plasmids

EGFP-tagged wild-type (WT) dynamin (DynII) and dominant-negative (DN) dynamin (DynII) constructs were kindly provided by Mark A. McNiven (Mayo Clinic, Rochester, MN, USA) (Cao et al., 2000). EGFP-tagged DN Eps15 (DIII) and a control construct (DIIIΔ2) were obtained from Alexandre Benmerah (Hôpital Necker-Enfants Malades, Paris, France) (Benmerah et al., 1998). An EGFP-fused WT and DN form of equine caveolin-1 (Cav1) were generated. Briefly, total RNA was extracted from NBL6 cells, and cDNA was obtained using RevertAid H minus reverse transcriptase (Fermentas) and an oligo(dT) primer. WT Cav1 with a HA tag at the C terminus was PCR amplified using the forward primer Cav1 Fw and the reverse primer Cav1 Rv (Table 2.1). The PCR product was digested with *Hind*III and *Bam*HI and cloned into pEGFP-N1 vector (Clontech) to generate pCav1-EGFP. To obtain the DN form of Cav1, PCR was performed using primer Cav1Y14F Fw (Table 2.1) and Cav1 Rv, which introduced an amino acid substitution (tyrosine 14 to phenylalanine: [Y14F]) while maintaining the C-terminal HA tag. The PCR product was cloned into pEGFP-C1 (Clontech), resulting in pEGFP-Cav1(Y14F). Correct insertion of the genes into recombinant plasmids were confirmed by DNA sequencing. The expression of recombinant Cav1-EGFP and EGFP-Cav1(Y14F) was confirmed by Western blotting using the protocol described below.

To verify the biological functions of the caveolin-1 constructs, they were electroporated into NBL6 cells. Electroporation was performed using cuvettes with a 4-mm electrode gap and the GenePulser Xcell (Bio-Rad) with the following settings: 260 V, 1,050 μF and 335 Ω (Stroh et al., 2010). Electroporated cells were resuspended in fresh medium and incubated for 24 h, after which the cells were washed twice with EMEM and kept at 4^{o}C for 30 min in the presence of 0.5 μg/ml Alexa Fluor 647-conjugated cholera toxin B (CTxB) (Invitrogen). Cells were then shifted to 37°C and incubated for 15 min, followed by treatment with citrate-buffered saline (CBS, pH 3.0) for 1 min to remove the unabsorbed remnant of CTxB on the cell surface. After washing with 1X PBS, cells were fixed with 3.5% paraformaldehyde and

inspected with a Zeiss LSM 510 confocal microscope.

To examine whether the DN constructs inhibit pUL56-induced MHC-I downregulation, NBL6 cells were electroporated with either the WT or the DN construct. Twenty-four hours post-transfection, cells were infected with Ab4-dsRed2 at an MOI of 3. At 5 h post-infection (p.i.), cells were trypsinized and cell surface MHC-I was detected by MHC-I MAb H58A and Alexa Fluor 647-labeled goat anti-mouse IgG using a FACSCalibur flow cytometer. Cell surface MHC-I expression was determined in cells that had been gated for both EGFP and DsRed2 positivity after compensation.

2.3.6 Western blot analyses

To determine the expression kinetics of pUL56, NBL6 cells were infected with vAb4G or vAb4GΔ1 at an MOI of 5 and incubated at 37°C for 1h, and then the cells were treated with CBS for 3 min to deactivate remaining virus on the cell surface. Cells were washed twice with 1X PBS, and cells were collected at different times p.i. (0.5, 1, 1.5, 2, 2.5, 3, 4 and 6 h p.i.) by trypsinization and lysed with radioimmunoprecipitation assay (RIPA) buffer (20 mM Tris, pH 7.5; 150 mM NaCl; 1% Nonidet P-40; 0.5% sodium deoxycholate; 0.1% SDS) containing a protease inhibitor cocktail (Roche) and benzonase (Novagen). After separation by 12% sodium dodecyl sulfate (SDS)-polyacrylamide gel electrophoresis (PAGE) under reducing conditions, proteins were transferred to polyvinylidene fluoride (PVDF) membranes using the semi-dry method as previously described (Ma et al., 2012). After blocking with 5% nonfat dry milk in 1X PBS-T (PBS with 0.05% [vol/vol] Tween 20), the membrane was incubated with pUL56 PAbs (1/500), followed by HRP-labeled goat anti-rabbit IgG. Reactive bands were visualized by enhanced chemoluminescence (ECL plus, GE Health Care).

To verify the expression of recombinant caveolin-1, plasmids pCav1-EGFP and pEGFP-Cav1(Y14F) were transfected into NBL6 cells by electroporation. At 48 h after transfection, cells were lysed and analyzed by Western blotting using rabbit anti-HA PAb.

2.3.7 Indirect immunofluorescence

NBL6 cells were grown on coverslips coated with 0.5 mg/ml collagen A (Biochrom AG) in double-distilled water (ddH_2O) (pH 3.5) and infected with vAb4 at an MOI of 5. At different times p.i., cells were fixed with 3.5% PFA for 5 min at room temperature (RT), followed by permeabilization with 0.1% saponin. After blocking with 3% bovine serum albumin (BSA) in 1X PBS for 1 h, cells were incubated with a mixture of mouse anti-MHC-I MAb H58A (1/1,000) and rabbit anti-LAMP-1 PAb (1/1,000) or rabbit anti-pUL56 PAb (1/200) for 1 h at RT. After 3 washing steps, cells were incubated with a mixture of Alexa Fluor 568 goat

anti-mouse (1/1,000) and Alexa Fluor 488 goat anti-rabbit IgG (1/1,000) for 1 h at RT. After the washes, coverslips were mounted and inspected using a Zeiss LSM 510 confocal microscope. To quantify colocalization, correlation analysis using PSC, a plugin for ImageJ (http://www.cpib.ac.uk/tools-resources/software/psc-colocalization-plugin) was applied. Areas of interest were analyzed according to the program instructions with a threshold setting at 40. The calculations are presented as Pearson and Spearman correlation coefficients. The Pearson coefficient accounts for the linear relationship between the green and the red channel, whereas the Spearman coefficient describes the non-linear relationship. For both measurements, the degree of overlap of pixels is associated with values from 0 to 1, where 0 indicates that there is no overlap of pixels and 1 indicates complete overlap.

2.4 Results

2.4.1 Cell surface MHC-I in EHV-1-infected cells is redirected to and degraded in the lysosomal compartment

It was proposed that downregulation of MHC-I in EHV-1-infected cells might occur through accelerated endocytosis (Rappocciolo et al., 2003), but the evidence was circumstantial. We sought to address the question of whether surface MHC-I molecules are indeed internalized and where they are re-directed. First, we asked whether pUL56 accelerates endocytosis of MHC-I by internalization assays that labeled MHC-I on the cell surface with the CZ3 antibody. A decrease of MHC-I levels was observed at 4 h p.i. in cells infected with vAb4G or vAb4GΔ1 virus, but internalization was significantly slower in cells infected with vAb4G lacking pUL56 than in vAb4G-infected cells ($P < 0.05$) (Fig. 2.1A). We concluded that pUL56 indeed plays a role in MHC-I internalization, and we next began to explore possible endocytic processes that may be responsible for MHC-I downregulation. We started with assessing the role of the proteasome in MHC-I turnover by using the proteasome inhibitor lactacystin. In vAb4G-infected NBL6 cells, both surface and total MHC-I expression was dramatically downregulated at 6 h p.i. With lactacystin treatment, a slight increase of cell surface MHC-I expression in infected cells was observed, while total MHC-I was still detected at low levels that were comparable to those determined in the absence of the inhibitor ($P > 0.05$) (Fig. 2.1B). This result suggested that the proteasome is not responsible for MHC-I degradation in EHV-1-infected cells.

Lysosomes are responsible for the disposal of many internalized cell surface proteins (Luzio et al., 2007). We speculated that MHC-I from the plasma membrane may be rerouted to lysosomes and degraded in these organelles. To test our hypothesis, chloroquine and ammonium chloride, drugs known to impair lysosomal function, were used. Both drugs are basic compounds that neutralize vesicular transition from endosome to lysosome (Dutta and

Donaldson, 2012; Fredericksen et al., 2002). By inactivating lysosomal function, we found that cell surface MHC-I was still dramatically downregulated after infection, but total MHC-I levels were restored to those seen in uninfected cells (Fig. 2.1B), indicating that MHC-I is indeed internalized and degraded in this compartment in EHV-1-infected cells. We also examined the effect of bafilomycin A1, an inhibitor of vacuolar H^+-ATPase that retards the maturation of early endosomes (Drose and Altendorf, 1997). This endocytic inhibitor also

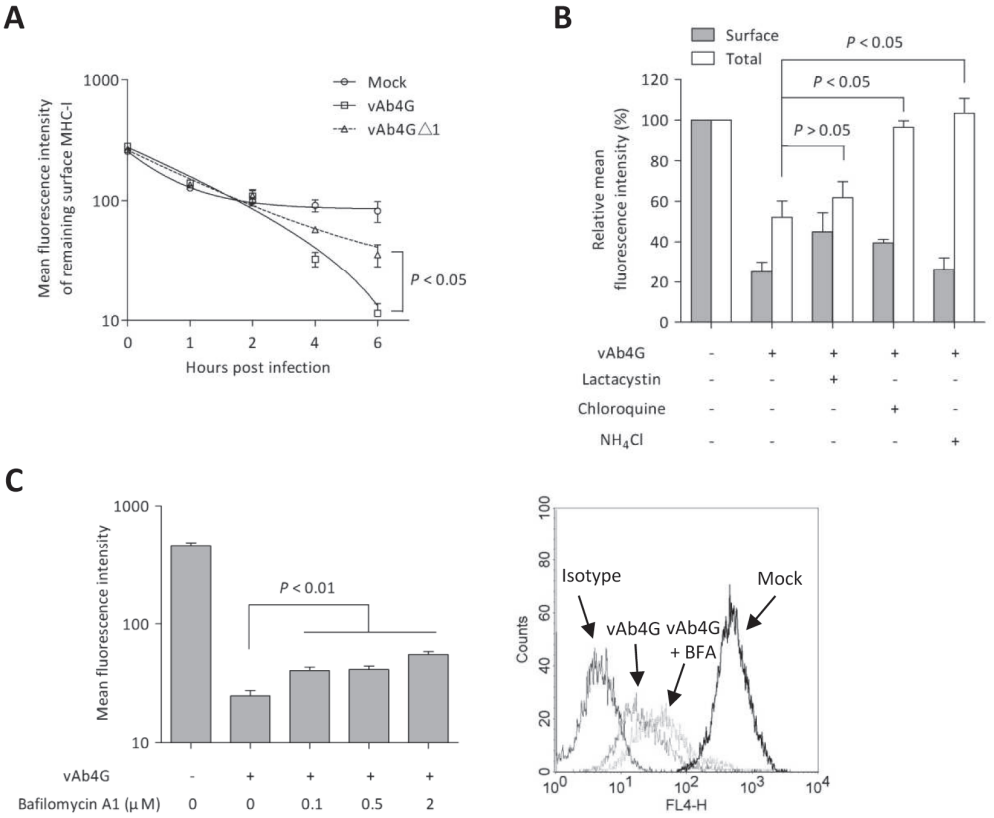

Figure 2.1 Cell surface MHC-I in EHV-1 infected cells is degraded in lysosomes. NBL6 cells were mock infected, or infected with vAb4G or vAb4GΔ1 at an MOI of 5**. (A)** Cells were incubated on ice for 30 min with excess amounts of MAb CZ3 directed against equine MHC-I. At 0, 1, 2, 4, 6 h p.i., cells were stained with Alexa Fluor 647-conjugated goat anti-mouse IgG and subjected to analyses using flow cytometry. The trend curves were fitted based on a logarithmic non-linear regression model. **(B)** Cells were incubated with the pharmacological inhibitors or 0.1% DMSO as a control. At 6 h p.i., cells were trypsinized and harvested. Monoclonal antibody against MHC-I (H58A) was used to detect cell surface expression of MHC-I. After fixation and permeablization, total MHC-I levels were assessed. **(C)** Bafilomycin A1 counteracted the MHC-I downregulation induced by viral infection. Infected cells were treated with the inhibitor at concentrations of 0.1, 0.5 and 2.0 μM, respectively. After 4 h of inhibition, cells were collected and analyzed by flow cytometry. A representative histogram for bafilomycin A1 (BFA) treatment at 2 μM is shown. The data are means ± standard deviation (error bars) from at least three independent experiments. A *P* value of <0.05 indicates a statistically significant difference as determined by one-way analysis of variance (ANOVA).

mitigated the effect of virus infection on the levels of cell surface MHC-I significantly ($P < 0.05$) (Fig. 2.1C). Overall, the results with the inhibitors clearly demonstrated that endocytosis and lysosomal degradation play a central role in governing the turnover of MHC-I in EHV-1-infected cells.

2.4.2 Trafficking of MHC-I molecules into lysosome depends on the expression of pUL56

EHV-1 encodes pUL49.5, a type I transmembrane protein that blocks TAP-mediated peptide transport into the ER lumen, where the MHC-I complex is retained as a consequence of the absence of antigenic peptides. With respect to MHC-I downregulation, pUL49.5 and pUL56 are functionally independent (Said et al., 2012), suggesting that pUL56 likely targets an alternative pathway to prevent MHC-I presentation. To examine whether pUL56 facilitates lysosomal proteolysis, we recorded the co-localization of MHC-I with lysosomes in a time course experiment by confocal laser scanning microscopy (CLSM). LAMP-1 (lysosome-associated membrane protein 1) was used as a marker to label the lysosomal compartment. At 3 h p.i., MHC-I molecules appeared in the form of vesicles, and co-localization of MHC-I with LAMP-1 was evident (Fig. 2.2A, top). At 4 h p.i., more MHC-I reactivity was apparent in LAMP-1-containing vesicles, which also seemed to accumulate at the periphery of the nucleus (Fig. 2.2A, middle). In contrast, infection with the pUL56-negative mutant did not affect the distribution of LAMP-1 in the cytoplasm, and accumulation of MHC-I could not be observed (Fig. 2.2A, bottom). These findings indicated that degradation of MHC-I is associated with pUL56 expression and redistribution of lysosomal vesicles.

To further assess the relationship between lysosomal degradation of MHC-I and expression of pUL56, co-localization of MHC-I with pUL56 was examined by CLSM. At 3 h p.i., co-localization of MHC-I and pUL56 was apparent (Fig. 2.2B, top). At 4 h p.i., vesicles that were specifically reactive with the H58A anti-MHC-I and the pUL56 antibodies predominantly clustered in the vicinity of the nucleus (Fig. 2.2B, middle), whereas no conspicuous relocalization of MHC-I was triggered in the absence of pUL56 (Fig. 2.2B, bottom). The early expression of pUL56 in vAb4-infected NBL6 cells was confirmed by Western blot analyses. Consistent with our previous report (Ma et al., 2012), pUL56 was detectable as early as 2 h p.i. With the progress of infection, pUL56 appeared as differently phosphorylated moieties that had increased apparent molecular masses (Fig. 2.2C). Higher pUL56 expression levels were detected from 4 h p.i., a time when dramatic downregulation of MHC-I on the surface of in fected cells was observed (Fig. 2.1A).Based on the co-localization and expression kinetics data, we surmised that pUL56 is abundantly produced at early times of infection, which allows rapid internalization of surface MHC-I and its subsequent degradation in the lysosomal compartment.

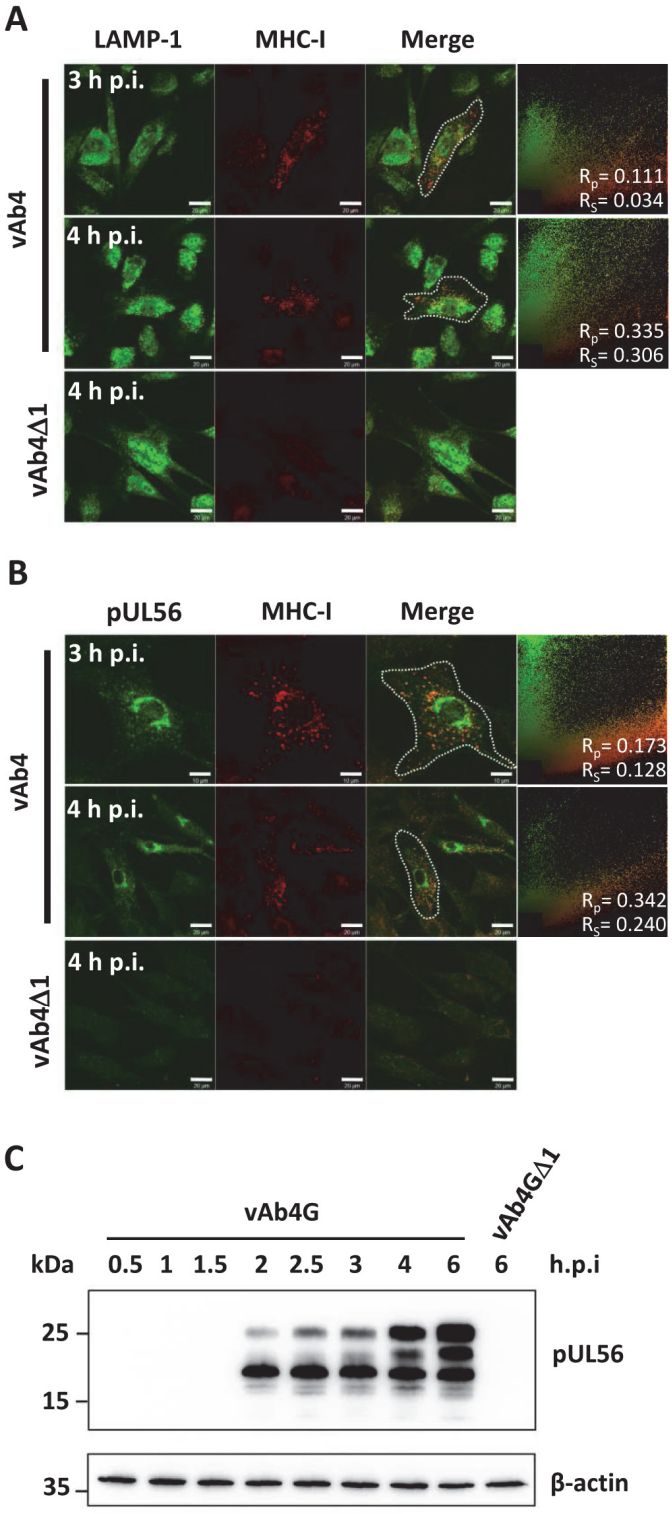

Figure 2.2 Engulfment of MHC-I molecules is associated with pUL56 expression and followed by lysosomal degradation. (A) Trafficking of MHC-I into the lysosomal vesicles in the presence of pUL56. Lysosome-associated membrane protein 1 (LAMP1; green) co-localizes with MHC-I (red). Bars, 20 μm. **(B)** pUL56 (green) and MHC-I (red) co-localize in vAb4-infected cells, while vAb4Δ1 virus deficient in *ORF1* is unable to trigger internalization and aggregation of MHC-I. All images were captured by confocal fluorescence microscopy. The top panels were inspected using 63X objective. Bars, 10 μm (top) and 20 μm (middle and bottom). Areas for quantitative co-localization analysis were masked with dotted curves. The results are shown in scatter plots, and the Pearson correlation coefficient (R_p) and Spearman correlation coefficient (R_s) are given. Higher values of R_p and R_s indicate stronger colocalization of two proteins. **(C)** Early expression profile of pUL56 in infection. vAb4G and vAb4GΔ1 at an MOI of 5 were used to infect NBL6 cells, and whole-cell lysates were extracted at the indicated times p.i. After separation using SDS-12% PAGE, proteins were transferred to PVDF membranes and then probed with the pUL56 PAbs. β-actin served as a gel-loading control. Molecular mass (kDa) was established by PageRuler Plus from Thermo Scientific.

2.4.3 Dynamin-mediated endocytosis is involved in cell surface depletion of MHC-I

Prior to the formation of endosomal vesicles, dynamin is integral in the formation of the invagination structure that ultimately leads to membrane abscission (Doherty and McMahon, 2009). We confirmed the role of dynamin in MHC-I downregulation by chemical interference and the use of dominant-negative molecules, respectively. Dynasore is a synthetic inhibitor that specifically targets the GTPase domain and is commonly used to block dynamin-dependent endocytosis (Macia et al., 2006). At low concentrations of dynasore, levels of cell surface MHC-I were largely unaffected in infected cells; however, they were restored at higher concentrations of the drug. This effect was particularly apparent when cells were incubated in the presence of 80 μM dynasore (Fig. 2.3A).

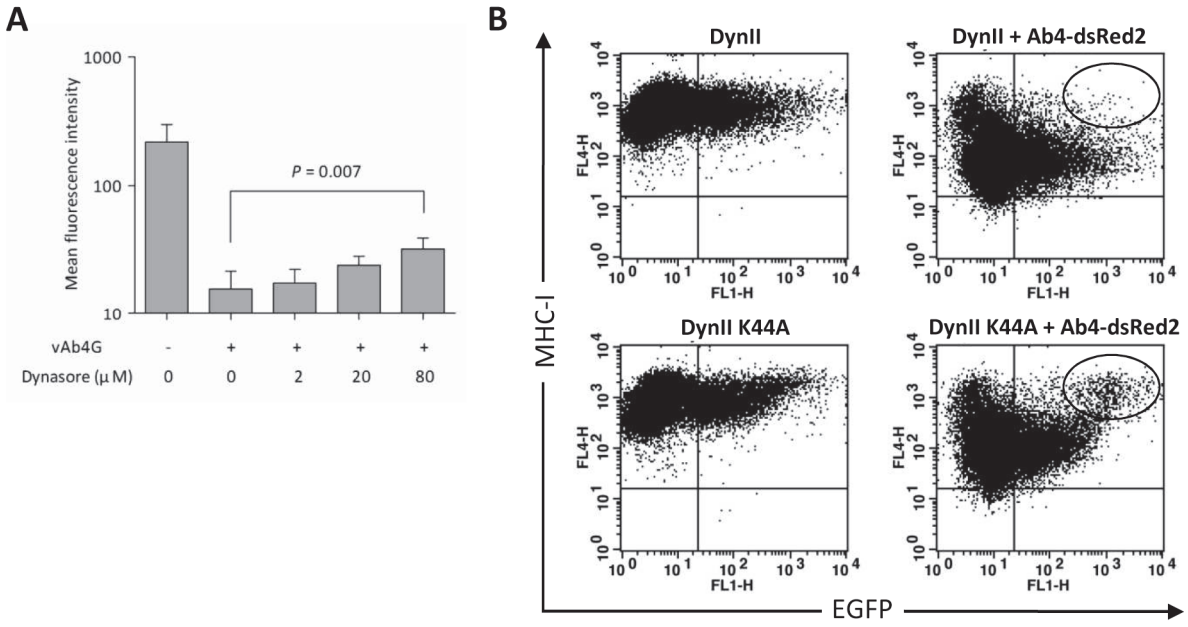

Figure 2.3 Dynamin-mediated endocytosis regulates cell surface MHC-I. (A) After entry of vAb4G into NBL6 cells, incubation was continued in the presence of increasing amounts of dynasore (2, 20 and 80 μM). Statistical significance was analyzed using one-way ANOVA. **(B)** NBL6 cells were transfected with WT dynamin (DynII; top) or its DN mutant (DynII-K44A; bottom), both of which are EGFP-tagged. Twenty-four hours after transfection, cells were infected with the Ab4-dsRed2 virus. At 5 h p.i., infected cells in which dsRed2 was expressed were gated and analyzed using both EGFP (control or dominant negative) and Alexa Fluor 647 (MHC-I) filters. Differential cell populations are highlighted in ellipses. Results are representative of three replicates.

DynII-K44A conjugated with EGFP has been confirmed to specifically target dynamin-mediated endocytosis and can be used as a dominant negative form of dynamin (Cao et al., 2000). To allow dual-color fluorescence detection, an EHV-1 mutant expressing dsRed2 as a marker of infection (Ab4-dsRed2) was generated. MHC-I downregulation induced by Ab4-dsRed2 was indistinguishable from that induced by vAb4G or vAb4 (data not shown).

Before infection with Ab4-dsRed2, NBL6 cells were transfected with plasmids expressing WT (DynII) or DN (DynII-K44A) dynamin. The sizes of cell populations expressing DynII and DynII-K44A were largely identical at 24 h after transfection and no difference in cell surface MHC-I levels was observed in uninfected cells transfected with the WT or DN DynII (Fig. 2.3B, left). In infected cells (5 h p.i.), cell surface MHC-I expression was analyzed in the cell population expressing both EGFP and dsRed2. In the presence of DynII-K44A, expression of cell surface MHC-I in infected cells was clearly restored (Fig. 2.3B, right), while WT DynII had no effect. We concluded from the data that EHV-1 enhances MHC-I internalization via dynamin-mediateted endocytosis.

2.4.4 Clathrin is not required for surface MHC-I uptake

The best studied endocytic pathways include clathrin- and caveolae-mediated endocytosis. To examine which endocytic pathway is responsible for pUL56-mediated MHC-I down-regulation, the role of the clathrin-mediated endocytosis was assessed. In the first set of experiments, we used chlorpromazine, a drug commonly used for inhibiting clathrin-mediated endocytosis (Wang et al., 1993). In the presence of chlorpromazine, the levels of MHC-I on the surface of infected cells remained as low as those in cells without treatment. With higher concentrations, there was still no significant restoration of MHC-I levels (Fig. 2.4A). To further examine the role of the clathrin-dependent pathway, we included Pitstop2, a novel inhibitor that blocks clathrin-mediated endocytosis by selectively binding to the terminal domain (TD) of clathrin (von Kleist et al., 2011). Consistent with the results obtained with chlorpromazine treatment, MHC-I levels in vA4G-infected cells were not restored after treatment with Pitstop2 and were indistinguishable from those after treatment with Pitstop2-Neg (Fig. 2.4B). A dominant negative Eps15 mutant fused to EGFP has been shown to cause substantial delay of clathrin-mediated uptake processes (Benmerah et al., 1999; Benmerah et al., 1998). We included this more specific construct to corroborate our findings using the chemical inhibitors. At 24 h after transfection, approximately 40% of NBL6 cells expressed either the control (DIIIΔ2) or the dominant negative form of the protein (DIII). Expression levels of cell surface MHC-I after transfection with either construct were virtually identical (Fig. 2.4C, left). Upon infection with Ab4-dsRed2 (MOI = 3), DIII had no impact on the inhibition of MHC-I downregulation (Fig. 2.4C, right), as the levels of surface MHC-I between control cells and those treated with the DN form were not significantly different. Collectively, these results suggested that internalization of MHC-I does not rely on clathrin-mediated endocytosis.

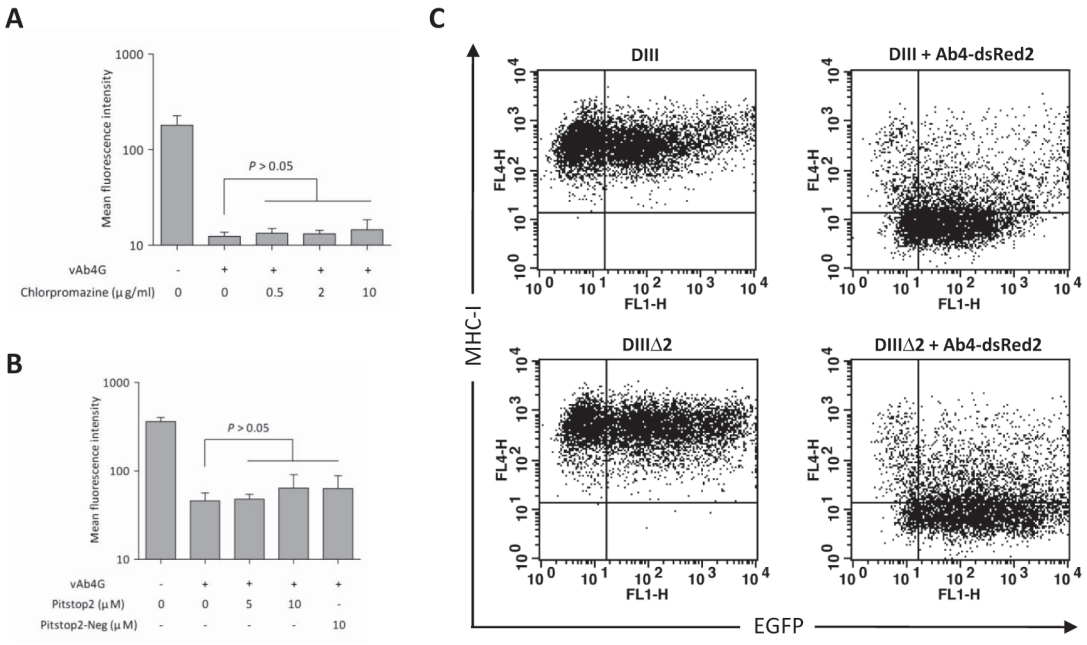

Figure 2.4 Clathrin-mediated endocytosis is not essential for MHC-I downregulation. (A) NBL6 cells were mock infected or infected with vAb4G in the presence of chlorpromazine (0.5, 2 or 10 μg/ml), an inhibitor commonly used to prevent clathrin recycling. **(B)** Infected cells were incubated with Pitstop2 at 5 μM or 10 μM. Pitstop2- Neg, a structural analogue of Pitstop2, was used as a control at 10 μM. Similar to chlorpromazine, no effects of Pitstop2 on virus-induced MHC-I downregulation were evident. One-way ANOVA was applied, and a *P* value >0.05 indicates that the difference is not significant. **(C)** Effect of the dominant negative Eps15 mutant. NBL6 cells were electroporated with equal amounts of pEGFP-DIIIΔ2 or pEGFP-DIII plasmids then cultured for 48 h. At 5 h p.i., infected cells expressing dsRed2 were gated and further examined by analyzing the mean fluorescence intensity of GFP (control or dominant negative Eps15) and Alexa Fluor 647 (MHC-I). Neither the WT nor the DN form restored the cell surface expression of MHC-I. Student's *t*-test was performed, and no statistical significance between the WT and the DN groups was seen. The dot plots are representative of three independent tests.

2.4.5 Inhibition of caveolae-mediated endocytosis does not affect internalization of MHC-I

Like clathrin-mediated endocytosis, caveolar internalization is another well characterized dynamin-dependent endocytic pathway, which is initiated by invagination of smooth patches of plasma membrane where cholesterol and sphingolipids are abundant (Nabi and Le, 2003). Numerous inhibitors have been reported to effectively block caveolar maturation, including genistein (Nabi and Le, 2003), filipin (Schnitzer et al., 1994), nystatin (Chen et al., 2011) and MβCD (Mundy et al., 2012). Treatment of cells with genistein resulted in a significant increase of cell surface MHC-I in infected cells in a dose-dependent manner (Fig. 2.5A). Therefore, we concluded that virus-mediated endocytosis of MHC-I depends on tyrosine kinase activity. We then tested the role of cholesterol in governing MHC-I internalization by

treatment with filipin. In the presence of filipin, particularly at higher concentrations, the recovery of internalized MHC-I was significantly increased compared to that in untreated cells or cells treated with lower concentrations ($P < 0.05$) (Fig. 2.5B). Thus, membrane-bound cholesterol seems to be involved in allowing the uptake of cell surface MHC-I during EHV-1 infection.

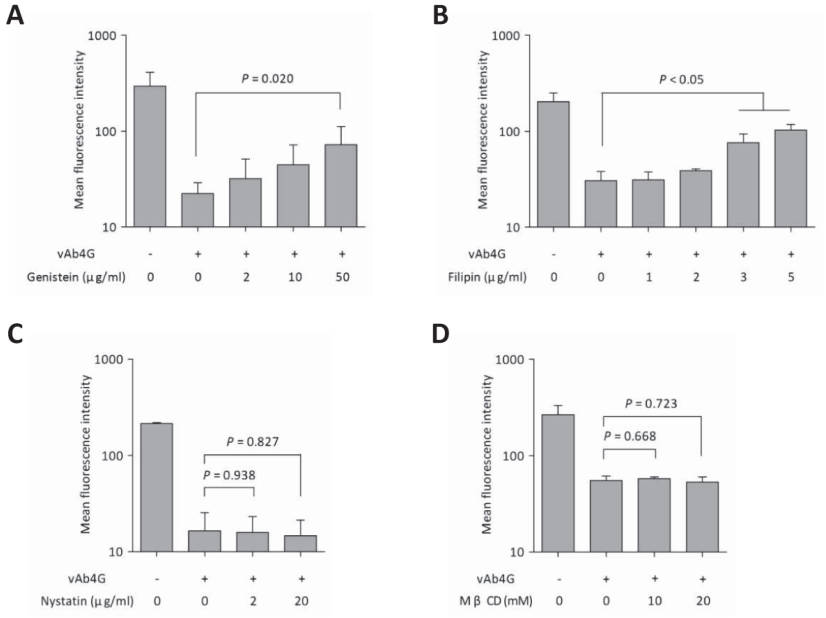

Figure 2.5 Chemical inhibition of clathrin-independent endocytic pathways. After infection with vAb4G, NBL6 cells were replenished with fresh medium containing genistein at concentrations at 2, 10, and 50 μg/ml **(A)**, filipin at 1, 2, 3, and 5 μg/ml **(B)**, nystatin at 2 and 20 μg/ml **(C)**, and methyl-β-cyclodextrin (MβCD) at 10 and 20 mM **(D)**. After 4 h of incubation, cells were processed for cell surface MHC-I labeling, and the mean fluorescence intensity of the populations was determined by flow cytometry. Values are expressed as means ± standard deviation (error bars) from at least three independent experiments. One-way ANOVA was used to analyze the statistical difference between groups.

There are multiple factors that control caveolar endocytosis and we used two additional drugs that interfere with different constituents of caveolar structures. When cells were incubated with nystatin after infection, the levels of MHC-I remained as low as those in untreated cells (Fig. 2.5C). Similarly, MβCD was unable to prevent virus-induced MHC-I downregulation in infected cells at different concentrations (Fig. 2.5D). It was not entirely surprising to see differences between the four drugs with respect to MHC-I internalization, because they have different molecular targets and interfere with different signaling pathways. Some of the drugs are known to be pleiotropic and affect other endocytic pathways as well; for example, nystatin and MβCD also interfere with the clathrin pathway (Chen et al., 2011; Vercauteren et al., 2010).

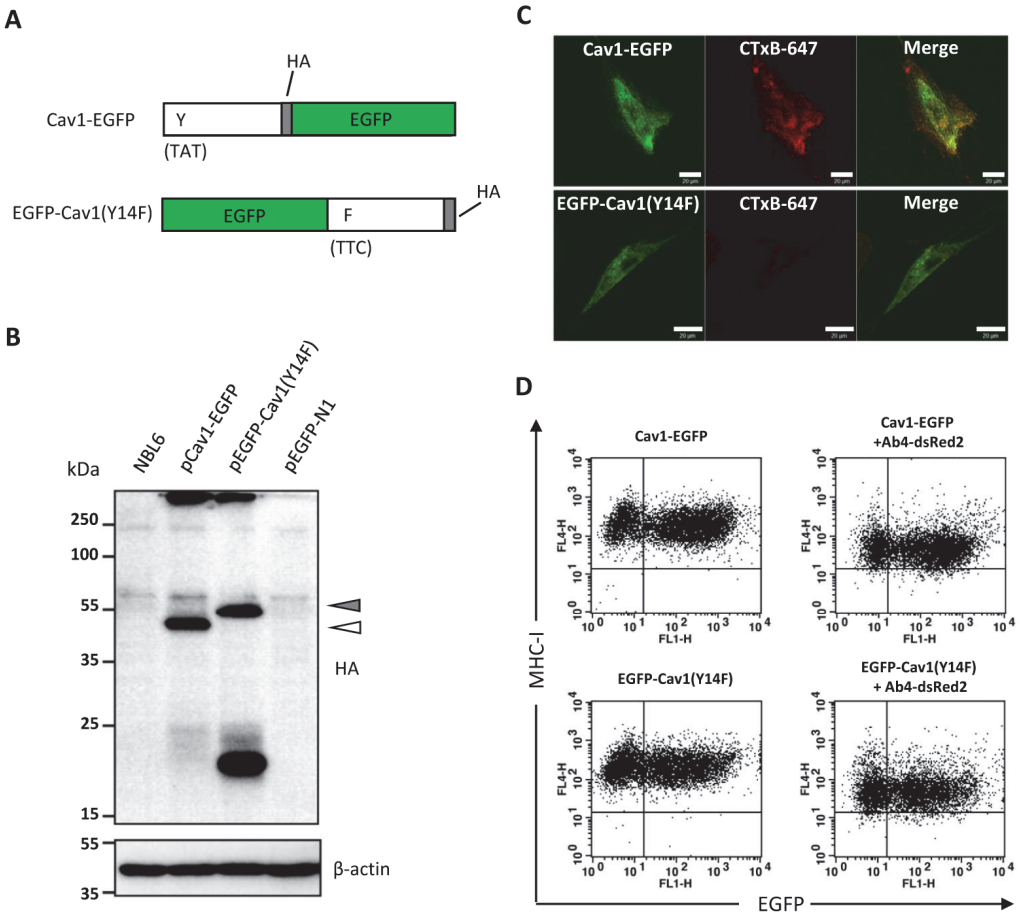

Figure 2.6 MHC-I downregulation is independent on caveolae-mediated endocytosis. **(A)** Schematic representation of the two forms of caveolin-1 used here, Cav1 (WT) and Cav1(Y14F) (DN), fused to the amino and carboxy termini of EGFP, respectively. **(B)** Expression of caveolin-1 constructs. At 48 h after transfection, whole-cell lysates were subjected to separation by SDS-12% PAGE followed by Western blot analysis. Specific bands corresponding to the WT (white triangle) or DN (gray triangle) proteins were detected using rabbit anti-HA MAb. β-actin was used as a loading control. PageRuler Plus from Thermo Scientific was run as a molecular ladder. **(C)** Inhibition of caveolae-mediated endocytosis by the DN mutant. EGFP-Cav1(Y14F) (green) effectively blocked the engulfment of cholera toxin B (CTxB), resulting in the reduced intensity of Alexa Fluor 647 (red). Bars, 20 μm. **(D)** MHC-I downregulation is not affected by expression of either the WT or the DN mutant after infection. After gating with dsRed2, the infected cells were analyzed by flow cytometry for expression of EGFP and MHC-I. Student's *t*-test was performed, and no statistical significance between the WT and the DN groups was seen. Representative dot plots from triplicate assays are presented.

In summary, however, the results obtained with chemical inhibitors suggest that MHC-I downregulation requires the activity of tyrosine kinase and is dependent on cholesterol, as deduced from the effects of genistein and filipin treatments, respectively. In contrast, sterol binding and lipid raft integrity seem to not be required, as nystatin and MβCD treatment did not affect virus-induced internalization of MHC-I. In order to further substantiate the role of caveolar endocytosis, a more specific tool in the form of a DN caveolin-1 (Cav1) mutant was employed. We altered the 14th amino acid residue of Cav1 by PCR-based mutagenesis and replaced the tyrosine with a phenylalanine residue (Y14F) (Orlichenko et al., 2006; Shatz et al., 2010). To facilitate detection of proteins by flow cytometry, both the WT and the DN mutant were fused to EGFP and tagged with an HA epitope (Fig. 2.6A). WT Cav1 was positioned upstream of EGFP (Cav1-EGFP), while the DN Cav1 construct containing the Y14F mutation was positioned downstream of EGFP [EGFP-Cav1(Y14F)]. We reasoned that the N-terminal fusion of Cav1 to EGFP together with the Y14F substitution would ensure the desired dominant negative effect, because caveolar uptake processes can be blocked by N-terminally tagged Cav1 (Pelkmans et al., 2001). Expression of both forms of Cav1 was readily detectable by Western blot analysis in NBL6 cell lysates (Fig. 2.6B). The effect of EGFP-Cav1(Y14F) was then evaluated by confocal imaging. Inhibition of caveolar endocytosis was noticeable, as the uptake of cholera toxin B (CTxB) was strongly attenuated in cells transfected with the plasmid expressing EGFP-Cav1(Y14F) (Fig. 2.6C). Furthermore, cell surface expression of MHC-I was analyzed in cells over-expressing either of the two forms of Cav1. In the absence of virus infection, over-expression of Cav1-EGFP or EGFP-Cav1(Y14F) did not alter levels of MHC-I on the cell surface (Fig. 2.6D, left). Likewise, at 5 h p.i., virus-induced downregulation of MHC-I was not affected, regardless of whether the wild-type or mutant form of Cav1 was used (Fig. 2.6D, right). Also, by using CLSM, we did not detect specific co-localization of caveolin-1 and MHC-I in infected cells (data not shown). We concluded from the experiments that caveolar endocytosis is not involved in MHC-I downregulation mediated by EHV-1.

2.4.6 Ubiquitination is essential for modulating cell surface levels of MHC-I in infected cells

It is known that over-expression of the gammaherpesvirus (Kaposi's sarcoma-associated herpesvirus [KSHV])-encoded ubiquitin E3 ligases K3 or K5 will reduce the levels of MHC-I at the cell surface. This process is mediated by linkage of polyubiquitin chains at lysine 63 (K63 polyubiquitination), which is sufficient to activate endocytosis (Duncan et al., 2006). Given that HSV-2 pUL56 strongly increases ubiquitination of host E3 ligase Nedd4 (Ushijima et al., 2010), we speculated that downregulation of MHC-I caused by EHV-1 pUL56 may be dependent on ubiquitination.

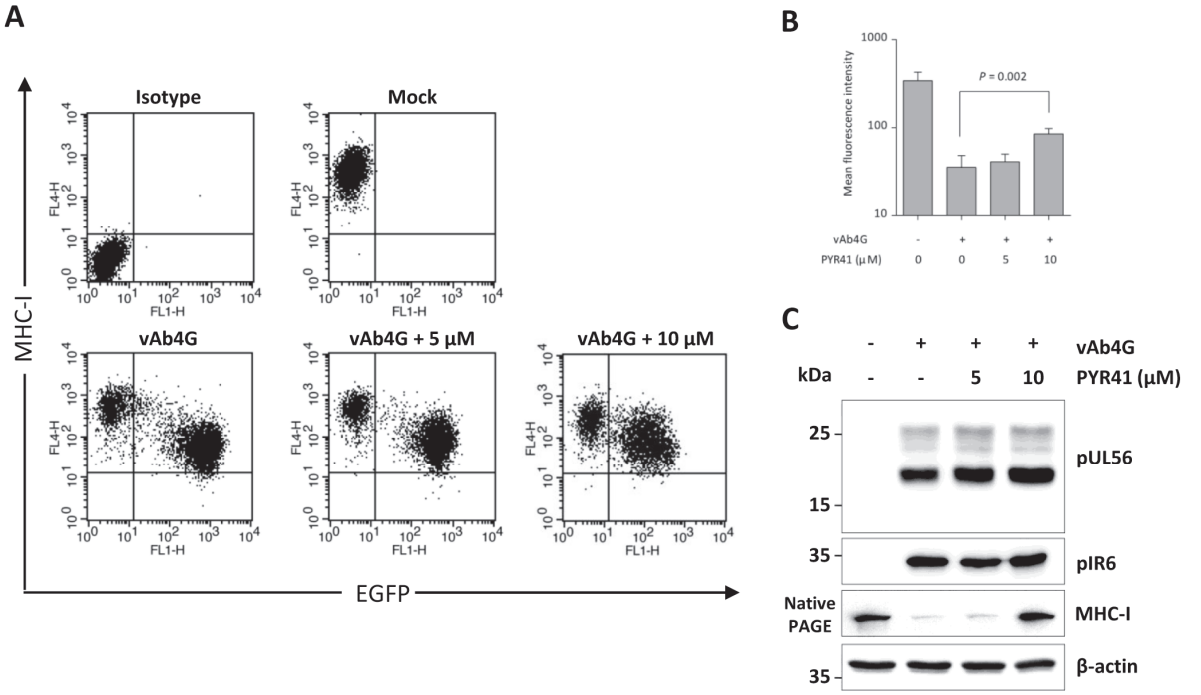

Figure 2.7 Ubiquitination affects cell surface MHC-I expression in EHV-1-infected cells. (A) Ubiquitination was blocked by PYR41, an E1 inhibitor. NBL6 cells were mock infected or infected with vAb4G for 2 h; afterwards, inhibitor at 5 µM or 10 µM was applied. At 4 h of inhibition, the levels of cell surface MHC-I were determined by flow cytometry. **(B)** The overall inhibitory effects are shown as dot plots and converted into a bar chart to quantitatively compare mean fluorescence intensities obtained with the treatments. Data analyses were performed using one-way ANOVA. **(C)** PYR41 inhibitor reduces MHC-I degradation but does not affect the expression of pUL56. At 4 h p.i., cell lysates were prepared with RIPA buffer and fractionated using SDS-12% PAGE. The expression levels of pUL56 and pIR6 were detected by Western blotting. For MHC-I detection, cell lysates were separated by non-denaturing 12% PAGE, and the blot was probed with anti-MHC-I MAb CZ3. β-actin was included as a gel loading control.

To test this hypothesis experimentally, infected cells were incubated with PYR41, which interferes with ubiquitination by E1 blockade (Yang et al., 2007). Incubation of infected cells with 10 µM PYR41 resulted in recovery of cell surface levels of MHC-I at 4 h p.i. compared to untreated cells (Fig. 2.7A and 2.7B). We ruled out the possibility that inhibition of the ubiquitination machinery might impair the expression of pUL56. Under PYR41 treatment, pUL56 and the early viral protein IR6 (pIR6) remained stable in infected cells (Fig. 2.7C). We concluded from the results of this experiment that MHC-I downregulation and degradation caused by EHV-1 require ubiquitination, more specifically an interaction between EHV-1 pUL56 and components of the cellular ubiquitination machinery.

2.4.7 Downregulation of additional cell surface markers by pUL56

Finally, we determined if pUL56-mediated internalization was specific to MHC-I. To this end, cell surface expression of a number of cell surface markers, specifically, CD46, CD58, CD59, CD63 and CD95, was analyzed. All the targeted molecules play critical roles in modulation of host innate or adaptive immunity. CD46 negatively regulates the pathways for complement activation (Liszewski et al., 1991), while CD58 and CD59 facilitate the adhesion and activation of T cells (Deckert et al., 1992). Being a co-stimulatory factor, CD63 is required for the steady activation and proliferation of T cells (Pfistershammer et al., 2004). CD95, best

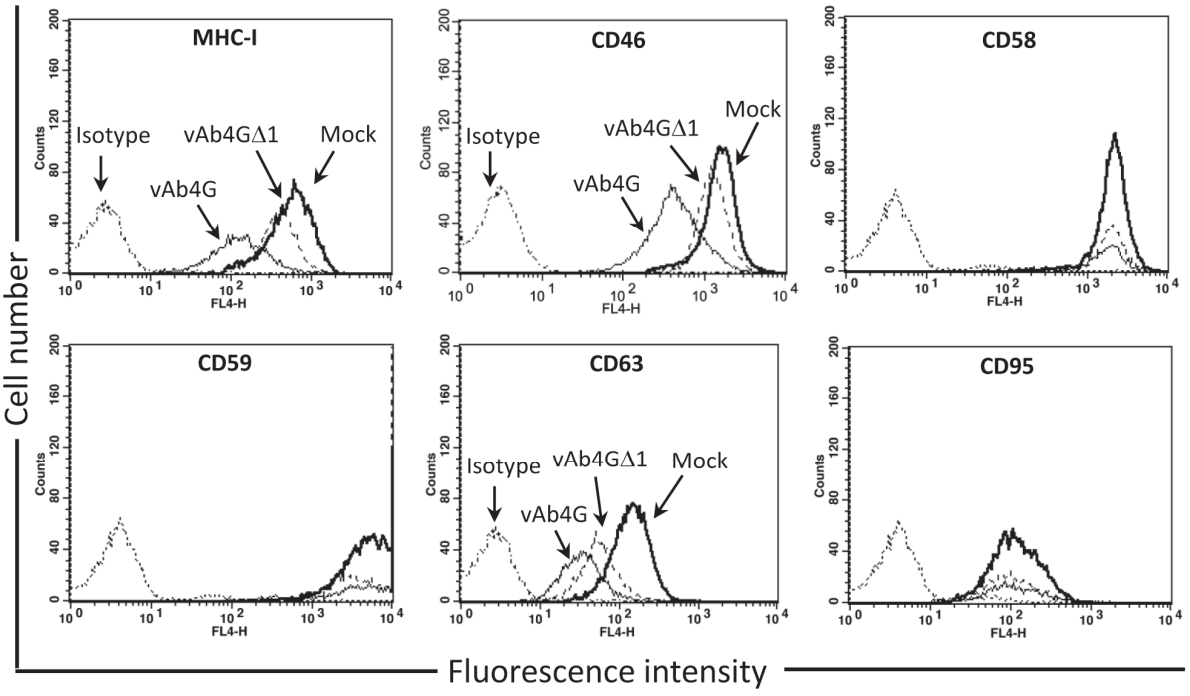

Figure 2.8 A broader range of surface markers is decreased during EHV-1 infection in a pUL56-dependent fashion. Hela cells were mock infected (black solid line) or infected with vAb4G (gray solid line) or vAb4GΔ1 (black dashed line). Unspecific binding of antibodies was controlled for by staining with corresponding isotype antibodies (gray dashed line). At 24 h p.i., all cells were sampled and incubated with monoclonal primary antibodies against MHC-I, CD46, CD58, CD59, CD63, and CD95. Alexa Fluor 647-conjugated goat anti-mouse IgG was used as a secondary antibody. Samples were detected by flow cytometry. The FL4-H axis refers to the fluorescence intensity of the given surface markers. Downregulation of MHC-I, CD46 and CD63, but not that of other markers, was rescued by abrogation of *ORF1*. The histograms are representative of two independent tests.

known as Fas receptor, initiates apoptosis when the target cells are recognized by CTLs (Krammer, 2000). Because the available antibodies show exclusive reactivity with human and murine but not equine CD molecules, our experiments were conducted using HeLa cells in which MHC-I downregulation dependent on pUL56 had previously been documented (Ma et

al., 2012). For testing each marker, HeLa cells were infected with vAb4G or vAb4GΔ1, the mutant devoid of pUL56. At 24 h p.i., cell surface levels of each maker were analyzed by flow cytometry and plotted as mean fluorescence intensity in histograms. Of the selected markers, pUL56 induced a significant reduction of CD46 and CD63, whereas it did not affect the levels of CD58, CD59 or CD95 (Fig. 2.8). On the basis of these data, we concluded that pUL56 is able to reduce cell surface levels of molecules other than MHC-I and, hence, may have a more general effect on immunomodulatory molecules in infected cells.

2.5 Discussion

Over the past 2 decades, a number of viral inhibitors targeting different stages of MHC-I presentation have been characterized (Hansen and Bouvier, 2009). The majority of such inhibitors were found in herpesviruses, although their mechanisms of action vary greatly. Recently, we discovered that pUL56, encoded by the gene *ORF1* of EHV-1, affects MHC-I expression (Ma et al., 2012). Phylogenetic analyses reveal that pUL56 is conserved in many alphaherpesviruses and the pUL56 homologue of EHV-4 also downregulates MHC-I at the cell surface (Said et al., 2012). It was speculated that loss of cell surface MHC-I is induced by endocytosis in the early stages of EHV-1 infection (Rappocciolo et al., 2003), and here, we investigated the putative relationship between pUL56 and endocytosis that might result in the reduction of MHC-I on the cell surface. By using inhibitors that disrupt endosomal or lysosomal function, we initially determined that endosomal acidification and lysosomal proteolysis govern the fate of internalized MHC-I. This finding was further corroborated by confocal microscopy showing that MHC-I co-localized with the lysosome marker LAMP-1.

Endocytosis is an important intracellular transport mechanism that initiates signal transduction and internalization of a number of nutrients, lipids, membrane proteins and pathogens (Doherty and McMahon, 2009). The endocytic pathways that allow infectious entry have been extensively studied for a number of viruses (Mercer et al., 2010); however, it is less well understood how viruses induce endocytosis of key immune-related receptors to achieve immune evasion. Notable exceptions are the KSHV K3 and K5 proteins, which promote MHC-I endocytosis in infected cells. It was shown in transiently transfected cells that these two virus-encoded enzymes directly increase endocytic activity and lead to the uptake of MHC-I molecules from the cell surface (Coscoy and Ganem, 2000). Likewise, the HIV Nef protein was shown to downregulate MHC-I through an endocytic pathway (Blagovesh-chenskaya et al., 2002), which may imply that enhancing endocytosis as a means of preventing or reducing presentation of antigenic (viral) peptides by MHC-I might be evolutionarily conserved among many viruses.

We were able to demonstrate here that EHV-1 pUL56 co-localizes from 4 h p.i. with MHC-I-containing vesicles and the lysosomal marker LAMP-1 in infected cells. This co-localization correlates with decreased cell surface MHC-I levels. The results, therefore, suggest that it is indeed pUL56 that mediates the trafficking of MHC-I molecules to lysosomes for degradation. The two known viral MHC-I inhibitors encoded by alphaherpesviruses, ICP47 and pUL49.5, prevent translocation of antigenic peptide into the ER and formation of the tri-molecular complex. Specifically, ICP47 is present in the cytoplasm and exhibits high affinity to TAP, which results in functional inactivation of peptide transport into the ER (Ahn et al., 1996; Tomazin et al., 1996). For pUL49.5, although it also restricts the supply of peptides to the ER, homologues in different viral species are mechanistically diverse. For example, BHV-1 pUL49.5 reduces TAP stability by promoting its proteasomal degradation (Koppers-Lalic et al., 2005), whereas pUL49.5 of EHV-1 and -4 inhibit the recruitment of ATP, which is indispensible for TAP activity (Koppers-Lalic et al., 2008). Unlike ER-based interference with MHC-I maturation, pUL56 is predominantly localized to the Golgi apparatus and endosomal vesicles. It does not perturb peptide transport to the ER (Ma et al., 2012; Said et al., 2012), and its mechanism of action is clearly distinct from those of ICP47 and pUL49.5. Therefore, pUL56 has a novel mode of action with respect to MHC-I downregulation in members of the *Alphaherpesvirinae* and functions more like gammaherpesviral K3 and K5 by promoting endocytosis.

Based on their constituent elements, endocytic pathways are classified into categories that include clathrin-, caveolae- and Arf6-dependent endocytosis as well as phagocytosis and macropinocytosis (Mayor and Pagano, 2007); however, a growing body of evidence now suggests that unidentified endocytic pathways might exist, and thus the classification scheme has been simplified by discriminating only between clathrin-dependent endocytosis (CDE) and clathrin-independent endocytosis (CIE) (Le Roy and Wrana, 2005). Endocytosis inhibitors are commonly used to investigate endocytic pathways responsible for homeostasis of cell surface proteins, but attention should be given to their possibly pleiotrophic effects (Vercauteren et al., 2010). Given that the turnover of cell surface proteins is dynamically regulated under normal physiological conditions, we tested the influence of our inhibitors on the metabolism of MHC-I, which might distort the interpretation of our results in infected cells. Except for the significant MHC-I reduction seen with the treatment of chloroquine, the other reagents used showed no or very little effect on the presence of MHC-I on the cell surface of mock-infected cells (Fig. 2.S1), ensuring that they target only MHC-I in infected cells. With inhibition of virus-induced MHC-I downregulation by chlorpromazine and Pitstop2 as well by dominant negative molecules, we demonstrated that MHC-I down-regulation is not through the CDE pathway. This observation for EHV-1 differs from that for KSHV, where the K3 protein interferes with the classical CDE pathway (Duncan et al., 2006),

while a unique Arf6-dependent pathway is targeted by HIV-1 Nef to divert mature cell surface MHC-I to lysosomes for degradation (Blagoveshchenskaya et al., 2002). Despite the differences, lysosomes are the ultimate cellular compartment where degradation of MHC-I occurs in the case of KSHV, HIV-1, and EHV-1.

Caveolae-dependent endocytosis is considered an important CIE pathway. Along with the involvement of dynamin, caveolin-1 is primarily responsible for the formation of the flask-shaped caveolae (Liu et al., 2002). Moreover, tyrosine kinase activity is necessary for the aggregation and fusion of caveolae or caveolar vesicles (Nomura and Fujimoto, 1999). Therefore, it is not surprising that a number of viruses gain access to host cells by non-classical endocytic pathways that are all dependent on the action of dynamin and tyrosine kinases but differ in other factors involved (Azab et al., 2013; Damm et al., 2005; Mulherkar et al., 2011; Qie et al., 1999). Here, we studied the role of caveolae-dependent endocytosis in virus-induced MHC-I downregulation. Despite the various effects of four inhibitors for CIE, transfection of a specific dominant negative form of caveolin-1 was unable to rescue cell surface expression of MHC-I, suggesting that caveolae-dependent endocytosis is not involved in MHC-I internalization. In contrast, we found that the decrease of surface MHC-I was remarkably attenuated when the action of dynamin was inhibited with dynasore or a dominant negative form of dynamin. These findings led us to conclude that MHC-I downregulation is associated with dynamin, which facilitates vesicle scission at the plasma membrane and as such is integral to many endocytic pathways (Hinshaw and Schmid, 1995; Marks et al., 2001). To our knowledge, our report describes the first example of an alphaherpesvirus that downregulates cell surface MHC-I through an endocytic pathway, which is associated with dynamin but unrelated to clathrin and caveolae. However, there might be another unknown viral protein(s) that can drive MHC-I downregulation through endocytic processes, as knockout of pUL56 alone cannot completely prevent endocytosis of MHC-I mediated by EHV-1 infection.

Ubiquitination determines the destiny of endocytosed membrane proteins (Strous and Govers, 1999). On the one hand, the formation of vesicles at different stages of endocytosis requires mono- or poly-ubiquitination (Hicke, 2001). On the other hand, the nature of ubiquitin linkage to lysine results in cargo sorting and degradation either in the proteasome or in the lysosome (Pickart and Fushman, 2004). KSHV K3 and K5 are E3 ubiquitin ligases that directly bind to membrane substrates and trigger endocytosis (Duncan et al., 2006; Means et al., 2007). In the case of HSV-2, pUL56 is able to increase ubiquitination of the E3 ligase Nedd4. This interaction is thought to affect protein sorting or vesicle trafficking but does not affect virus release, as originally surmised (Ushijima et al., 2008). Here, EHV-1 pUL56, which is structurally similar to its HSV-2 orthologue, was shown to direct MHC-I molecules for

lysosomal degradation. This process is greatly affected when ubiquitination is chemically blocked. It is therefore tempting to speculate that the function of pUL56 depends on its interaction with an E3 ligase, a hypothesis that we are currently testing.

To address the specificity of pUL56 action, several other cell surface markers were screened in this study. We found that pUL56 can reduce the expression of CD46 and CD63 on the cell surface. CD46 is critical for efficient T cell responses and bridges between the complement system and cellular immunity (Riley-Vargas et al., 2004); for instance, expression of CD46 facilitates destruction of the cells infected with measles virus by CTLs, a process that depends on MHC-I antigen presentation (Cardoso et al., 1996). CD63 is a membrane protein containing four transmembrane domains (tetraspanin), which is widely distributed on endosomal membranes and known to modulate immune signaling pathways (Levy and Shoham, 2005; Pols and Klumperman, 2009). In dendritic cells, for example, intracellular transport of CD63 is associated with antigen presentation by MHC-II (Engering and Pieters, 2001). The implication of pUL56 in downregulating CD46 and CD63 may suggest that it functions as a more promiscuous immune modulator, a notion that is supported by the results obtained in equids infected with the Ab4 mutant unable to express the protein (Soboll Hussey et al., 2011).

Removal of cell surface MHC-I seems a wise strategy for persistent infection, as CTLs would be unable to eliminate infected cells due to a failure to recognize antigens. However, cells devoid of surface MHC-I are unlikely to survive and might be subject to clearance by natural killer (NK) cells. KSHV K5 targets other surface molecules to counteract the threat from NK cells. Along with CD31, CD86, CD144, CD166, and intracellular adhesion molecule 1 (ICAM1) (Means et al., 2007), KSHV K5 also downregulates activation-induced C-type lectin (AICL), MHC-I polypeptide-related sequence A (MICA), and MICB, which are required for NK cell lysis (Nathan and Lehner, 2009; Thomas et al., 2008). Whether pUL56 targets these surface molecules sensed by NK cells remains to be explored.

Taken together, we investigated the pathway by which pUL56 induces downregulation of cell surface MHC-I. The endocytic process responsible for MHC-1 removal from the cell surface is mediated by dynamin but not clathrin or caveolae. Importantly, tyrosine kinase activity and membrane-bound cholesterol are required for MHC-I endocytosis as is ubiquitination. The latter may imply that pUL56 function is dependent on the E3 ligase activity. Since pUL56 is able to regulate other cell surface molecules, it may have a more comprehensive role in regulation of the immune response to infection. Future studies will focus on how pUL56 interacts with ubiquitination and the yet-unidentified viral protein(s) it needs to fulfill its functions.

Acknowledgements

We thank Dr. Walid Azab for helpful suggestions on inhibitors and maintenance of equine cells. We express gratitude for the Pitstop2 inhibitors, kindly provided by Dr. Volker Haucke from the Leibniz-Institut für Molekulare Pharmakologie (FMP), Berlin-Buch, Germany, and the anti-MHC MAb CZ3, provided by Dr. Douglas F. Antczak (Cornell University, USA). We also gratefully acknowledge the dominant negative mutants kindly provided by Dr. Mark A. McNiven (Mayo Clinic, Rochester, MN, USA) and Dr. Alexandre Benmerah (Hôpital Necker-Enfants Malades, Paris, France).

T.H. was supported by a grant from the China Scholarship Council. This study was financed by DFG grant OS143/3-1 and unrestricted funds of Freie Universität Berlin to N.O.

Author contributions

T.H., G.M. and K.O. jointly conceived the study and designed the experiments. T.H. and G.M. performed most of the experiments and interpreted the data. M.J.L. assisted in confocal microscopy. A.S. constructed the virus mutant expressing dsRed and tested some inhibitors. T.H. and G.M. prepared the manuscript; and K.O. revised it critically. All authors provided comments on the paper and gave their final approval to submission.

References

Ahn, K., Meyer, T.H., Uebel, S., Sempe, P., Djaballah, H., Yang, Y., Peterson, P.A., Fruh, K., Tampe, R., 1996, Molecular mechanism and species specificity of TAP inhibition by herpes simplex virus ICP47. EMBO J 15, 3247-3255.

Azab, W., Lehmann, M.J., Osterrieder, N., 2013, Glycoprotein H and alpha4beta1 integrins determine the entry pathway of alphaherpesviruses. J Virol 87, 5937-5948.

Benmerah, A., Bayrou, M., Cerf-Bensussan, N., Dautry-Varsat, A., 1999, Inhibition of clathrin-coated pit assembly by an Eps15 mutant. J Cell Sci 112 (Pt 9), 1303-1311.

Benmerah, A., Lamaze, C., Begue, B., Schmid, S.L., Dautry-Varsat, A., Cerf-Bensussan, N., 1998, AP-2/Eps15 interaction is required for receptor-mediated endocytosis. J Cell Biol 140, 1055-1062.

Blagoveshchenskaya, A.D., Thomas, L., Feliciangeli, S.F., Hung, C.H., Thomas, G., 2002, HIV-1 Nef downregulates MHC-I by a PACS-1- and PI3K-regulated ARF6 endocytic pathway. Cell 111, 853-866.

Burgert, H.G., Kvist, S., 1985, An adenovirus type 2 glycoprotein blocks cell surface expression of human histocompatibility class I antigens. Cell 41, 987-997.

Cao, H., Thompson, H.M., Krueger, E.W., McNiven, M.A., 2000, Disruption of Golgi structure and function in mammalian cells expressing a mutant dynamin. J Cell Sci 113 (Pt 11), 1993-2002.

Cardoso, A.I., Gerlier, D., Wild, T.F., Rabourdin-Combe, C., 1996, The ectodomain of measles virus envelope glycoprotein does not gain access to the cytosol and MHC class I presentation pathway following virus-cell fusion. J Gen Virol 77 (Pt 11), 2695-2699.

Chen, Y., Wang, S., Lu, X., Zhang, H., Fu, Y., Luo, Y., 2011, Cholesterol sequestration by nystatin enhances the uptake and activity of endostatin in endothelium via regulating distinct endocytic pathways. Blood 117, 6392-6403.

Coscoy, L., Ganem, D., 2000, Kaposi's sarcoma-associated herpesvirus encodes two proteins that block cell surface display of MHC class I chains by enhancing their endocytosis. Proc Natl Acad Sci U S A 97, 8051-8056.

Damm, E.M., Pelkmans, L., Kartenbeck, J., Mezzacasa, A., Kurzchalia, T., Helenius, A., 2005, Clathrin- and caveolin-1-independent endocytosis: entry of simian virus 40 into cells devoid of caveolae. J Cell Biol 168, 477-488.

Deckert, M., Kubar, J., Bernard, A., 1992, CD58 and CD59 molecules exhibit potentializing effects in T cell adhesion and activation. J Immunol 148, 672-677.

Doherty, G.J., McMahon, H.T., 2009, Mechanisms of endocytosis. Annu Rev Biochem 78, 857-902.

Drose, S., Altendorf, K., 1997, Bafilomycins and concanamycins as inhibitors of V-ATPases and P-ATPases. J Exp Biol 200, 1-8.

Duncan, L.M., Piper, S., Dodd, R.B., Saville, M.K., Sanderson, C.M., Luzio, J.P., Lehner, P.J., 2006, Lysine-63-linked ubiquitination is required for endolysosomal degradation of class I molecules. EMBO J 25, 1635-1645.

Dutta, D., Donaldson, J.G., 2012, Search for inhibitors of endocytosis: Intended specificity and unintended consequences. Cell Logist 2, 203-208.

Engering, A., Pieters, J., 2001, Association of distinct tetraspanins with MHC class II molecules at different subcellular locations in human immature dendritic cells. Int Immunol 13, 127-134.

Fredericksen, B.L., Wei, B.L., Yao, J., Luo, T., Garcia, J.V., 2002, Inhibition of endosomal/lysosomal degradation increases the infectivity of human immunodeficiency virus. J Virol 76, 11440-11446.

Fruh, K., Ahn, K., Djaballah, H., Sempe, P., van Endert, P.M., Tampe, R., Peterson, P.A., Yang, Y., 1995, A viral inhibitor of peptide transporters for antigen presentation. Nature 375, 415-418.

Fruh, K., Gruhler, A., Krishna, R.M., Schoenhals, G.J., 1999, A comparison of viral immune escape strategies targeting the MHC class I assembly pathway. Immunol Rev 168, 157-166.

Goodman, L.B., Loregian, A., Perkins, G.A., Nugent, J., Buckles, E.L., Mercorelli, B., Kydd, J.H., Palu, G., Smith, K.C., Osterrieder, N., Davis-Poynter, N., 2007, A point mutation in a

herpesvirus polymerase determines neuropathogenicity. PLoS Pathog 3, e160.

Hansen, T.H., Bouvier, M., 2009, MHC class I antigen presentation: learning from viral evasion strategies. Nat Rev Immunol 9, 503-513.

Hicke, L., 2001, A new ticket for entry into budding vesicles-ubiquitin. Cell 106, 527-530.

Hill, A., Jugovic, P., York, I., Russ, G., Bennink, J., Yewdell, J., Ploegh, H., Johnson, D., 1995, Herpes simplex virus turns off the TAP to evade host immunity. Nature 375, 411-415.

Hinshaw, J.E., Schmid, S.L., 1995, Dynamin self-assembles into rings suggesting a mechanism for coated vesicle budding. Nature 374, 190-192.

Koppers-Lalic, D., Reits, E.A., Ressing, M.E., Lipinska, A.D., Abele, R., Koch, J., Marcondes Rezende, M., Admiraal, P., van Leeuwen, D., Bienkowska-Szewczyk, K., Mettenleiter, T.C., Rijsewijk, F.A., Tampe, R., Neefjes, J., Wiertz, E.J., 2005, Varicelloviruses avoid T cell recognition by UL49.5-mediated inactivation of the transporter associated with antigen processing. Proc Natl Acad Sci U S A 102, 5144-5149.

Koppers-Lalic, D., Verweij, M.C., Lipinska, A.D., Wang, Y., Quinten, E., Reits, E.A., Koch, J., Loch, S., Marcondes Rezende, M., Daus, F., Bienkowska-Szewczyk, K., Osterrieder, N., Mettenleiter, T.C., Heemskerk, M.H., Tampe, R., Neefjes, J.J., Chowdhury, S.I., Ressing, M.E., Rijsewijk, F.A., Wiertz, E.J., 2008, Varicellovirus UL 49.5 proteins differentially affect the function of the transporter associated with antigen processing, TAP. PLoS Pathog 4, e1000080.

Krammer, P.H., 2000, CD95's deadly mission in the immune system. Nature 407, 789-795.

Kydd, J.H., Wattrang, E., Hannant, D., 2003, Pre-infection frequencies of equine herpesvirus-1 specific, cytotoxic T lymphocytes correlate with protection against abortion following experimental infection of pregnant mares. Vet Immunol Immunopathol 96, 207-217.

Le Roy, C., Wrana, J.L., 2005, Clathrin- and non-clathrin-mediated endocytic regulation of cell signalling. Nat Rev Mol Cell Biol 6, 112-126.

Levy, S., Shoham, T., 2005, The tetraspanin web modulates immune-signalling complexes. Nat Rev Immunol 5, 136-148.

Lilley, B.N., Ploegh, H.L., 2005, Viral modulation of antigen presentation: manipulation of cellular targets in the ER and beyond. Immunol Rev 207, 126-144.

Liszewski, M.K., Post, T.W., Atkinson, J.P., 1991, Membrane cofactor protein (MCP or CD46): newest member of the regulators of complement activation gene cluster. Annu Rev Immunol 9, 431-455.

Liu, P., Rudick, M., Anderson, R.G., 2002, Multiple functions of caveolin-1. J Biol Chem 277, 41295-41298.

Luzio, J.P., Pryor, P.R., Bright, N.A., 2007, Lysosomes: fusion and function. Nat Rev Mol Cell Biol 8, 622-632.

Ma, G., Azab, W., Osterrieder, N., 2013, Equine herpesviruses type 1 (EHV-1) and 4 (EHV-4)--masters of co-evolution and a constant threat to equids and beyond. Vet Microbiol 167, 123-134.

Ma, G., Feineis, S., Osterrieder, N., Van de Walle, G.R., 2012, Identification and characterization of equine herpesvirus type 1 pUL56 and its role in virus-induced downregulation of major histocompatibility complex class I. J Virol 86, 3554-3563.

Macia, E., Ehrlich, M., Massol, R., Boucrot, E., Brunner, C., Kirchhausen, T., 2006, Dynasore, a cell-permeable inhibitor of dynamin. Dev Cell 10, 839-850.

Marks, B., Stowell, M.H., Vallis, Y., Mills, I.G., Gibson, A., Hopkins, C.R., McMahon, H.T., 2001, GTPase activity of dynamin and resulting conformation change are essential for endocytosis. Nature 410, 231-235.

Mayor, S., Pagano, R.E., 2007, Pathways of clathrin-independent endocytosis. Nat Rev Mol Cell Biol 8, 603-612.

Means, R.E., Lang, S.M., Jung, J.U., 2007, The Kaposi's sarcoma-associated herpesvirus K5 E3 ubiquitin ligase modulates targets by multiple molecular mechanisms. J Virol 81, 6573-6583.

Mercer, J., Schelhaas, M., Helenius, A., 2010, Virus entry by endocytosis. Annu Rev Biochem 79, 803-833.

Mulherkar, N., Raaben, M., de la Torre, J.C., Whelan, S.P., Chandran, K., 2011, The Ebola virus glycoprotein mediates entry via a non-classical dynamin-dependent macropinocytic pathway.

Virology 419, 72-83.

Mundy, D.I., Li, W.P., Luby-Phelps, K., Anderson, R.G., 2012, Caveolin targeting to late endosome/lysosomal membranes is induced by perturbations of lysosomal pH and cholesterol content. Mol Biol Cell 23, 864-880.

Nabi, I.R., Le, P.U., 2003, Caveolae/raft-dependent endocytosis. J Cell Biol 161, 673-677.

Nathan, J.A., Lehner, P.J., 2009, The trafficking and regulation of membrane receptors by the RING-CH ubiquitin E3 ligases. Exp Cell Res 315, 1593-1600.

Nomura, R., Fujimoto, T., 1999, Tyrosine-phosphorylated caveolin-1: immunolocalization and molecular characterization. Mol Biol Cell 10, 975-986.

O'Callaghan, D.J., Colle, C.F., 3rd, Flowers, C.C., Smith, R.H., Benoit, J.N., Bigger, C.A., 1994, Identification and initial characterization of the IR6 protein of equine herpesvirus 1. J Virol 68, 5351-5364.

Orlichenko, L., Huang, B., Krueger, E., McNiven, M.A., 2006, Epithelial growth factor-induced phosphorylation of caveolin 1 at tyrosine 14 stimulates caveolae formation in epithelial cells. J Biol Chem 281, 4570-4579.

Peaper, D.R., Cresswell, P., 2008, Regulation of MHC class I assembly and peptide binding. Annu Rev Cell Dev Biol 24, 343-368.

Pelkmans, L., Kartenbeck, J., Helenius, A., 2001, Caveolar endocytosis of simian virus 40 reveals a new two-step vesicular-transport pathway to the ER. Nat Cell Biol 3, 473-483.

Pfistershammer, K., Majdic, O., Stockl, J., Zlabinger, G., Kirchberger, S., Steinberger, P., Knapp, W., 2004, CD63 as an activation-linked T cell costimulatory element. J Immunol 173, 6000-6008.

Pickart, C.M., Fushman, D., 2004, Polyubiquitin chains: polymeric protein signals. Curr Opin Chem Biol 8, 610-616.

Pols, M.S., Klumperman, J., 2009, Trafficking and function of the tetraspanin CD63. Exp Cell Res 315, 1584-1592.

Qie, L., Marcellino, D., Herold, B.C., 1999, Herpes simplex virus entry is associated with tyrosine phosphorylation of cellular proteins. Virology 256, 220-227.

Rappocciolo, G., Birch, J., Ellis, S.A., 2003, Down-regulation of MHC class I expression by equine herpesvirus-1. J Gen Virol 84, 293-300.

Riley-Vargas, R.C., Gill, D.B., Kemper, C., Liszewski, M.K., Atkinson, J.P., 2004, CD46: expanding beyond complement regulation. Trends Immunol 25, 496-503.

Said, A., Azab, W., Damiani, A., Osterrieder, N., 2012, Equine herpesvirus type 4 UL56 and UL49.5 proteins downregulate cell surface major histocompatibility complex class I expression independently of each other. J Virol 86, 8059-8071.

Schnitzer, J.E., Oh, P., Pinney, E., Allard, J., 1994, Filipin-sensitive caveolae-mediated transport in endothelium: reduced transcytosis, scavenger endocytosis, and capillary permeability of select macromolecules. J Cell Biol 127, 1217-1232.

Shatz, M., Lustig, G., Reich, R., Liscovitch, M., 2010, Caveolin-1 mutants P132L and Y14F are dominant negative regulators of invasion, migration and aggregation in H1299 lung cancer cells. Exp Cell Res 316, 1748-1762.

Soboll Hussey, G., Hussey, S.B., Wagner, B., Horohov, D.W., Van de Walle, G.R., Osterrieder, N., Goehring, L.S., Rao, S., Lunn, D.P., 2011, Evaluation of immune responses following infection of ponies with an EHV-1 ORF1/2 deletion mutant. Vet Res 42, 23.

Stroh, T., Erben, U., Kuhl, A.A., Zeitz, M., Siegmund, B., 2010, Combined pulse electroporation--a novel strategy for highly efficient transfection of human and mouse cells. PLoS One 5, e9488.

Strous, G.J., Govers, R., 1999, The ubiquitin-proteasome system and endocytosis. J Cell Sci 112 (Pt 10), 1417-1423.

Thomas, M., Wills, M., Lehner, P.J., 2008, Natural killer cell evasion by an E3 ubiquitin ligase from Kaposi's sarcoma-associated herpesvirus. Biochem Soc Trans 36, 459-463.

Tischer, B.K., von Einem, J., Kaufer, B., Osterrieder, N., 2006, Two-step red-mediated recombination for versatile high-efficiency markerless DNA manipulation in Escherichia coli. Biotechniques 40, 191-197.

Tomazin, R., Hill, A.B., Jugovic, P., York, I., van Endert, P., Ploegh, H.L., Andrews, D.W., Johnson,

D.C., 1996, Stable binding of the herpes simplex virus ICP47 protein to the peptide binding site of TAP. EMBO J 15, 3256-3266.

Ushijima, Y., Koshizuka, T., Goshima, F., Kimura, H., Nishiyama, Y., 2008, Herpes simplex virus type 2 UL56 interacts with the ubiquitin ligase Nedd4 and increases its ubiquitination. J Virol 82, 5220-5233.

Ushijima, Y., Luo, C., Kamakura, M., Goshima, F., Kimura, H., Nishiyama, Y., 2010, Herpes simplex virus UL56 interacts with and regulates the Nedd4-family ubiquitin ligase Itch. Virol J 7, 179.

Vercauteren, D., Vandenbroucke, R.E., Jones, A.T., Rejman, J., Demeester, J., De Smedt, S.C., Sanders, N.N., Braeckmans, K., 2010, The use of inhibitors to study endocytic pathways of gene carriers: optimization and pitfalls. Mol Ther 18, 561-569.

von Kleist, L., Stahlschmidt, W., Bulut, H., Gromova, K., Puchkov, D., Robertson, M.J., MacGregor, K.A., Tomilin, N., Pechstein, A., Chau, N., Chircop, M., Sakoff, J., von Kries, J.P., Saenger, W., Krausslich, H.G., Shupliakov, O., Robinson, P.J., McCluskey, A., Haucke, V., 2011, Role of the clathrin terminal domain in regulating coated pit dynamics revealed by small molecule inhibition. Cell 146, 471-484.

Wang, L.H., Rothberg, K.G., Anderson, R.G., 1993, Mis-assembly of clathrin lattices on endosomes reveals a regulatory switch for coated pit formation. J Cell Biol 123, 1107-1117.

Wong, P., Pamer, E.G., 2003, CD8 T cell responses to infectious pathogens. Annu Rev Immunol 21, 29-70.

Yang, Y., Kitagaki, J., Dai, R.M., Tsai, Y.C., Lorick, K.L., Ludwig, R.L., Pierre, S.A., Jensen, J.P., Davydov, I.V., Oberoi, P., Li, C.C., Kenten, J.H., Beutler, J.A., Vousden, K.H., Weissman, A.M., 2007, Inhibitors of ubiquitin-activating enzyme (E1), a new class of potential cancer therapeutics. Cancer Res 67, 9472-9481.

Supplemental material

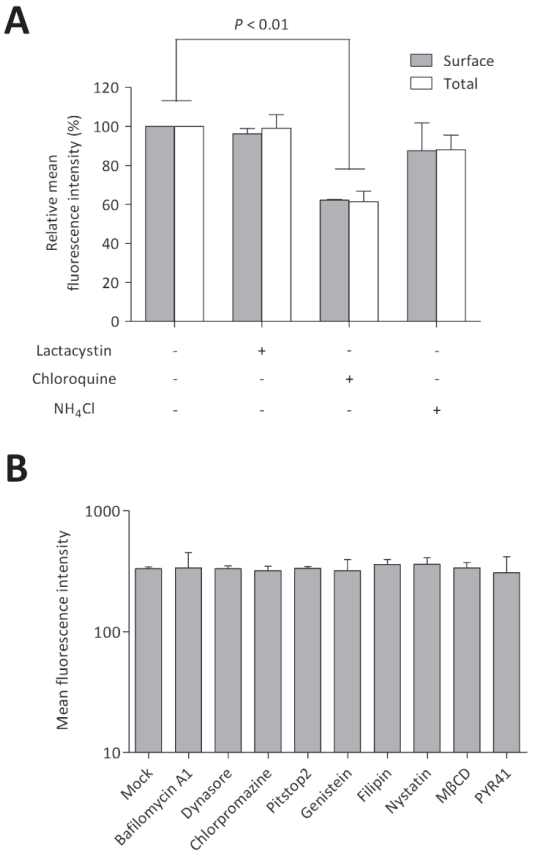

Figure 2.S1 Effects of inhibitors on the turnover of MHC-I in uninfected cells. NBL6 cells were treated with the following inhibitors: **(A)** 5 μM lactacystin, 150 μM chloroquine and 10 mM NH_4Cl. **(B)** 2 μM bafilomycin A1, 80 μM Dynasore, 10 μg/ml chlorpromazine, 10 μM Pitstop2, 50 μg/ml genistein, 5 μg/ml filipin, 20 μg/ml nystatin, 20 mM MβCD and 10 μM PYR41. After inhibition for 4 h, cells were suspended and reacted with MAb anti-MHC-I, followed by staining with Alexa Fluor 647-conjugated goat anti-mouse IgG. To detect total levels of MHC-I, cells were fixed in 3.5% PFA and permeablized in PBS supplemented with 0.02% saponin before proceeding to incubation with primary antibody. Expression levels of MHC-I were detected by flow cytometry. Data were obtained from three independent experiments and presented as means ± standard deviation.

CHAPTER 3

Equine herpesvirus type 1 (EHV-1) multiply transmembrane protein pUL43 cooperates with pUL56 in downregulation of cell surface MHC class I

Teng Huang[a], Guanggang Ma[a], Nikolaus Osterrieder[a]

[a] Institut für Virologie, Freie Universität Berlin, Zentrum für Infektionsmedizin - Robert von Ostertag-Haus, 14163 Berlin, Germany.

 [Journal of Virology, 2015, 89: 6251-6263. doi: 10.1128/JVI.00032-15].

3.1 Summary

Herpesviruses have evolved an array of strategies to counteract antigen presentation by major histocompatibility complex class I (MHC-I). Previously, we have identified pUL56 of equine herpesvirus type 1 (EHV-1) as one major determinant of downregulation of cell surface MHC-I (G. Ma, S. Feineis, N. Osterrieder, and G. R. Van de Walle, J. Virol. 86:3554–3563, 2012, doi:10.1128/JVI.06994-11; T. Huang, M. J. Lehmann, A. Said, G. Ma, and N. Osterrieder, J. Virol. 88:12802-12815, 2014, doi:10.1128/JVI.02079-14). Since pUL56 was able to exert its function only in the context of virus infection, we hypothesized that pUL56 cooperates with another viral protein. Here, we generated and screened a series of EHV-1 single gene deletion mutants and found that the pUL43 orthologue was required for downregulation of cell surface MHC-I expression at the same time of infection when pUL56 exerts its function. We demonstrate that the absence of pUL43 was not deleterious to virus growth and that expression of pUL43 was detectable from 2 h post-infection (h p.i.), but decreased after 8 h p.i due to lysosomal degradation. pUL43 localized within Golgi vesicles and required a unique hydrophilic N-terminal domain to function properly. Finally, co-expression of pUL43 and pUL56 in transfected cells reduced cell surface expression of MHC-I. This process was dependent on PPxY motifs present in pUL56, suggesting that late domains are required for pUL43- and pUL56-dependent sorting of MHC class I for lysosomal degradation.

3.2 Introduction

The interplay between viruses and their hosts has lead to evolution of a number of strategies that facilitate evasion from the recognition and clearance of virus infection by the host immune system. Upon successful entry into the cell, viruses are uncoated. Structural

components of the invading virus as well as newly produced proteins are poly-ubiquitinated and then fragmented into peptides by the proteasome (Gao and Luo, 2006). The processed antigenic peptides are transported into the endoplasmic reticulum (ER) and presented by histocompatibility complex class I (MHC-I) molecules on the cell surface. Cytotoxic $CD8^+$ T lymphocytes (CTL) whose T-cell receptor (TCR) specifically recognizes small peptides bound in the groove of MHC-I ultimately eliminate the infected cell (Neefjes et al., 2011; Zhang and Bevan, 2011). However, CTL-mediated immunity may fail or be delayed, because many viruses encode specific inhibitors that interfere with various stages of MHC-I antigen presentation (Hansen and Bouvier, 2009). As a consequence, infected cells have reduced MHC-I expression and become invisible to patrolling CTL.

Equine herpesvirus type 1 (EHV-1) is an important veterinary pathogen that poses a severe risk to the health of horse populations around the world. EHV-1 infection results in various clinical syndromes involving upper respiratory ailments, miscarriage, death of neonates and neurological disease (Ma et al., 2013). Classified as a member of the *Alphaherpesvirinae* subfamily, EHV-1 is a double-stranded DNA virus featuring a large genome of approximately 150 kbp in size. The EHV-1 genome contains at least 80 open reading frames (ORFs), in which at least 4 ORFs are duplicated in the inverted-repeat regions (Telford et al., 1992). Historically, the EHV-1 genome has been annotated in accordance with those of herpes simplex virus type 1 (HSV-1) and varicella zoster virus (VZV), prototype viruses of the *Alphaherpesvirinae.* This approach has also been applied to other closely related viruses, e.g., EHV-4 and pseudorabies virus (PRV) (Klupp et al., 2004; Telford et al., 1998). Hence, the role of a particular EHV-1 gene product can be deduced on the basis of its HSV-1 or VZV counterpart and extended to predict the function of the orthologues that are conserved in the genus, subfamily or even family. Nevertheless, several genes and/or gene functions are unique to HSV-1, VZV or EHV-1. For instance, HSV-1 ICP47 was the first protein identified in the *Alphaherpesvirinae* to induce downregulation of MHC-I at the cell surface by directly interacting with the transporter associated with antigen processing (TAP). ICP47 irreversibly prevents the transport of cytoplasmic peptides into the ER (Fruh et al., 1995), but ICP47 homologues are absent in EHV-1 and other varicelloviruses, including VZV. EHV-1 also causes MHC-I downregulation in a species-independent fashion and the pUL49.5 and pUL56 proteins have been shown to modulate cell surface MHC-I expression (Koppers-Lalic et al., 2008; Ma et al., 2012); however, pUL49.5 and pUL56 of HSV-1 do not affect MHC-I levels (Koppers-Lalic et al., 2005).

The pUL56 and pUL49.5 homologues of various *Alphaherpesvirinae* differ in expression patterns and subcellular localization (Ma et al., 2012; Wei et al., 2011), indicating that they are mechanistically different. EHV-1 pUL49.5, a small type I transmembrane protein that

interacts with viral glycoprotein M (gM) (Rudolph et al., 2002), inhibits the formation of peptide-loaded MHC-I complexes by preventing ATP binding to TAP (Koppers-Lalic et al., 2008). pUL56, a type II transmembrane protein, enhances internalization of MHC-I through dynamin-dependent endocytosis (Huang et al., 2014). In our previous studies, we reported that pUL56 induced cell surface MHC-I reduction solely in the context of infection and that MHC-I levels were not completely restored when cells were infected with a virus mutant lacking both pUL49.5 and pUL56 (Ma et al., 2012). These findings gave rise to the hypothesis that another viral protein partners with pUL56 and participates in downregulation of cell surface MHC-I.

The efforts of our work presented here focused on the identification of viral gene products that contribute to downregulation of MHC-I in cells after EHV-1 infection. By screening a single-gene knockout library of EHV-1, the product of the HSV-1 UL43 homologue was identified to potently block surface MHC-I presentation in EHV-1-infected cells. Further characterization showed that pUL43 is non-essential for virus growth *in vitro* and degraded in lysosomes at later times of infection. pUL43 also localizes to Golgi vesicles and requires its four C-terminal transmembrane (TM) domains for proper intracellular distribution. We also found that a unique hydrophilic domain of EHV-1 pUL43 is indispensible for reducing MHC-I levels. Finally, co-transfection of pUL43 and pUL56 resulted in robust inhibition of cell surface MHC-I expression. Taken together, these results suggest a novel mechanism by which alphaherpesviruses utilize a combination of viral transmembrane proteins to negatively regulate MHC-I antigen presentation and achieve immune evasion.

3.3 Materials and methods

3.3.1 Cells and viruses

Equine dermal (NBL6) cells were propagated in Eagle's minimum essential medium (EMEM; Biochrom AG) supplemented with 20% fetal calf serum (FCS; Biochrom AG), 1% Pen/Strep (100 U/ml penicillin, 100 µg/ml streptomycin; Sigma-Aldrich), 1 mM sodium pyruvate and 1 X non-essential amino acids (Biochrom AG). RK13 (rabbit kidney) cells, HeLa (human epithelial carcinoma) cells and HEK293 (human embryonic kidney) cells were grown in EMEM containing 5% FCS and 1% Pen/Strep. RK13 cells that constitutively express either the ER marker calreticulin or the Golgi marker β-1,4-galactosyltransferase fused to enhanced green fluorescent protein (EGFP) were generated by transfection of the plasmids pER-EGFP and pGolgi-EGFP, respectively, which were kindly provided by Dr. Michael Veit (Freie Universität Berlin, Germany). The transfected cell lines were purified and maintained in the medium for RK13 cells supplemented with 500 µg/ml G418 disulfate salt (Sigma-Aldrich). The parental and mutant viruses were derived from EHV-1 strain Ab4, which was cloned as

an infectious bacterial artificial chromosome (BAC). The BAC for Ab4 virus (pAb4) contains a mini-F cassette in which the *egfp* gene is driven by the HCMV IE promoter (Goodman et al., 2007). Viruses were reconstituted by transfection of BAC DNA into RK13 cells with polyethylenimine (PEI) (Polysciences) as previously described (Ma et al., 2012). To delete the *egfp* gene from viral genome, RK13 cells expressing Cre were infected with the engineered virus at a multiplicity of infection (MOI) of 0.0001 (Azab et al., 2009). Non-fluorescent viral plaques were picked for purification on RK13 cells. Unless otherwise indicated, RK13 cells were used for virus propagation and titration.

3.3.2 Antibodies and reagents

Rabbit anti-β-actin (13E5) monoclonal antibody (MAb), rabbit and mouse anti-hemagglutinin (HA) tag MAbs were purchased from Cell Signaling Technologies. Rabbit polyclonal antibodies (PAbs) against EHV-1 pUL56 were prepared previously (Ma et al., 2012). Rabbit anti-EHV-1 IR6 PAbs, anti-EHV-1 gM (F6) and anti-EHV-1 gC (2A2) MAbs were used as in our earlier studies (Osterrieder, 1999; Osterrieder et al., 1996a; Osterrieder et al., 1996b). Mouse anti-MHC-I MAb specific for an equine haplotype (CZ3) was kindly provided by Dr. Douglas F. Antczak (Cornell University, Ithaca). Mouse anti-HLA class I (W6/32) MAb was a gift from Dr. Hartmut Hengel (Universität Freiburg, Germany). Mouse anti-CD58 MAb was obtained from Biolegend. Mouse IgG isotype control was from Santa Cruz Biotechnology. Alexa Fluor 647 or 568-labeled goat anti-mouse immunoglobulin G (IgG), Alexa Fluor 488-labeled goat anti-rabbit and goat anti-mouse IgG were produced by Invitrogen. Horseradish peroxidase (HRP)-conjugated goat anti-mouse and goat anti-rabbit IgG were obtained from Southern Biotech. Phosphonoacetic acid (PAA), an inhibitor for viral DNA synthesis was obtained from Alfa Aesar. Chloroquine and Lactacystin were purchased from Sigma-Aldrich. Restriction enzymes were supplied by New England Biolabs.

3.3.3 Engineering of BAC mutants

The pAb4 BAC was maintained in *Escherichia coli* GS1783 cells that were grown in Luria-Bertani (LB) broth in the presence of 30 μg/ml chloramphenicol (Ma et al., 2012). Genetic modification of the BAC was performed by *en passant* mutagenesis exactly as described (Tischer et al., 2006). To start the mutagenesis, a fragment flanked by homologous arms for the target region was PCR-amplified using a kanamycin resistance (*Kan*^{r}) gene present in the pEP-Kan-S2 plasmid using the primers in Table 1. After gel electrophoresis, PCR products were purified and subjected to *Dpn*I digest to eliminate residual plasmid. GS1783 competent cells were electroporated with the PCR products and incubated at 32^{o}C for 48 h. Kanamycin-resistant colonies were screened by restriction fragment length polymorphism (RFLP) analysis and compared to the predicted digestion pattern. Correct

intermediates were used for a second round of Red-mediated recombination in the presence of 1% L-(+)-Arabinose (Alfa Aesar) that induced removal of the *Kan*^{r} sequence from the BAC construct. Following the resolution step, candidate colonies were examined by RFLP and confirmed by DNA sequencing (LGC sequencing service). The BAC DNA from desired colonies was prepared by standard alkaline lysis (Sambrook et al., 1989) and applied for virus reconstitution.

Table 3.1 List of primers for viral mutagenesis, plasmid construction and DNA sequencing

Primers	Sequence (5'-3')
BAC muatagenesis	
43STOP_Fw[a]	CAAAGGTTGGCTTGCTACATCAAGGTTATCAATCATGATG***TAA***CAGCCAGATAGAGAGCCCGGTAGGGATAACAGGGTAATCGAT
43STOP_Rv	GCACCAGACACGAGTCTTCACCGGGCTCTCTATCTGGCTG***TTA***CATCATGATTGATAACCTTGCCAGTGTTACAACCAATTAACC
43Rev_Fw[b]	CAAAGGTTGGCTTGCTACATCAAGGTTATCAATCATGATG***TAC***CAGCCAGATAGAGAGCCCGGTAGGGATAACAGGGTAATCGAT
43Rev_Rv	GCACCAGACACGAGTCTTCACCGGGCTCTCTATCTGGCTG***GTA***CATCATGATTGATAACCTTGCCAGTGTTACAACCAATTAACC
HA43_Fw[c]	CAAAGGTTGGCTTGCTACATCAAGGTTATCAATCATGATGTACCCATACGACGTCCCAGACTACGCTTACCAGCCAGATAGAGAGCCCCAGTGTTACAACCAATTAACC
HA43_Rv	CCAGACACGAGTCTTCACCGGGCTCTCTATCTGGCTGGTAAGCGTAGTCTGGGACGTCGTATGGGTACATCATGATTGATAACCTTGTAGGGATAACAGGGTAATCGATT
HA_ΔN_43_Fw	ATCAATCATGATGTACCCATACGACGTCCCAGACTACGCTAAAGCTTTCGTTGGAATCGGTAGGGATAACAGGGTAATCGATT
HA_ΔN_43_Rv	TGAGGACGCAAGCTTGTAGTCCGATTCCAACGAAAGCTTTAGCGTAGTCTGGGACGTCGTCCAGTGTTACAACCAATTAACC
Expression vectors	
pUL43/UL43s-EGFP	
pUL43-EGFP_Fw[c]	GC*GAATTC*ACCATGATGTACCCATACGACGTCCCAGACTACGCTTACCAGCCAGATAGAGAGCC
pUL43-EGFP_Rv	CG*GGATCC*ATGTGTGATTATAGTTGCATAACAC
pUL43s-EGFP_Rv	CG*GGATCC*CGGCATCTCCTTGAAAAACTTGAAC
pUL43-UL56-P2A-EGFP pHA43_Fw[c]	CG*GGATCC*ACCATGATGTACCCATACGACGTCCCAGACTACGCTTACCAGCCAGATAGAGAGCC
pHA43_Rv	GC*GAATTC*TTTAATGTGTGATTATAGTTGCATAAC
P2A-EGFP_Fw[d]	CG*GAATTC*GGAAGCGGAGCTACTAACTTCAGCCTGCTGAAGCAGGCTGGAGACGTGGAGGAGAACCCTGGACCTATGGTGAGCAAGGGCGAGGAGC
P2A-EGFP_Rv	CG*TCTAGA*TTACTTGTACAGCTCGTCCATG
Sequencing	
UL43_Seq_Fw1	CACTTGTAGAAACACGCCCA
UL43_Seq_Fw2	CGTCATATGCTCAGCCAATG
UL43_Seq_Rv	AACATACCATGCACCAAAGG

[a] Italic bold letters stand for the stop codon introduced to *UL43* gene; [b] Italic bold letters indicate the original codon of *UL43* gene; [c] Underlined nucleotides are sequence for a hemagglutinin epitope; [d] Underlined letters represent the P2A sequence with a GSG linker (italic).

3.3.4 Construction of expression vectors

Full-length UL43 or a truncated form was amplified by PCR using appropriate primers (Table 3.1). For cloning, PCR products were digested with *EcoR*I and *BamH*I and inserted in plasmid pEGFP-N3 (Clontech) to obtain fusion proteins with an EGFP tag at the C-terminus and were termed pUL43-EGFP (wild-type) and pUL43s-EGFP (truncated mutant), respectively. In addition, a construct that allows co-expression of pUL43 and pUL56 was generated. First, a transfer vector containing pUL56 and EGFP was created based on pcDNA3 (Invitrogen), with the two genes connected by a P2A linker. Using the linker, pUL56 and EGFP should be expressed with similar stoichiometry due to the cotranslational “ribosome skipping” event mediated by the P2A peptide. This property and the P2A sequence used for this study have been reported elsewhere (Kim et al., 2011). Specifically, PCR products were amplified using a forward primer containing the P2A sequence and a reverse primer for the *egfp* gene (Table

3.1). After digestion with *EcoR*I and *Xba*I, the purified P2A-EGFP fragment was ligated into the corresponding sites of a pcDNA3 plasmid harboring UL56 plasmid, which resulted in the transfer vector pcUL56-P2A-EGFP. Second, the UL56-P2A-EGFP fragment was released from the transfer plasmid by cutting with *BamH*I and *Xba*I. The chimeric sequence was then inserted into the first cloning site of pVITRO2-mcs-Hygro (InvivoGen) where pUL43 was placed in the second cloning site. Similarly, a co-expression vector for pUL43 and pUL56(AY) was constructed, in which all the PPxY motifs in pUL56 had been mutated to AAxY.

3.3.5 Virus growth properties and plaque morphology

The role of the *UL43* gene in production of progeny virus was evaluated by one-step growth kinetics. Confluent NBL6 cells were infected with the parental virus vAb4G (Goodman et al., 2007), the virus mutant vUL43STOP or its revertant vUL43STOP_R at a multiplicity of infection (MOI) of 3. Cells were incubated at 4^{o}C for 1 h to allow attachment of the viruses then shifted to 37^{o}C for virus entry. After 1.5 h of penetration, infected cells were treated with ice-cold citrate buffer (0.062 M Na_2HPO4, 0.132 M citric acid, 0.5% bovine serum albumin [BSA], pH 3.0) for 30 seconds to remove surface-bound virions that had not entered the cells. After washing with PBS three times, fresh medium was added and the cells were kept at 37^{o}C. To determine the extracellular and intracellular virus titers, supernatants and infected cell pellets were separately harvested at 0, 4, 8, 12, 24, 36 h post infection (p.i.). Samples were titrated on RK13 monolayers and overlaid with 1.5% (w/v) methylcellulose in EMEM. At 72 h p.i. when viral plaques were clearly visible, the methylcellulose was discarded and the cells were fixed with 3.5% paraformaldehyde (PFA) in PBS for 5 min. Plaques were counted after staining with 0.1% (w/v) crystal violet solution. The data were presented as plaque-forming units per ml (PFU/ml) from three independent experiments.

The influence of *UL43* on viral cell-to-cell spread was investigated by measuring plaque sizes. To this end, each virus at an MOI of 0.0001 was inoculated on 6-well plates where RK13 cells were seeded and grown to confluency. After incubation for 2 h at 37^{o}C, residual virus was removed and cell monolayers were covered with 1.5% (w/v) methylcellulose in EMEM. At 72 h p.i., viral plaques were inspected under a Zeiss Axiovert S100 microscope. For each virus, at least 50 plaques were randomly acquired with a digital camera. Diameters of the plaques were measured by the ImageJ program (http://imagej.nih.gov/ij/) using a line tool. The measurements were normalized to those from the parental virus, which were set as 100%. Three independent assays were conducted.

3.3.6 Immunofluorescence and microscopy

Cells were seeded on coverslips and grown to 70-80% confluency. After transfection or infection, cells were fixed in 3.5% PFA in PBS for 5 min and permeabilized with 0.1% Triton X-100 lysis buffer for 10 min. Coverslips were blocked in PBS supplemented with 3% BSA for 2 h at room temperature (RT). Later, cell samples were probed with primary antibodies, including anti-HA MAb (1/200), anti-EHV-1 gC MAb (1/100) and anti-pUL56 PAbs (1/200) for 1 h. After three washes with PBS, cells were reacted with Alexa Fluor 568-conjugated goat anti-mouse IgG (1/500) or Alexa Fluor 488-conjugated goat anti-rabbit IgG (1/500) for another hour at RT. After washing, coverslips were mounted and stained with DAPI medium (Vector Laboratories) on glass slides and examined under a Zeiss Axio Imager M1 microscope or a confocal laser-scanning microscope (LSM510, Zeiss).

3.3.7 Western blotting

Cell lysates were extracted by radioimmunoprecipitation assay (RIPA) buffer (25 mM Tris, pH 7.5, 150 mM NaCl, 1% Nonidet P-40, 0.25% sodium deoxycholate, 0.1% sodium dodecyl sulfate [SDS], 1 mM EDTA) containing protease inhibitor cocktail (Roche) and benzonase (Novagen). Samples were separated by SDS-12% polyacrylamide gel electrophoresis (PAGE) as described before (Huang et al., 2014). After fractionation, proteins were transferred to polyvinylidene difluoride (PVDF) membranes (Carl Roth). To prevent unspecific binding, membranes were blocked in PBS containing 0.05% Tween 20 (PBST) with 5% (w/v) skim milk powder overnight at 4^{o}C. Membranes were then probed with the following primary antibodies: anti-HA MAb (1/1,000), anti-pUL56 PAbs (1/500), anti-EHV-1 IR6 PAbs (1/500), anti-EHV-1 gM MAb (1/500) and anti-β-actin MAb (1/1,000) for 1 h at RT. Membranes were washed with PBST three times and incubated with suitable HRP-conjugated secondary antibodies (1/10,000) for 1 h at RT. After three washing steps with PBST, reactive proteins on membranes were visualized by an enhanced chemiluminescence (ECL) detection kit (Amersham ECL Prime; GE Healthcare).

3.3.8 Flow cytometry

Mock-infected, infected or transfected cells were trypsinized and suspended in PBS with 2% FCS. To determine cell surface MHC-I levels, NBL6 cells were incubated with anti-MHC-I (CZ3) MAb (1/50) or isotype control IgG (1/100); alternatively, HeLa or HEK293 cells were incubated with mouse anti-HLA class I (W6/32) MAb (1/50). After 30 min incubation on ice, cells were washed with PBS plus 2% FCS for three times and reacted with Alexa Fluor 647-conjugated goat anti-mouse IgG (1/1,000) for 30 min. At least 10,000 live cells from each sample were analyzed by a FACSCalibur flow cytometry system according to the manufacturer's instructions (BD Biosciences). The data from flow cytometry are presented as mean fluorescence intensity.

3.4 Results

3.4.1 Identification of EHV-1 pUL43 as a novel inhibitor of MHC-I presentation

Our previous studies had shown that pUL56 failed to reduce cell surface expression of MHC-I molecules in the absence of virus infection (Ma et al., 2012), suggesting that there is at least one additional viral gene product that directly or indirectly cooperates with pUL56 to mediate MHC-I downregulation. To identify viral proteins functionally cooperating with pUL56, we engineered a library of 26 single-gene knockout mutants of EHV-1 strain Ab4. The library was based on predictions of gene functions, and we particularly focused on genes that are putatively non-essential for virus growth and expressed with early kinetics. The mutants were generated by insertion of a positive selection marker (*Kan*^{r}) and removal of the respective open reading frames (ORFs) using en passant mutagenesis. The reconstituted viruses were tested for their potential to downregulate expression levels of cell surface MHC-I in equine NBL6 cells (Table 3.2). Among the generated mutant viruses, only the *ORF17*–negative virus was unable to significantly induce downmodulation of cell surface MHC-I levels. The *ORF17* gene product is homologous to HSV-1 pUL43 as established by sequence and structure comparisons (Telford et al., 1992).

Table 3.2 List of deletion mutants that were tested for MHC-I downregulation

Deletion mutant	Homologue of HSV-1 and function	Virus growth[a]	MHC-I recovery[b]
ORF3	N/A, unknown	+	N
ORF4	UL55, unknown	+	N
ORF5	UL54, transcriptional activatior	+	N
ORF8	UL51, unknown	+	N
ORF11	VP22, tegument protein	-	N/A
ORF12	UL48, tegument protein	+	N
ORF13	UL47, tegument protein	-	N/A
ORF14	UL46, unknown	+	N
ORF15	UL45, virion protein	+	N
ORF17	UL43, multiply hydrophobic prote	+	Y
ORF19	UL41, host shutoff virion protein	+	N
ORF23	UL37, unknown	-	N/A
ORF34	N/A, ubiquitinated virion protein	+	N
ORF38	UL23, Thymidine kinase	+	N
ORF40	UL21, unknown	-	N/A
ORF41	UL20, multiply hydrophobic prote	-	N/A
ORF46	UL16, unknown	-	N/A
ORF48	UL14, unknown	-	N/A
ORF51	UL11, myristylated virion protein	-	N
ORF55	UL7, unknown	-	N/A
ORF58	UL4, unknown	+	N
ORF59	N/A, cytosolic virion protein	-	N/A
ORF63	ICP0, transcriptional activator	+	N
ORF68	US2, unknown	+	N
ORF67	N/A, nucleocapsid egress	+	N
ORF76	US9, tegument protein	+	N

[a] The mark (+) means that the deletion mutant could be reconstituted and grew efficiently, while the mark (-) indicates that the deletion mutant could not be rescued; [b] At 6 h p.i., levels of cell surface MHC-I expression in equine NBL6 cells were measured and compared between the individual mutant and parental virus; “Y” means responsible for MHC-I downregulation and “N” means not. N/A: not assessed.

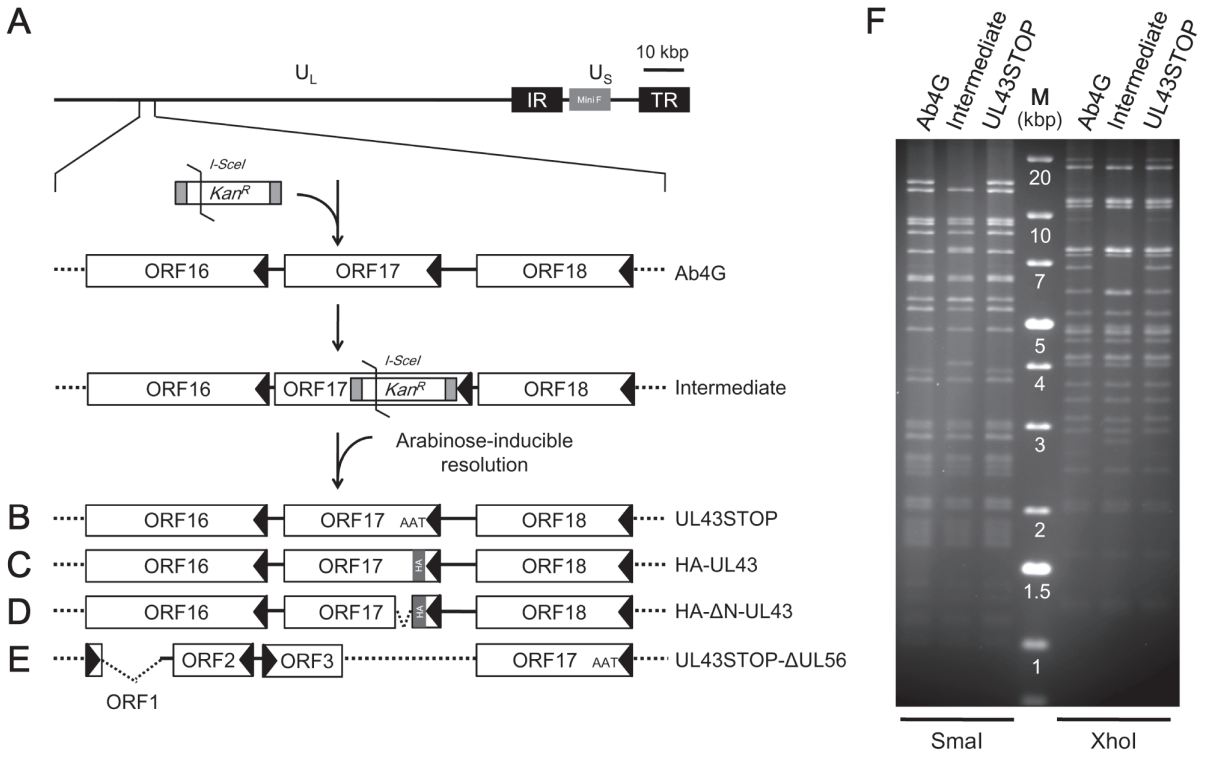

Figure 3.1 Schematic for virus mutagenesis and RFLP analysis of the infectious BAC mutants. **(A)** Parental EHV-1 strain rAb4 was derived from a BAC, which harbors an *egfp* gene driven by the HCMV IE promoter. U_L: Unique long region; U_S: Unique short region; IR: Internal repeats; TR: Terminal repeats. *En passant* mutagenesis was performed to generate the following mutants for the present study: **(B)** UL43STOP, a stop codon TAA in reverse direction was introduced into the *ORF17* gene downstream of the second codon; **(C)** HA-UL43, in which an HA tag (YPYDVPDYA in amino acid sequence) was fused to the N-terminus of ORF17; **(D)** HA-ΔN-UL43, in which amino acids (3-40) at the N-terminus of ORF17 were deleted; **(E)** UL43STOP-ΔUL56, a mutant based on our previous Ab4GΔ1 (Ma, et al., 2012) with introduction of a stop codon into the *ORF17* gene as described above. All mutants were confirmed by DNA sequencing. **(F)** Representative gel of an RFLP analysis. DNA from the parental or indicated BAC mutants was digested with *Sma*I or *Xho*I and separated by electrophoresis using 0.8% agarose gel. Changes in the digestion profile are consistent with those predicted *in silico*.

Given that the selection marker may interfere with expression of neighboring ORFs, we minimized the alterations in the viral genome and abolished expression of pUL43 by replacing the 3rd codon of the ORF (TAC) with a stop codon (TAA, Fig. 3.1A and 3.1B). Prior to virus reconstitution, the pAb4 mutant BAC (pUL43STOP) was confirmed by RFLP (Fig. 3.1E) and DNA sequencing (data not shown). Transfection of pUL43STOP DNA resulted in viable virus and the mutant was termed vUL43STOP. In comparison to the parental virus, the ability of vUL43STOP to induce MHC-I downregulation was substantially attenuated ($P < 0.05$), consistent with the results of the library screening (Fig. 3.2A and 3.2B). When the stop codon introduced at position 3 of the ORF was repaired to the original TAC, the resulting

virus mutant vUL43STOP_R was able to trigger reduction of MHC-I with kinetics and efficiency indistinguishable from those of the parental virus ($P > 0.05$) (Fig. 3.2B). This effect was exclusively mediated by the *UL43* gene, as we confirmed that the expression of the downstream *UL44* (*gC*) gene was not affected by the stop codon (data not shown). Our results demonstrated that pUL43 plays an important role in regulating cell surface expression of MHC-I during virus infection. Furthermore, we found that pUL43 not only exerted this function in equine cells but also induced considerable decrease of cell surface MHC-I expression in human cells (Fig. 3.2C), indicating that pUL43 might govern a conserved pathway in mammalian cells to redistribute MHC-I.

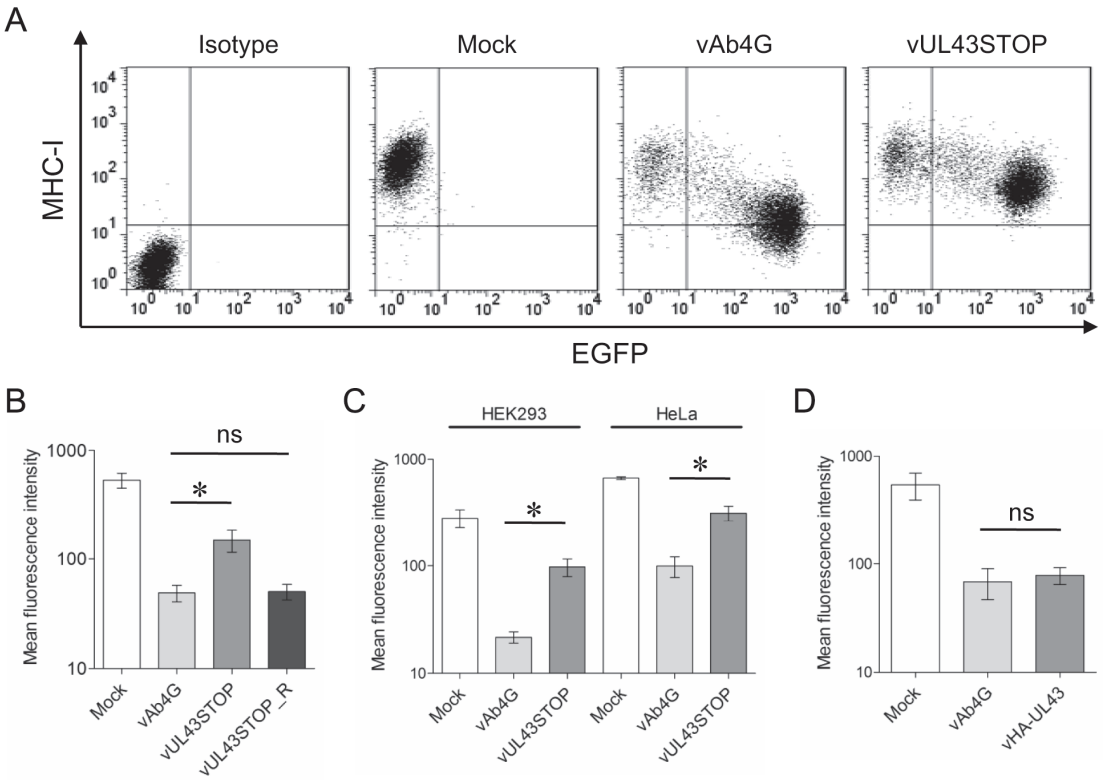

Figure 3.2 pUL43 induces downregulation of cell surface MHC-I. (A) Equine NBL6 cells were infected with vAb4G or vUL43STOP virus at an MOI of 3. At 6 h p.i., cells were analyzed using flow cytometry after incubation with mouse anti-MHC-I (CZ3) MAb and Alexa Fluor 647-labeled goat anti-mouse IgG. Representative dot plots are derived from three independent experiments. **(B)** vAb4G, vUL43STOP or vUL43STOP_R virus was used to infect NBL6 cells at an MOI of 3. Surface MHC-I levels were measured after 6 h p.i. as described above. **(C)** At 16 h p.i., HEK293 and HeLa cells infected with vAb4G or vUL43STOP virus were probed with mouse anti-HLA class I (W6/32) MAb and subjected to flow cytometry. **(D)** NBL6 cells were exposed to infection with vHA-UL43 mutant. At 6 h p.i., cells were analyzed after incubation with mouse anti-MHC-I (CZ3) MAb and staining with Alexa Fluor 647-labeled goat anti-mouse IgG. All experiments were independently performed in triplicate and analyzed using the Student's *t* test. Data are presented as means ± standard deviations (error bars). Asterisk (*) represents statistical significance ($P < 0.05$); ns means not significant.

To facilitate detection of pUL43 in further experiments and due to the lack of a specific antibody, we constructed a virus mutant, named vHA-UL43, in which the N-terminus of pUL43 was tagged with an HA epitope (YPYDVPDYA) (Fig. 3.1C). With inclusion of the HA sequence, the virus mutant was still able to induce reduction of cell surface expression of MHC-I and did so as efficiently as the parental virus *(P* > 0.05) (Fig. 3.2D).

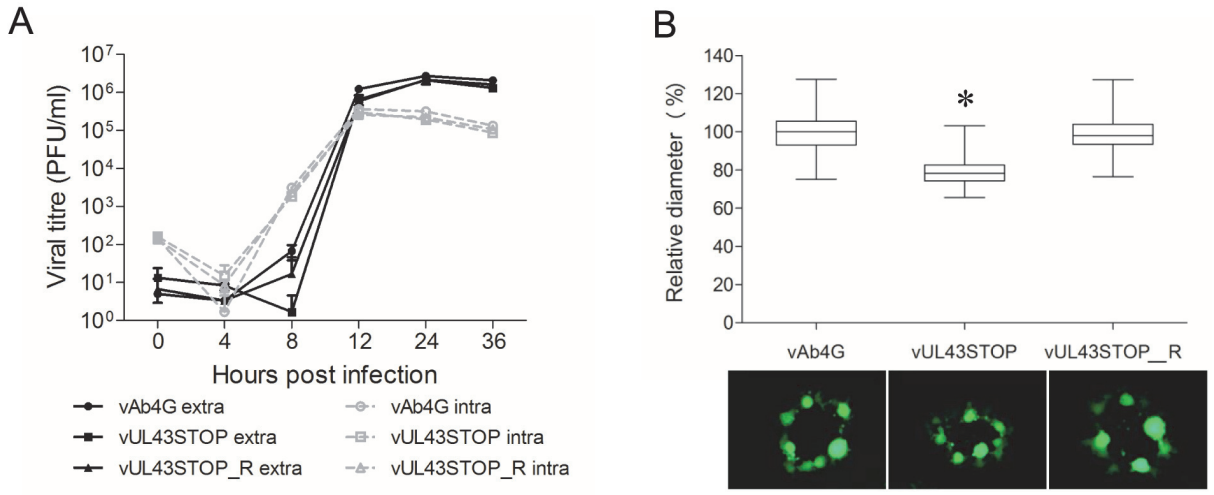

Figure 3.3 Effects of pUL43 on virus replication and cell-to-cell spread. (A) Single-step growth kinetics. NBL6 cells were infected with the parental virus vAb4G, vUL43STOP or revertant vUL43STOP_R at an MOI of 3. At the indicated times following infection, supernatants and cell pellets were harvested for determination of extracellular and intracellular titers, respectively. Data are from triplicate measurements and expressed as means ± standard deviations (error bars). **(B)** Comparison of plaque sizes. Individual viruses were used to infect RK13 cells at an MOI of 0.0001 and overlaid with methylcellulose. Three days after infection, images of at least 80 plaques for each virus were acquired with a camera. The plaque diameter of vAb4G was set as 100% and then the relative plaque sizes for other viruses were calculated. Representative phenotype of viral plaque is shown (green). Statistical significance ($P < 0.05$) is marked with an asterisk (*).

3.4.2 Abrogation of pUL43 does not impair virus production but slightly affects cell-to-cell spread

It was unknown whether pUL43 is required for EHV-1 replication in horse fibroblasts. We, therefore, performed one-step growth assays with the parental virus vAb4G, mutant vUL43STOP and revertant vUL43STOP_R on equine NBL6 cells. At the indicated times after infection, extracellular and intracellular titers were determined. With respect to the production of virus progeny, there was no significant difference between the virus mutants lacking *UL43* (*ORF17*) (Fig. 3.3A), suggesting that pUL43 is non-essential for virus replication. In parallel, we analyzed the effects of pUL43 on viral cell-to-cell spread by measuring plaque sizes. The average diameter of plaques induced by vUL43STOP was approximately 20% smaller than those of the parental virus ($P < 0.05$). Repair of the stop codon in pUL43 restored plaque

formation to the morphology seen for the parental virus (Fig. 3.3B). These results demonstrate that pUL43 is non-essential for virus growth but involved in virus spread between cells. Our findings are in agreement with the earlier studies on PRV and HSV-1, in which deletion of *UL43* proved dispensable for virus growth *in vitro* (Klupp et al., 2005; MacLean et al., 1991; Powers et al., 1994).

3.4.3 Determination of the pUL43 expression pattern and degradation in lysosomes

In earlier reports on HSV-1 and PRV *UL43*, mRNA was detected as early as 2 h p.i. even in the presence of phosphonoacetic acid (PAA), an inhibitor of viral DNA synthesis (Carter et al., 1996; Powers et al., 1994). However, the expression kinetics of pUL43 throughout an infection cycle has not been addressed in detail. Detection of pUL43 homologues by SDS-PAGE and western blot analysis is complicated by the fact that they are predicted to be highly hydrophobic polypeptides, which presents problems for the design and generation of specific antibodies. After repeated failure to raise antibodies to EHV-1 pUL43, we decided to fuse an HA tag with the N-terminus of the target protein. As mentioned before, insertion of this epitope into the virus mutant (vHA-UL43) did not impair pUL43 function in MHC-I downreglation or virus growth. In infected cells, the gene product of pUL43 was expressed as a specific moiety of 34 kDa that could be detected from 2 h p.i. and the amount of protein continued to increase until the 8 h time point; afterwards, the levels of detectable protein began to decline (Fig. 3.4A). The single band was considered specific although it is considerably smaller in apparent molecular weight compared to the predicted Mr of 43,000. To determine the temporal class of pUL43 expression, viral DNA synthesis was chemically inhibited with PAA, which noticeably inhibited the expression of pUL43 as well as the production of gM that was used as a control. In contrast, the levels of the product of the early IR6 gene were not affected by PAA treatment (Fig. 3.4A).

To determine whether pUL43 is degraded at later times of infection, we used different inhibitors to block the pathways responsible for breakdown of cellular proteins. Our results showed that expression levels of pUL43 were stabilized when infected cells were incubated with chloroquine, an inhibitor of lysosomes. In contrast, lactacystin that inhibits the proteasome did not protect pUL43 from degradation (Fig. 3.4B). Next, a combination of PAA and chloroquine was used to confirm whether pUL43 is indeed an early protein. Compared to the treatment with PAA alone, supplement of chloroquine in the presence of PAA resulted in increased levels of pUL43 in infected cells (Fig. 3.4C). From these data, we concluded that pUL43 is an early gene product and directed to the lysosomal pathway for degradation at later times of infection.

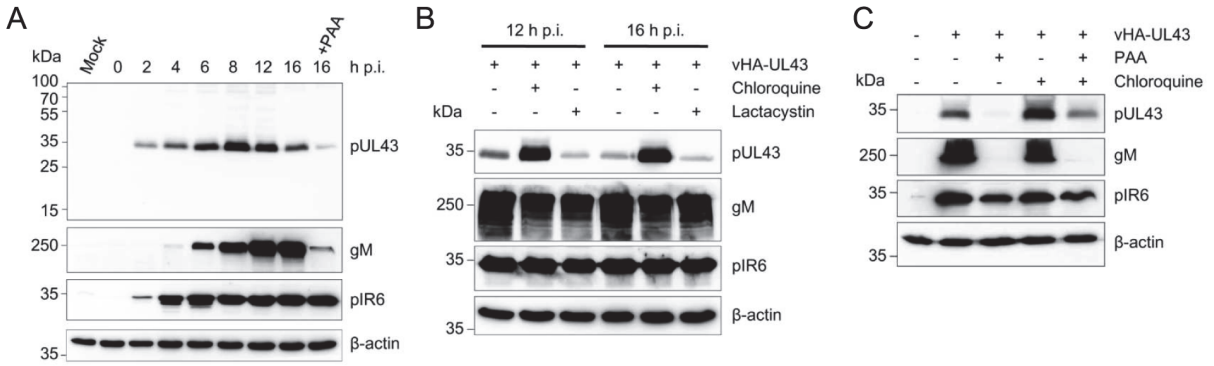

Figure 3.4 Determination of pUL43 expression pattern and degradation by lysosomes. (A) Expression profile of pUL43 after infection. Cells were mock-infected or infected with vHA-UL43 at an MOI of 3 in the absence or presence of PAA. Samples were harvested at different times p.i. **(B)** Lysosomes rather than proteasomes are responsible for degradation of pUL43. After infection, cells were maintained in culture media supplemented with 150 μM of chroloquine or 5 μM of lactacystin, respectively, for 12 h and 16 h. **(C)** pUL43 is an early gene product and subjected to lysosomal degradation during infection. Infected cells were treated with PAA, chroloquine or with both inhibitors for 12 h. To detect proteins, cell lysates were prepared in RIPA buffer. After separation by SDS-12% PAGE, proteins were transferred to PVDF membranes and incubated with anti-HA MAb, anti-gM MAb or anti-pIR6 PAbs. The immunoblots were developed by enhanced chemiluminescence. β-actin was included as a loading control. Molecular mass markers were run for each blot in parallel and sizes indicated as kDa.

3.4.4 pUL43 is present in the Golgi and requires the transmembrane domains at the C-terminus for correct localization

As the intracellular distribution of pUL43 was poorly defined, we performed indirect immunofluorescence microscopy to follow pUL43 subcellular distribution. RK13 cell lines that constitutively express EGFP-conjugated β-1,4-galactosyltransferase or calreticulin were generated by transfection and selection in the presence of G418. Calreticulin and β-1,4-galactosyltransferase are commonly used markers for the ER and Golgi compartments, respectively (Gelebart et al., 2005; Russo et al., 1992). To avoid conflicts of EGFP signals during visualization, the mini-F cassette present in vHA-UL43 was excised by Cre-mediated recombination, resulting in a modified virus vHA-UL43_M that lacks EGFP expression in infected cells. RK13 cells expressing the individual compartment markers were infected with vHA-UL43_M. After reaction with anti-HA monoclonal antibody, pUL43 was found to predominantly localize to the Golgi apparatus. Moreover, the Golgi complex seemed partially fragmented and pUL43 became dispersed into vesicles in infected cells (Fig. 3.5A). In contrast, pUL43 was not apparently associated with structures that expressed the ER marker (Fig. 3.5B). In transiently transfected cells, pUL43 was still distributed in a vesicular fashion, which is consistent with the observations in infected cells (Fig. 3.5D).

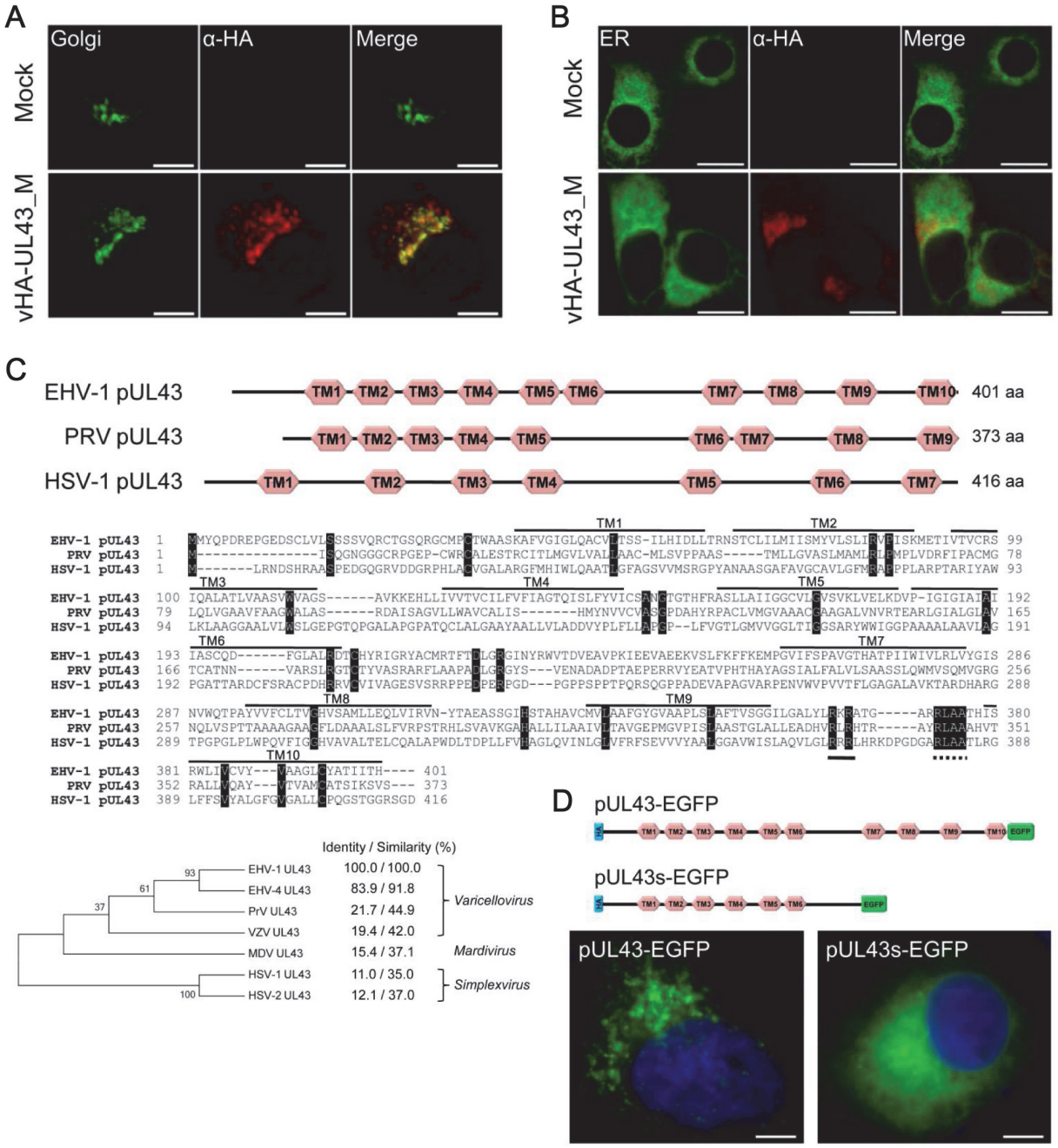

Figure 3.5 Subcellular localization of pUL43 and the role of TM domains at the C-terminus. (A) Cells expressing EGFP-labeled β-1,4-galactosyltransferase, a Golgi marker (green). **(B)** Cells expressing EGFP-labeled calreticulin, an ER marker (green). The two cell lines were mock-infected or infected with vHA-UL43_M virus. At 6 h p.i., samples were fixed with 3.5% PFA in PBS and then permeablized with 0.1% Triton X-100. A confocal laser scan microscope was used to visualize the expression of pUL43 after sequential incubation with anti-HA MAb and Alex Fluor 568-conjugated goat anti mouse IgG (red). Scale bar: 10 µm. **(C)** Domains of pUL43 homologues and phylogenic analysis. Putative transmembrane (TM) domains were predicted by SOSUI, http://bp.nuap.nagoyau.ac.jp/sosui). Identical amino acids are highlighted in black after multiple sequence alignment with ClustalW 2.0 (http://www.ebi.ac.uk/Tools/msa/clustalw2). The RxR and RLAA motifs are underlined with solid and dotted lines, respectively. Sequences of pUL43 proteins were derived from

(Figure 3.5 continued) GenBank, including EHV-1 (YP_053062), EHV-4 (NP_045234), PRV (AFI70808), VZV (NP_040138), MDV (YP_001033972), HSV-1 (AER37980) and HSV-2 (NP_044513). The phylogeny tree was constructed using the UPGMA method, after ten-thousand bootstraps were executed by the MEGA 6.0 toolkit. Identity and similarity of the amino acid sequences were calculated using the SIAS online tool with default settings (http://imed.med.ucm.es/Tools/sias.html). **(D)** Expression of pUL43 and the truncated mutant lacking 4 TM domains at the C-terminus. At 24 h after transfection with the indicated plasmids (green), cells were fixed and stained with DAPI (blue). Images were acquired using an upright fluorescence microscope under a 100X oil objective. Scale bar: 5 μm.

Structurally, the C-terminus of pUL43 homologue contains 4 putative TM domains, which are more conserved than those at the N-terminus in terms of their relative positions of amino acids. Additionally, two motifs, RxR and RLAA, were identified within the C-terminus, which are conserved amongst related viruses (Fig. 3.5C). When the protein was truncated by removal of these four predicted TM regions, the shortened pUL43 appeared with a diffuse pattern in the cytoplasm after transfection of an expression plasmid (Fig. 3.5D). Taken together, these data demonstrated that pUL43 primarily localizes to the Golgi network and suggested that at least one of the four predicted TM domains at the C-terminus are required for correct subcellular localization.

3.4.5 The hydrophilic domain at the N-terminus plays a critical role in MHC-I downregulation mediated by pUL43

The pUL43 homologues of HSV-1 and PRV are predicted to represent type III transmembrane proteins (MacLean et al., 1991; Powers et al., 1994) (Fig. 3.5C). Apart from 10 putative TM regions, the topology of EHV-1 pUL43 is characterized by a unique hydrophilic domain at its N-terminus and an extremely short C-terminal domain. In addition, *in silico* analyses revealed that no cleavable signal sequence is present, which led us to investigate the possible involvement of the flexible domain in pUL43-mediated downregulation of MHC-I. Using *en passant* mutagenesis, the region encompassing amino acids 3 to 40 was deleted, resulting in the vHA-ΔN-UL43 virus mutant (Fig. 3.1D). In infected cells, the pUL43 mutant lacking the N-terminus appeared more focally localized and was present in fewer vesicles compared with the full-length protein (Fig. 3.6A). Flow cytometry showed that expression of cell surface MHC-I was higher in cells infected with vHA-ΔN-UL43 or vUL43STOP, whereas dramatic reduction of MHC-I levels was induced by vHA-UL43 ($P < 0.05$) (Fig. 3.6B). These results suggest that the hydrophilic N-terminus is essential for the function of pUL43, possibly by modulating intracellular sorting and/or trafficking of pUL43.

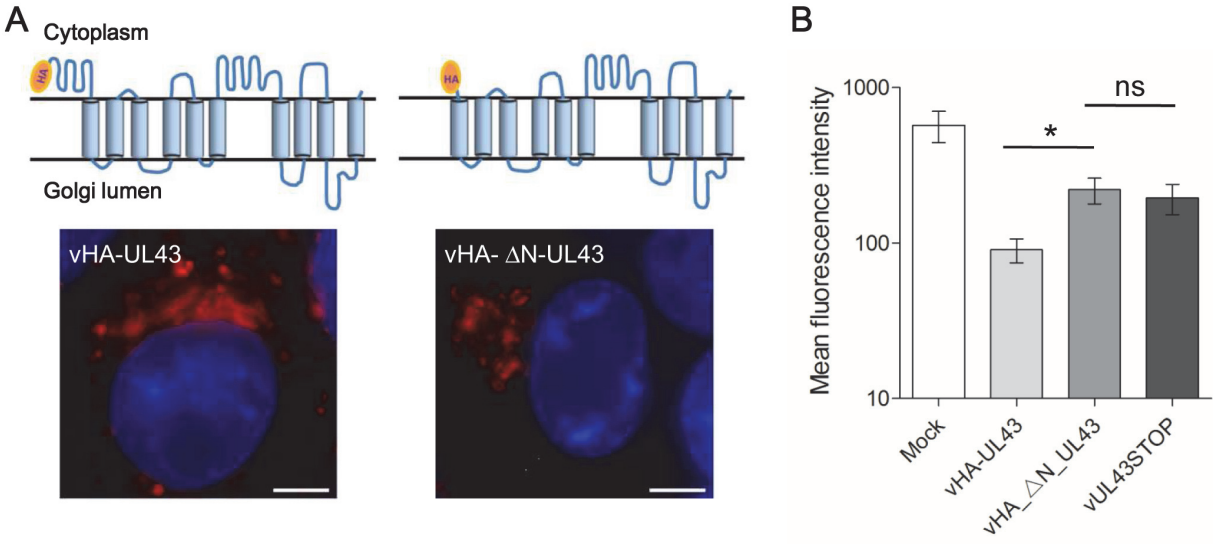

Figure 3.6 The hydrophilic domain at the N-terminus plays a critical role in MHC-I downregulation mediated by pUL43. (A) Putative structures of the pUL43 and the mutant lacking the N-terminal 40 amino acids. Cells were infected with virus vHA-UL43 or mutant vHA-ΔN-UL43. At 6 h p.i., cells were incubated with anti-HA MAb and visualized after staining with Alex Fluor 568-conjugated goat anti mouse IgG (red) and DAPI (blue). Coverslips were inspected with a 100X oil objective. Scale bar: 5 µm. **(B)** Virus vHA-UL43, vHA-ΔN-UL43 or vUL43STOP was used to infect NBL6 cells for 6 h. Cellsells were collected for flow cytometry and triplicate assays were performed independently. Data are expressed as means ± standard deviations (error bars). Differences between various treatments were evaluated by Student's *t* test. Asterisk (*) represents the significant level ($P < 0.05$); ns indicates no significant difference.

3.4.6 pUL43 and pUL56 cooperate to downregulate cell surface MHC-I in transfected cells

Altough pUL56 was shown to be an inhibitor of cell surface MHC-I presentation at early times of EHV-1 infection, this effect could not be achieved by transfection of a UL56 expression vector (Ma et al., 2012). As pUL43 and pUL56 share similarities in terms of intracellular localization and expression patterns and deletion of both genes in one virus did not have an additive effect (Fig. 3.1E and Fig. 3.7A), we hypothesized that the two proteins cooperate to trigger downregulation of MHC-I molecules. To test our hypothesis, an expression vector was constructed, which allows expression of pUL43 and pUL56 from a single vector. In addition, we introduced a self-cleavable EGFP marker that was separated from pUL56 by a P2A sequence to facilitate detection of transfected cells (Fig. 3.7B). We also replaced all PPxY motifs of pUL56 with AAxY elements in this plasmid, resulting in the pUL56(AY) mutant (Fig. 3.7C).

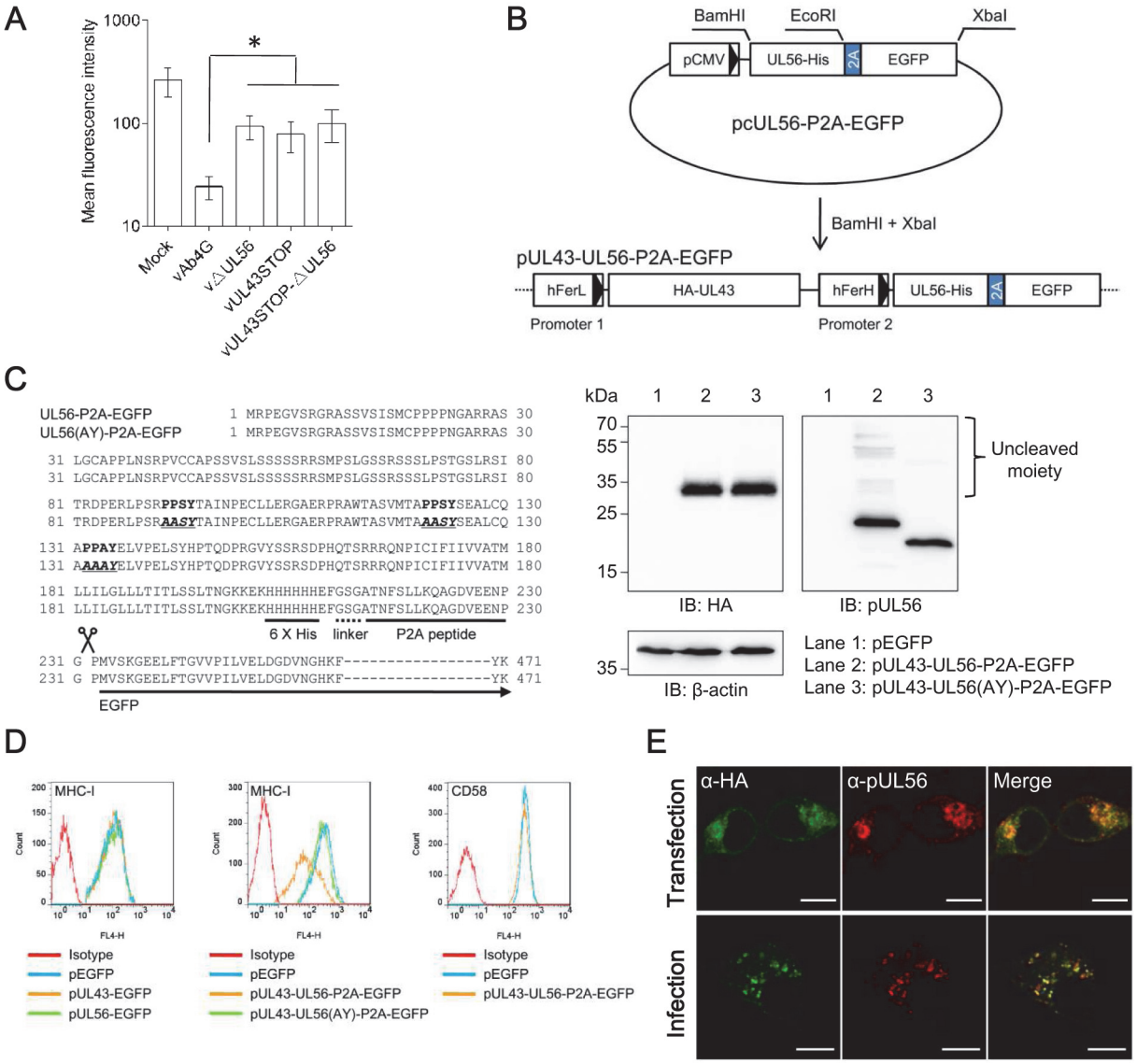

Figure 3.7 Downregulation of MHC-I is induced by co-expression of pUL43 and pUL56 in transfected cells. (A) Deletion of both pUL43 and pUL56 does not induce additional increase of MHC-I expression. NBL6 cells were infected with individual viral mutant at an MOI of 3. At 6 h p.i., levels of cell surface MHC-I were measured by flow cytometry. There is no significant difference between single and double deletion mutants. Asterisk (*) indicates statistical significance ($P < 0.05$). **(B)** Strategy of engineering the co-expression vectors with a self-cleavable EGFP marker. The P2A sequence was inserted between pUL56 and EGFP. The fragment of pUL56-P2A-EGFP was subcloned into the pVITRO-UL43 vector after digestion with *BamH*I and *Xba*I. **(C)** Sequence alignment and detection of the co-expression vectors. Mutations are highlighted in bold and italics. HEK293 cells were transfected with the indicated vectors. At 24 h, expression of individual gene was detected by immunoblotting (IB), following incubation with anti-HA MAb and anti-pUL56 PAbs, respectively. β-actin was used as a loading control. **(D)** Downregulation of MHC-I caused by pUL43 and pUL56. HEK293 cells were transfected with 500 ng of different expression plasmids. At 24 h, cells were harvested and processed for flow cytometry analysis. Anti-HLA class I MAb (W6/32) was used to react with cell surface MHC-I. CD58 was included as a negative control. Representative histograms

(Figure 3.7 continued) are from three independent assays. **(E)** Colocalization of pUL43 with pUL56. HEK293 cells were transfected with plasmid pUL43-pUL56-P2A-EGFP for 24 h (upper). NBL6 cells were infected with vHA-UL43 virus for 6 h (lower). Samples were fixed with ice cold acetone until the EGFP fluorescence was quenched. After reaction with anti-HA MAb and anti-pUL56 PAbs, the coverslips were stained with Alexa Fluor 488-labeled goat anti-mouse IgG (green) and Alexa Fluor 568-labeled goat anti-rabbit IgG (red). Images were captured by a confocal microscope with a 60X oil objective. Scale bar: 10 μm.

At 24 h after transfection, pUL43 and pUL56 or pUL56(AY) were detectable by western blotting. As expected, some of the pUL56/UL56(AY)-P2A- EGFP protein was not completely cleaved and migrated more slowly as determined by SDS-PAGE (Fig. 3.7C). Separate expression of pUL43 or pUL56 did not induce downregulation of cell surface MHC-I (Fig. 3.7D; left panel). However, a dramatic reduction of cell surface MHC-I molecules was observed in cells expressing both wild-type pUL43 and pUL56. In contrast, levels of cell surface MHC-I remained stable in cells co-expressing pUL43 and pUL56(AY) (Fig. 3.7D; middle panel). Expression levels of CD58, which was used as a negative control, were not affected by co-expression of pUL43 and pUL56 (Fig. 3.7D; right panel). To further assess the cooperation of pUL43 and pUL56, we performed indirect immunofluorescence followed by confocal microscopy and found that pUL43 colocalized with pUL56 in transfected as well as infected cells (Fig. 3.7E). These results are consistent with the conclusion that pUL43 cooperates with pUL56 to specifically induce downregulation of MHC-I on the cell surface in transfected and infected cells.

3.5 Discussion

Antagonizing the MHC-I presentation pathway is an effective strategy to achieve immune evasion and a result of the long co-evolution of herpesviruses and their respective hosts. Different members of the *Herpesviridae* family encode a variety of viral proteins to reduce MHC-I molecules on the cell surface and they achieve this by exploiting diverse mechanisms. In the *Alphaherpesvirinae*, the ICP47 homologue of HSV-1 was the first protein identified that blocks peptide binding by direct interaction with TAP (Fruh et al., 1995). Likewise, the pUL49.5 homologues from the varicelloviruses, including bovine herpesvirus type 1 (BoHV-1), PRV, EHV-1 and EHV-4, interfere with the activity of TAP either by proteasomal degradation and/or by inhibiting the affinity of ATP to TAP (Koppers-Lalic et al., 2005; Koppers-Lalic et al., 2008). It is noted that the ICP47 homologues are absent in varicelloviruses, but the pUL49.5 homologue of HSV-1 cannot mediate MHC-I downregulation (Koppers-Lalic et al., 2005), suggesting that suppression of MHC-I pathway by a particular gene product can be restricted to specific viruses and that it is not the action of an individual protein but the end result that is conserved. Moreover, the US3 kinases of VZV,

PRV and HSV-1 have also been demonstrated to be necessary for induction of downregulation of MHC-I during productive infection (Deruelle et al., 2009; Eisfeld et al., 2007; Imai et al., 2013). The mechanisms by which pUS3 homologues achieve downregulation vary greatly between viruses and were shown to be highly dependent on the particular cell type infected. Therefore, it is necessary to explore the entire repertoire of viral genes that hold the potential of blocking MHC-I presentation based on the virus species of interest.

In our previous studies, the pUL56 homologue of EHV-1 was identified as a novel viral protein that modulates presentation of MHC-I molecules at the cell surface by accelerating dynamin-dependent endocytosis (Huang et al., 2014). However, pUL56 alone is not sufficient to induce downregulation of MHC-I as it did so only in the context of viral infection, implying that either direct or indirect interaction of a viral protein(s) with pUL56 is required for MHC-I depletion. To test this hypothesis, we screened a single gene knock-out library of EHV-1 and focused on genes that were predicted to be non-essential for virus growth and not well defined with respect to function. These efforts led to identification of a viral *ORF17* gene encoding the pUL43 homologue that we then showed to be involved in downregulation of MHC-I at early times of infection, coinciding with the time when pUL56 was shown to exert its function. Given that this is the first description of EHV-1 pUL43, we characterized its role in virus growth and examined its expression pattern and subcellular localization. We found that insertion of a stop codon within the open reading frame of pUL43 had little effect on virus growth in vitro and only mildly inhibited virus spread between cells. These findings on EHV-1 pUL43 are in agreement with its counterparts in HSV-1 and PRV (Klupp et al., 2005; MacLean et al., 1991; Powers et al., 1994). Due to the difficulty in generation of specific antibodies, the expression profiles of pUL43 homologues have not been well determined and most of the available studies only focused on detection of mRNA transcripts. Treatment with PAA to inhibit viral DNA synthesis revealed that mRNA transcripts of pUL43 homologues in HSV-1 and PRV are produced with early kinetics and detectable as early as 2 h p.i. (Carter et al., 1996; Powers et al., 1994). However, our expression kinetics showed that the production of pUL43 in cells after EHV-1 infection was reduced when viral DNA synthesis was blocked, suggesting that pUL43 could also be expressed as a late protein. However, in light of our observation that the pUL43 protein is degraded in lysosomes at later times of infection we currently surmise that pUL43 does represent a *bona fide* early and not a late protein and that the reduced expression levels under PAA treatment are a result of degradation. This conclusion is supported by an experiment in which addition of lysosome inhibitors resulted in levels of pUL43 that were only marginally affected in the presence of PAA (Fig. 3.4C). It is noteworthy that EHV-1 pUL43 is expressed as a single species without any detectable post-translational modifications regardless of infection or transfection; however, the protein migrates faster than predicted from its predicted molecular weight. This anomalous mobility

as assessed after SDS-PAGE gel is commonly seen in all studied pUL43 homologues (Carter et al., 1996; Klupp et al., 2005). A reasonable interpretation for this migration anomaly is that pUL43 exhibits extraordinary hydrophobicity and, consequently, may not be fully accessible to the detergent (Nybo, 2012). In this case, non-denatured pUL43 protein could aggregate and migrate with a mobility that is faster than expected. This abnormal mobility would certainly make difficult the identification of post-translational modification including ubiquitination.

Phylogenetic analysis predicts that pUL43 homologues are conserved in the *Alphaherpesvirinae* (Klupp et al., 2005). pUL43 homologues commonly consist of multiple TM regions, but have different numbers of TM domains and share low amino acid identity (Fig. 3.5C). To ascertain the intracellular localization of pUL43, we applied confocal microscopy, which revealed that pUL43 is primarily located to the Golgi apparatus, which appears to be critically dependent on the most conserved TM domains at the C-terminus of the protein. The pUL43 homologue of PRV is present in vesicles and inhibits syncytium formation, indicating that it might be involved in trafficking of membrane proteins and vesicles (Klupp et al., 2005). The Golgi is an organelle that directs sorting and trafficking of proteins (Fullekrug and Nilsson, 1998; Joyce, 1997), such as the mature MHC-I complex. Evidenced by localization of pUL56 to the Golgi network and its role in inhibiting MHC-I presentation (Ma et al., 2012), it is conceivable that localization of viral proteins to the Golgi compartment to obstruct MHC-I presentation would be an optimal strategy for immune evasion. Our current model predicts that, similar to pUL56, pUL43 is targeted to Golgi and endocytic vesicles. To this end, pUL43 specifies two pivotal domains. Firstly, the association of pUL43 with the Golgi complex is maintained by the TM domains at the C-terminus; secondly, the N-terminal hydrophilic domain determines the localization in vesicles that are involved in directing the intracellular transport of MHC-I molecules.

Although both pUL56 and pUL43 are Golgi-associated viral proteins, neither of them is able to cause downregulation of MHC-I independently. Arguably, the most significant finding of this report is our demonstration that pUL43 and pUL56 collaborate in decreasing cell surface MHC-I molecules (Fig. 3.7). This process requires the PPxY motifs present in the cytoplasmic domain of the type II transmembrane protein pUL56. Similar to HSV-2 pUL56 (Ushijima et al., 2008), the mutated EHV-1 protein also migrated faster as detected by SDS-PAGE when the AAxY motifs were introduced instead of PPxY (Fig. 3.7C). The possibility cannot be excluded that pUL56 is structurally altered, but we currently assume that the aberrant mobility is caused by difference in electric charge, similar to the HSV-2 orthologue. The changes may also be caused by the presumably absent interaction between EHV-1 pUL56 and Nedd4. Due to technical limitations, we did not further investigate the mechanisms that regulate MHC-I reduction after co-transfection of pUL43 and pUL56, but we favor a model in which pUL43

and pUL56 orchestrate sorting of MHC-I to and degradation in endo-lysosomes, which is mainly based on colocalization of pUL43 and pUL56 (Fig. 3.7E) and experimental evidence elsewhere that includes the following: (i) PPxY motifs are required for the interaction of pUL56 with the cellular E3 ubiquitin ligase Nedd4 (Ushijima et al., 2008); (ii) Trafficking of viral proteins containing PPxY motifs towards endo-lysosomal pathway requires Nedd4.1-mediated ubiquitination and recruitment of TSG101, a component of the ESCRT-1 complex (endosomal sorting complexes required for transport) (Blot et al., 2004); (iii) Nedd4 is known to ubiquitinate proteins with multiple transmembrane domains such as ion channels, thereby facilitating endocytosis and degradation (Bongiorno et al., 2011). It is conceivable that pUL43 is modified similarly and acts as an adaptor for MHC I class endocytosis where pUL56 is the recruiter for Nedd4. This interpretation is consistent with the colocalization of pUL56 and MHC-I in Golgi and endosomal vesicles during EHV-1 infection (Huang et al., 2014).

It has been shown that EHV-1 strains differ in their potential to reduce cell surface MHC-I expression. Infection with the Ab4 strain caused severe downregulation of MHC-I molecules, while the levels of surface MHC-I were moderately reduced by infection with the RacL11 strain (Ma et al., 2012). This difference in modulation of MHC-I largely depends on the presence of pUL56, but our results demonstrate that pUL43 and pUL56 cooperate to decrease expression of cell surface MHC-I during virus infection and after transient transfection. We surmise that EHV-1 strains, such as Ab4, which contain full-length pUL43 and pUL56, are likely to cause MHC-I downregulation through interaction between the two proteins. In contrast, RacL11 or other strains lacking pUL56 and/or pUL43 are unable to adopt this immune evasion strategy. Apart from MHC-I, a variety of cell surface molecules might be affected by cooperation of pUL43 with pUL56, as recently pUL56 has been shown to modulate a selection of cell surface markers in equine mesenchymal stem cells after EHV-1 infection (Claessen et al., 2015). In the future, we will address questions on the involvement of pUL43 in MHC-I downregulation by various EHV-1 strains, and the spectrum and functional consequences of pUL43-pUL56 interaction.

In summary, our present study identified a new function for the poorly understood pUL43 homologue of EHV-1. pUL43 has an important role in modulating MHC-I presentation, although it proves dispensable for virus growth and is subjected to lysosomal degradation in the course of infection. Interestingly, combination of pUL56 and pUL43 induces downregulation of cell surface MHC-I independently of viral infection. Our findings open a new aspect of the complex landscape of viral immune evasion and may provide useful insights into rational design of immunotherapies against EHV-1 infection.

Acknowledgements

We are grateful to Dr. Douglas F. Antczak (Cornell University, USA) for his generous supply of anti-MHC-I (CZ3) MAb. We would also like to appreciate Drs. Maik J. Lehmann and Walid Azab for assistance in confocal imaging. T.H. received financial support from the China Scholarship Council (CSC). The study was supported by DFG grant OS143/3-1 awarded to N.O.

Author contributions

T.H., G.M. and K.O. jointly conceived the study and designed the experiments. T.H. performed all the experiments, analyzed the data and wrote the manuscript. K.O. modified the paper with input from G.M. All authors critically read the paper and gave their final approval to submission.

References

Azab, W., Kato, K., Arii, J., Tsujimura, K., Yamane, D., Tohya, Y., Matsumura, T., Akashi, H., 2009, Cloning of the genome of equine herpesvirus 4 strain TH20p as an infectious bacterial artificial chromosome. Arch Virol 154, 833-842.

Blot, V., Perugi, F., Gay, B., Prevost, M.C., Briant, L., Tangy, F., Abriel, H., Staub, O., Dokhelar, M.C., Pique, C., 2004, Nedd4.1-mediated ubiquitination and subsequent recruitment of Tsg101 ensure HTLV-1 Gag trafficking towards the multivesicular body pathway prior to virus budding. J Cell Sci 117, 2357-2367.

Bongiorno, D., Schuetz, F., Poronnik, P., Adams, D.J., 2011, Regulation of voltage- gated ion channels in excitable cells by the ubiquitin ligases Nedd4 and Nedd4-2. Channels (Austin) 5, 79-88.

Carter, K.L., Ward, P.L., Roizman, B., 1996, Characterization of the products of the U(L)43 gene of herpes simplex virus 1: potential implications for regulation of gene expression by antisense transcription. J Virol 70, 7663-7668.

Claessen, C., Favoreel, H., Ma, G., Osterrieder, N., De Schauwer, C., Piepers, S., Van de Walle. G.R., 2015, Equid herpesvirus 1 (EHV1) infection of equine mesenchymal stem cells induces a pUL56-dependent downregulation of select cell surface markers. Vet Microbiol 176, 32-39.

Deruelle, M.J., Van den Broeke, C., Nauwynck, H.J., Mettenleiter, T.C., Favoreel, H.W., 2009, Pseudorabies virus US3- and UL49.5-dependent and -independent downregulation of MHC I cell surface expression in different cell types. Virology 395, 172-181.

Eisfeld, A.J., Yee, M.B., Erazo, A., Abendroth, A., Kinchington, P.R., 2007, Downregulation of class I major histocompatibility complex surface expression by varicella-zoster virus involves open reading frame 66 protein kinase-dependent and -independent mechanisms. J Virol 81, 9034-9049.

Fruh, K., Ahn, K., Djaballah, H., Sempe, P., van Endert, P.M., Tampe, R., Peterson, P.A., Yang, Y., 1995, A viral inhibitor of peptide transporters for antigen presentation. Nature 375, 415-418.

Fullekrug, J., Nilsson, T., 1998, Protein sorting in the Golgi complex. Biochim Biophys Acta 1404, 77-84.

Gao, G., Luo, H., 2006, The ubiquitin-proteasome pathway in viral infections. Can J Physiol Pharmacol 84, 5-14.

Gelebart, P., Opas, M., Michalak, M., 2005, Calreticulin, a Ca2+-binding chaperone of the endoplasmic reticulum. Int J Biochem Cell Biol 37, 260-266.

Goodman, L.B., Loregian, A., Perkins, G.A., Nugent, J., Buckles, E.L., Mercorelli, B., Kydd, J.H., Palu, G., Smith, K.C., Osterrieder, N., Davis-Poynter, N., 2007, A point mutation in a herpesvirus polymerase determines neuropathogenicity. PLoS Pathog 3, e160.

Hansen, T.H., Bouvier, M., 2009, MHC class I antigen presentation: learning from viral evasion strategies. Nat Rev Immunol 9, 503-513.

Huang, T., Lehmann, M.J., Said, A., Ma, G., Osterrieder, N., 2014, Major histocompatibility complex class I downregulation induced by equine herpesvirus type 1 pUL56 is through dynamin-dependent endocytosis. J Virol 88, 12802-12815.

Imai, T., Koyanagi, N., Ogawa, R., Shindo, K., Suenaga, T., Sato, A., Arii, J., Kato, A., Kiyono, H., Arase, H., Kawaguchi, Y., 2013, Us3 kinase encoded by herpes simplex virus 1 mediates downregulation of cell surface major histocompatibility complex class I and evasion of CD8+ T cells. PLoS One 8, e72050.

Joyce, S., 1997, Traffic control of completely assembled MHC class I molecules beyond the endoplasmic reticulum. J Mol Biol 266, 993-1001.

Kim, J.H., Lee, S.R., Li, L.H., Park, H.J., Park, J.H., Lee, K.Y., Kim, M.K., Shin, B.A., Choi, S.Y., 2011, High cleavage efficiency of a 2A peptide derived from porcine teschovirus-1 in human cell lines, zebrafish and mice. PLoS One 6, e18556.

Klupp, B.G., Altenschmidt, J., Granzow, H., Fuchs, W., Mettenleiter, T.C., 2005, Identification and characterization of the pseudorabies virus UL43 protein. Virology 334, 224-233.

Klupp, B.G., Hengartner, C.J., Mettenleiter, T.C., Enquist, L.W., 2004, Complete, annotated sequence of the pseudorabies virus genome. J Virol 78, 424-440.

Koppers-Lalic, D., Reits, E.A., Ressing, M.E., Lipinska, A.D., Abele, R., Koch, J., Marcondes

Rezende, M., Admiraal, P., van Leeuwen, D., Bienkowska-Szewczyk, K., Mettenleiter, T.C., Rijsewijk, F.A., Tampe, R., Neefjes, J., Wiertz, E.J., 2005, Varicelloviruses avoid T cell recognition by UL49.5-mediated inactivation of the transporter associated with antigen processing. Proc Natl Acad Sci U S A 102, 5144-5149.

Koppers-Lalic, D., Verweij, M.C., Lipinska, A.D., Wang, Y., Quinten, E., Reits, E.A., Koch, J., Loch, S., Marcondes Rezende, M., Daus, F., Bienkowska-Szewczyk, K., Osterrieder, N., Mettenleiter, T.C., Heemskerk, M.H., Tampe, R., Neefjes, J.J., Chowdhury, S.I., Ressing, M.E., Rijsewijk, F.A., Wiertz, E.J., 2008, Varicellovirus UL 49.5 proteins differentially affect the function of the transporter associated with antigen processing, TAP. PLoS Pathog 4, e1000080.

Ma, G., Azab, W., Osterrieder, N., 2013, Equine herpesviruses type 1 (EHV-1) and 4 (EHV-4)-Masters of co-evolution and a constant threat to equids and beyond. Vet Microbiol.

Ma, G., Feineis, S., Osterrieder, N., Van de Walle, G.R., 2012, Identification and characterization of equine herpesvirus type 1 pUL56 and its role in virus-induced downregulation of major histocompatibility complex class I. J Virol 86, 3554-3563.

MacLean, C.A., Efstathiou, S., Elliott, M.L., Jamieson, F.E., McGeoch, D.J., 1991, Investigation of herpes simplex virus type 1 genes encoding multiply inserted membrane proteins. J Gen Virol 72 (Pt 4), 897-906.

Neefjes, J., Jongsma, M.L., Paul, P., Bakke, O., 2011, Towards a systems understanding of MHC class I and MHC class II antigen presentation. Nat Rev Immunol 11, 823-836.

Nybo, K., 2012, Molecular biology techniques Q&A. Western blot: protein migration. Biotechniques 53, 23-24.

Osterrieder, N., 1999, Construction and characterization of an equine herpesvirus 1 glycoprotein C negative mutant. Virus Res 59, 165-177.

Osterrieder, N., Holden, V.R., Brandmuller, C., Neubauer, A., Kaaden, O.R., O'Callaghan, D.J., 1996a, The equine herpesvirus 1 IR6 protein is nonessential for virus growth in vitro and modified by serial virus passage in cell culture. Virology 217, 442-451.

Osterrieder, N., Neubauer, A., Brandmuller, C., Braun, B., Kaaden, O.R., Baines, J.D., 1996b, The equine herpesvirus 1 glycoprotein gp21/22a, the herpes simplex virus type 1 gM homolog, is involved in virus penetration and cell-to-cell spread of virions. J Virol 70, 4110-4115.

Powers, L., Wilkinson, K.S., Ryan, P., 1994, Characterization of the prv43 gene of pseudorabies virus and demonstration that it is not required for virus growth in cell culture. Virology 199, 81-88.

Rudolph, J., Seyboldt, C., Granzow, H., Osterrieder, N., 2002, The gene 10 (UL49.5) product of equine herpesvirus 1 is necessary and sufficient for functional processing of glycoprotein M. J Virol 76, 2952-2963.

Russo, R.N., Shaper, N.L., Taatjes, D.J., Shaper, J.H., 1992, Beta 1,4-galactosyltransferase: a short NH2-terminal fragment that includes the cytoplasmic and transmembrane domain is sufficient for Golgi retention. J Biol Chem 267, 9241-9247.

Sambrook, J., Fritsch, E.F., Maniatis, T., 1989, Molecular cloning : a laboratory manual, 2nd Edition. Cold Spring Harbor Laboratory, Cold Spring Harbor, N.Y.

Telford, E.A., Watson, M.S., McBride, K., Davison, A.J., 1992, The DNA sequence of equine herpesvirus-1. Virology 189, 304-316.

Telford, E.A., Watson, M.S., Perry, J., Cullinane, A.A., Davison, A.J., 1998, The DNA sequence of equine herpesvirus-4. J Gen Virol 79 (Pt 5), 1197-1203.

Tischer, B.K., von Einem, J., Kaufer, B., Osterrieder, N., 2006, Two-step red-mediated recombination for versatile high-efficiency markerless DNA manipulation in Escherichia coli. Biotechniques 40, 191-197.

Ushijima, Y., Koshizuka, T., Goshima, F., Kimura, H., Nishiyama, Y., 2008, Herpes simplex virus type 2 UL56 interacts with the ubiquitin ligase Nedd4 and increases its ubiquitination. J Virol 82, 5220-5233.

Wei, H., Wang, Y., Chowdhury, S.I., 2011, Bovine herpesvirus type 1 (BHV-1) UL49.5 luminal domain residues 30 to 32 are critical for MHC-I down-regulation in virus-infected cells. PLoS One 6, e25742.

Zhang, N., Bevan, M.J., 2011, CD8(+) T cells: foot soldiers of the immune system. Immunity 35, 161-168.

CHAPTER 4

Cumulative discussion

4.1 Inhibition of MHC-I antigen presentation pathway at various stages

Under the selective pressure caused by co-evolution, viruses have developed a series of ingenious strategies, which ensure their persistent infection and protect them from being eliminated by the host immune system. The crucial role of MHC-I presentation pathway in the defense against viral infection is realized by activation of CTL-mediated immune responses (Neefjes et al., 2011). Therefore, a variety of stages that control the production of functional MHC-I molecules and stabilize MHC-I distribution at the cell surface have become the inhibition targets of many viruses, especially herpesviruses (Hansen and Bouvier, 2009).

Prior to the assembly of MHC-I molecules in the ER compartment, some components from invading viruses are processed into short endogenous peptides by proteasomal degradation. These antigenic peptides are essential for the production of virus-specific MHC-I species. Two viral proteins from gammaherpesviruses, named EBNA1 and LANA1 (Levitskaya et al., 1995; Bennett et al., 2005), are known to resist the activity of proteasomes and reduce the supply of antigenic peptides for MHC-I loading, but no homologues are discovered in other herpesviral subfamilies.

It is not surprising that the ER is a main organelle targeted by many viruses for MHC-I downregulation, because the premature MHC-I heterodimers composed of a heavy chain and a β_2-microglobulin reside in the lumen of ER. To become mature, the newly synthesized MHC-I molecules need to properly carry viral peptides and migrate to the Golgi for further modifications (Hewitt, 2003). To interfere with this stage, viruses exploit at least three distinct mechanisms, including blocking the translocation of peptides, aberrant retention of MHC-I to the ER, and induction of ER-associated degradation (Iannello et al., 2006). By far, all representative members of *Herpesviridae* are equipped with their own proteins to impair the assembly of the tri-molecular complex (MHC-I heavy chain, β_2-miroglobulin and peptide) in the ER through one of the mechanisms above.

During the modification process in the Golgi, the trafficking of MHC-I molecules encounters another level of inhibition. CMV gp48 protein and HIV Nef protein represent the striking examples of this category (Reusch et al., 1999; Roeth et al., 2004). Before reaching the cell surface, MHC-I molecules are re-directed by these proteins from the *trans*-Golgi network to the endo-lysosomal pathway for degradation. For herpesviruses, only CMV has been

described to make use of such molecular mechanism. At the cytosolic tail of gp48, there is a di-leucine (LL) motif that affects the normal sorting of MHC-I molecules by the Golgi apparatus, thereby leading to their relocation and degradation in the lysosomes (Reusch et al., 1999). Although the gp48 homologues are not present in other herpesviral subfamilies, the possibility cannot be ruled out that similar strategy might be manipulated by other viral proteins, particularly the Golgi-associated ones that contain putative sorting motifs.

Even if a few MHC-I molecules are eventually delivered to the plasma membrane, there is still the last opportunity for viruses to subvert the stable presentation of MHC-I. By accelerating endocytosis of MHC-I, the link between the infected cells and CTLs is directly interrupted. Evidence for this mechanism has been well documented in the characterization of KSHV kk3 and kk5 proteins. Levels of cell surface MHC-I were significantly decreased after transfection of kk3 or kk5 (Coscoy and Ganem, 2000). Further studies revealed that these two viral proteins have the activity of E3 ubiquitin ligase and catalyze the elongation of K63 ubiquitin chain at the cytoplasmic domain of MHC-I heavy chain (Duncan et al., 2006). As a result of polyubiquitination, the targeted MHC-I molecules are internalized into endosomal vesicles via recruitment of clathrin and ultimately degraded in the lysosomal compartments. Except for the example of KSHV, it remains enigmatic whether other herpesviral species have evolved comparable strategies.

4.2 A unique array of viral inhibitors targeting MHC-I in alphaherpesviruses

With respect to their biological properties and evolutionary similarities, viral species from the *Herpesviridae* can be further grouped into the alpha-, beta- or gamma- subfamilies. In common, herpesviruses are able to propagate in permissive cells by lytic infection, and target specialized cell types for persistent infection and reactivation. Specifically, alphaherpesviruses tend to be neurotropic, while beta- and gamma- herpesviruses have the predisposition to establish latency in lymphocytes (Paludan et al., 2011). Owing to such a great distinction between these subfamilies, it is conceivable that alphaherpesviruses might depend on another different kind of MHC-I inhibitors to circumvent CTL-mediated immunity. To date, there are 5 gene products encoded by the *Alphaherpesvirinae*, which account for MHC-I down-regulation, including those of *ICP47*, *US3*, *UL41*, *UL49.5* and *UL56*.

HSV ICP47 is the best characterized viral protein that interferes with the antigen presentation pathway by targeting the assembly of MHC-I in the ER. The fundamental role of ICP47 is determined by its direct interaction with TAP. Mechanistically, cytoplasmic distribution of ICP47 competes with antigenic peptides for binding to the ER-resident TAP complex, thereby reducing the production rate of functional MHC-I molecules (Fruh et al., 1995); however,

ICP47 orthologue is exclusively present in the *Simplexvirus* genus. Recently, some pUL49.5 homologues from the genus *Varicellovirus* have also been shown to inhibit the activity of TAP required for peptide transport. Interestingly, the mechanisms of pUL49.5 proteins vary greatly, which depend on virus species. BoHV-1 pUL49.5 undermines the integrity of TAP by inducing abnormal degradation in proteasomes (Koppers-Lalic et al., 2005), whereas the pUL49.5 homologues of PRV, EHV-1 and EHV-4 function as a barrier that limits the transfer of ATP to TAP (Koppers-Lalic et al., 2008). Collectively, ICP47 and pUL49.5 represent a sort of MHC-I inhibitors that play their roles by interfering with the formation of peptide loading complex, a process that occurs in the ER lumen.

pUS3 is an extensively studied protein and has been shown to inhibit the surface expression of MHC-I, but the precise molecular basis remains poorly understood. VZV pUS3 by itself is able to restrain the process of MHC-I maturation in the *cis*/*medial*-Golgi compartment, which requires its activity of serine/threonine protein kinase (Eisfeld et al., 2007). In contrast, levels of MHC-I at the cell surface were not affected by overexpression of HSV-1 pUS3 (Imai et al., 2013). For the varicelloviruses of veterinary importance, PRV pUS3 has been reported to decrease surface remaining MHC-I levels (Deruelle et al., 2009), but such an effect cannot be achieved in the example of EHV-1 pUS3 (Ma et al., 2012). Although it has been clear that the pUS3 kinase activity plays a central role in MHC-I downregulation, the action mode of a given pUS3 homologue is dictated by different cell types, potential phosphorylation targets and infection stages. Obviously, these multiple factors will make it difficult to elucidate how pUS3 functions. In addition, the virion host shutoff (vhs) protein pUL41 is conserved in all members of the *Alphaherpesvirinae* subfamily and posseses the RNase activity that indiscriminately degrades mRNA transcripts of MHC-I and other proteins for antigen presentation in host cells (Smiley, 2001; Smiley et al., 2004). However, not all pUL41 homologues can inhibit the *de novo* synthesis of MHC-I and its subsequent display on the cell surface, at least EHV-1 pUL41 represents an exception (Chapter 3; Table 3.2).

Unlike the other alphaherpesviruses, EHV-1 does not have the homologue of ICP47, and both its pUS3 and pUL41 fail to exert influence on the production and surface expression of MHC-I, indicating that EHV-1 encodes a distinct collection of candidate proteins involved in modulating MHC-I distribution. This speculation has been confirmed by our recent identification of pUL56 as a novel MHC-I inhibitor (Ma et al., 2012; Said et al., 2012). In Chapter 2, the first study of this thesis experimentally corroborated the idea that endocytosis contributes to downregulation of MHC-I mediated by pUL56. Upon internalization, MHC-I vesicles are delivered to lysosomal compartments for degradation. This machinery is initiated by activation of dynamin and requires ubiquitination. Based on these major findings, pUL56 emerges as the third viral protein, following KSHV kk3 and kk5, that triggers decrease of cell

surface MHC-I through induction of endocytosis; however, the precise mechanism by which pUL56 causes surface MHC-I reduction seems completely different from that of kk3 and kk5, as pUL56 on its own is neither a kinase nor an E3 ubiquitin ligase.

Besides the 5 proteins discussed above, the entire repertoire of MHC-I modulators in alphaherpesvirus should embrace more candidates to establish overwhelming suppression of the virus-specific CTL-dependent immunity. Over the past 2 decades, our growing knowledge of herpesviruses has benefited a lot from the widespread application of infectious bacterial artificial chromosomes (BACs) (Hall et al., 2012). For EHV-1, the genomes of several isolates that cause differential clinical symptoms have been constructed as BACs and preserved in *Escherichia coli* (Rosas et al., 2006). Meanwhile, the improvement of BAC mutagenesis techniques enables rapid deletion and alteration of sequences (Tischer et al., 2006). Based on the available EHV-1 BACs and our efficient *en passant* protocol, creation of a single-gene knockout library has become feasible, and screening of EHV-1 mutants holds promise to discover more viral gene products that antagonize the MHC-I antigen presentation pathway (Fig. 4.1). As a rule of thumb, this strategy can also be extended to other members of the *Alphaherpesvirinae*.

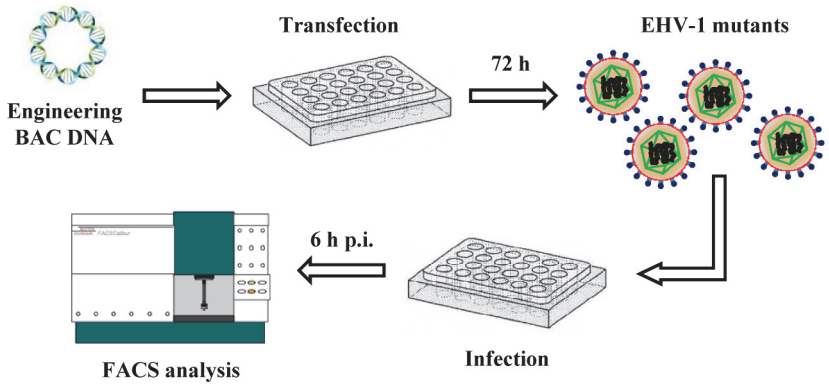

Figure 4.1 Procedure for screening EHV-1 mutants. The EHV-1 Ab4 strain was previously cloned as an infectious BAC in our lab. According to the information from its reference genome (GenBank accession number: NC_001491.2), each ORF in the BAC was disrupted by integration of a selection gene using *en passant* mutagenesis. RK13 cells were transfected with the engineered BAC DNA to reconstitute the deletion mutant. Then equine NBL6 cells were infected with individual knockout virus. In early time of infection (6 h p.i.), cells were harvested and subjected to detection of surface MHC-I levels by flow cytometry.

4.3 Cooperation of pUL43 and pUL56 as a novel model for MHC-I downregulation

Although EHV-1 infection in the presence of pUL56 causes significant reduction of MHC-I at the cell surface, transfection of pUL56 is insufficient to trigger similar effect (Ma et al., 2012), suggesting that there is at least one additional viral gene product that directly or indirectly

cooperates with pUL56 to mediate MHC-I downregulation. Based on this hypothesis, the second study of this thesis (Chapter 3) was designed to look for the potential partner in cooperation with pUL56. By screening a single-gene knockout library of EHV-1, the homologue of UL43 (pUL43) was identified to potently block surface MHC-I presentation in EHV-1-infected cells. Coincidently, the expression kinetics and subcellular localization of pUL43 are in line with those of pUL56. This clue inspired us to test the putative effect of co-expression of pUL43 and pUL56 on modulating the turnover of MHC-I. Our results demonstrate that pUL43 and pUL56 virtually act in concert to prevent cell surface MHC-I expression. Furthermore, we found that the cooperation leading to reduced MHC-I expression is dependent on the PPxY motifs of pUL56.

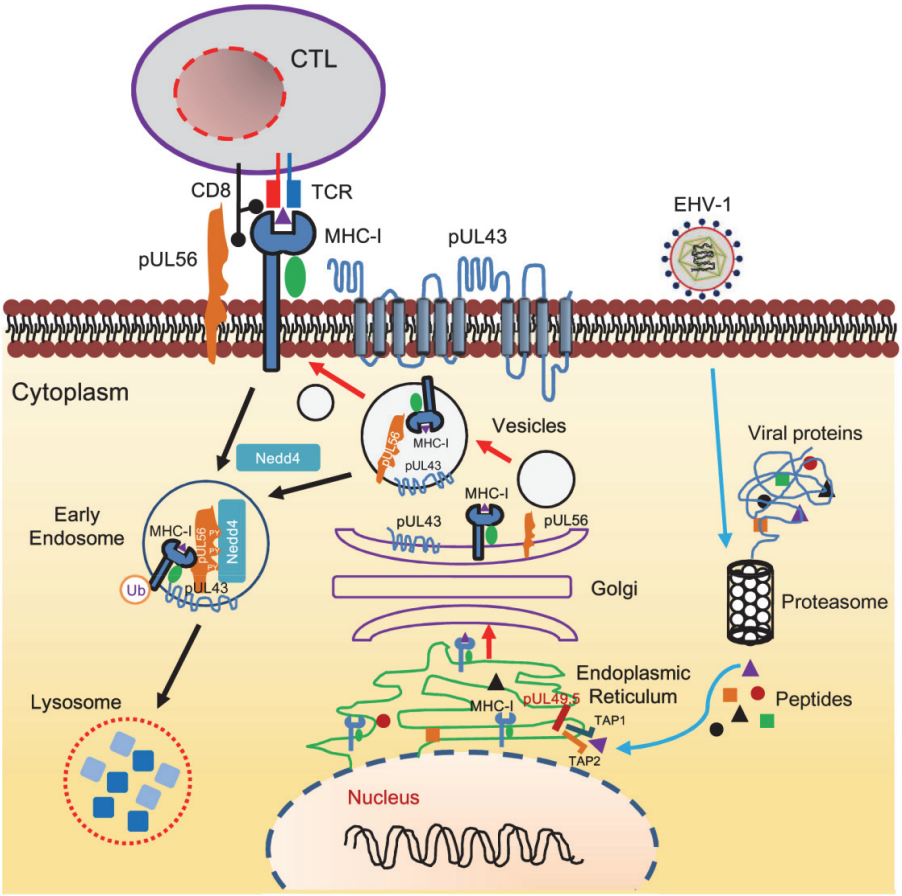

Figure 4.2 EHV-1 antagonizes the MHC-I pathway for immune evasion. Upon virus entry, breakdown of EHV-1 particles occurs and viral proteins are processed by the proteasomal system. Then the viral peptides are presented by MHC-I to the cell surface. During this process, EHV-1 employs two strategies to reduce expression of cell surface MHC-I. In the first strategy, pUL49.5 interferes with the activity of TAP1-TAP2 heterodimer, thereby inhibiting the production of mature MHC-I. In the second strategy, pUL43 and pUL56 cooperate to enhance internalization of MHC-I molecules at the cell surface, resulting in the subsequent degradation of MHC-I and pUL43 in lysosomal compartments. As a consequence of insufficient virus-specific MHC-I, the infected cells are less sensitive to the elimination by CTLs and serve as reservoir for progeny virus. CTL: cytotoxic T lymphocyte; TAP: transporter associated with antigen processing; TCR: T cell receptor; Ub: ubiquitin.

Phylogenetic analyses revealed that the homologues of pUL43 and pUL56 are conserved in the *Alphaherpesvirinae* subfamily (Klupp et al., 2005; Ushijima et al., 2010). In different virus species, pUL43 homologues are predicted as type III tranmembrane (TM) proteins, but the number of their TM domains appears to be not constant. Regardless of its striking hydrophobicity, pUL43 harbors an N-terminus and a spanning in the middle, both of which are hydrophilic and face towards the cytoplasm (Fig. 3.6). Hence, it is assumed that these two regions likely contain the binding sites for viral and/or cellular proteins that affect the trafficking of MHC-I molecules. With regard to pUL56, it is characterized by the topology of a type II TM protein and has a cytoplasmic domain where its three proline-rich (PPxY) motifs interact with a cellular E3 ubiquitin ligase, Nedd4 (Ushijima et al., 2008). Owing to the limited time, this thesis did not experimentally address the concern about how pUL43 and pUL56 work synergistically to trigger MHC-I downregulation. However, a plausible explanation can be deduced based on the data from Chapter 2 along with the biological properties of pUL56 and PPxY motifs documented elsewhere (Blot et al., 2004; Ushijima et al., 2009). To be short, this model delineates that vesicles carrying pUL43, pUL56 and MHC-I are directed to the endo-lysosomal pathway via endocytosis or sorting at the *trans*-Golgi interface, which requires the ubiquitination cascade mediated by Nedd4 (Fig. 4.2). Given that pUL43 and pUL56 are evolutionarily prevalent in alphaherpesviruses, their collaboration may underlie an ancient mechanism that neutralizes the output of cell surface MHC-I during lytic infection to delay the ensuing CTL response *in vivo*. Currently, in-depth studies have been conceived to examine whether pUL43 is ubiquitinated and how the MHC-I molecules, in the presence of pUL43 and pUL56, are transported to the lysosomes for degradation.

4.4 Extensive roles of viral immunomodulatory proteins

Accumulating evidence suggests that inhibition of MHC-I antigen presentation can only provide limited evasion from the attack by the host immune system. Alternatively, NK cells constitute a complementary network dealing with those virus-infected cells that skip the killing by CTLs. Antibody-dependent , cell-mediated cytotoxicity (ADCC) allows NK cells to sense and eliminate the abnormal cells that are suspiciously dominated by invading pathogens (Iannello et al., 2006). To efficiently impede NK cell lysis, viruses are likely to broaden the modulation range of their immune evasion proteins. For instance, KSHV kk5 represents such a promiscuous inhibitor that not only affects binding of ligands (MICA and MICB) to NK cell activating receptors (Thomas et al., 2008) but also targets a selection of cell surface molecules involved in secretion of cytokines and chemokines (Nathan and Lehner, 2009). During EHV-1 infection, reduction of cell surface CD46 and CD63 was also induced by pUL56 and pUL43 (Fig. 2.8 and Fig. 4.3, respectively). Compared to the wild type, ponies challenged with pUL56-deficient mutant exhibited higher levels of IL-8 expression and suffered milder nasal

discharge and shorter primary fever (Soboll Hussey et al., 2011). Recently, pUL56 has been reported to affect cytokine expression and chemotaxis in equine respiratory epithelial cells, leading to a general modulation of innate immune responses (Soboll Hussey et al., 2014). In the future, it is tempting to investigate whether pUL43 brings about comprehensive immune effects on respiratory epithelium as well as host animals.

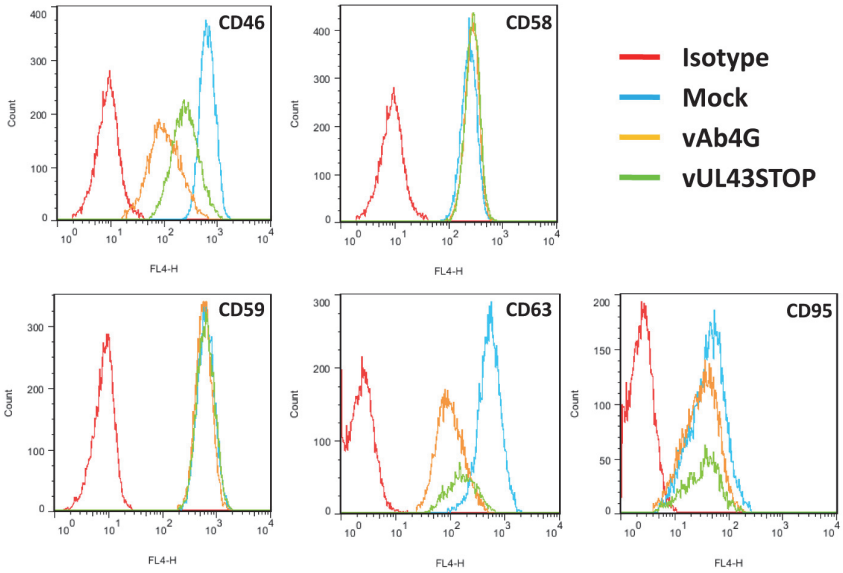

Figure 4.3 pUL43 affects additional surface proteins. After infection with each virus for 24 h, cells were harvested and incubated with primary MAb against CD46, CD58, CD59, CD63 or CD95. Alexa Fluor 647 conjugated goat anti-mouse IgG was used as a secondary antibody. Samples were analyzed by flow cytometry. The FL4-H axis indicates the mean fluorescence intensity of the given surface markers. Downregulation of CD46 and CD63 was dramatically alleviated by abrogation of *UL43* gene, but not for the other tested markers. Shown are the representative histograms of two independent tests.

4.5 Conversion of threat into welfare

Since there is no permanent treatment for any herpesvirus infection, vaccination remains the most effective measure to prevent the transmission of EHV-1 in horse populations. Current commercial vaccines are able to elicit robust humoral immunity but unable to fulfill satisfactory protection primarily because of scarce induction of cellular immunity (Kydd et al., 2006). Virus mutant incapable of repressing MHC-I expression can be developed as a candidate live vaccine, whch is supposed to safely induce antiviral T cell responses. This idea has been supported by a study of challenge infection in which calves immunized with a BoHV-1 mutant lacking *UL50*, *UL49.5*, *UL49* genes were least susceptible to clinical diseases (Liang et al., 1997). Therefore, our continuous understanding of the MHC-I inhibitor list, now at least including pUL43, pUL49.5 and pUL56 for EHV-1, will shed light on rational design of novel vaccines to better prime virus-specific $CD8^+$ CTLs. Moreover, these 3 proteins are encoded by genes non-essential for virus replication. In the context of modified live EHV-1 vector, these loci can be considered for insertion of multiple foreign sequences.

References

Bennett, N.J., May, J.S., Stevenson, P.G., 2005, Gamma-herpesvirus latency requires T cell evasion during episome maintenance. PLoS Biol 3, e120.

Blot, V., Perugi, F., Gay, B., Prevost, M.C., Briant, L., Tangy, F., Abriel, H., Staub, O., Dokhelar, M.C., Pique, C., 2004, Nedd4.1-mediated ubiquitination and subsequent recruitment of Tsg101 ensure HTLV-1 Gag trafficking towards the multivesicular body pathway prior to virus budding. J Cell Sci 117, 2357-2367.

Coscoy, L., Ganem, D., 2000, Kaposi's sarcoma-associated herpesvirus encodes two proteins that block cell surface display of MHC class I chains by enhancing their endocytosis. Proc Natl Acad Sci U S A 97, 8051-8056.

Deruelle, M.J., Van den Broeke, C., Nauwynck, H.J., Mettenleiter, T.C., Favoreel, H.W., 2009, Pseudorabies virus US3- and UL49.5-dependent and -independent downregulation of MHC I cell surface expression in different cell types. Virology 395, 172-181.

Duncan, L.M., Piper, S., Dodd, R.B., Saville, M.K., Sanderson, C.M., Luzio, J.P., Lehner, P.J., 2006, Lysine-63-linked ubiquitination is required for endolysosomal degradation of class I molecules. EMBO J 25, 1635-1645.

Eisfeld, A.J., Yee, M.B., Erazo, A., Abendroth, A., Kinchington, P.R., 2007, Downregulation of class I major histocompatibility complex surface expression by varicella-zoster virus involves open reading frame 66 protein kinase-dependent and -independent mechanisms. J Virol 81, 9034-9049.

Fruh, K., Ahn, K., Djaballah, H., Sempe, P., van Endert, P.M., Tampe, R., Peterson, P.A., Yang, Y., 1995, A viral inhibitor of peptide transporters for antigen presentation. Nature 375, 415-418.

Hall, R.N., Meers, J., Fowler, E., Mahony, T., 2012, Back to BAC: the use of infectious clone technologies for viral mutagenesis. Viruses 4, 211-235.

Hansen, T.H., Bouvier, M., 2009, MHC class I antigen presentation: learning from viral evasion strategies. Nat Rev Immunol 9, 503-513.

Hewitt, E.W., 2003, The MHC class I antigen presentation pathway: strategies for viral immune evasion. Immunology 110, 163-169.

Iannello, A., Debbeche, O., Martin, E., Attalah, L.H., Samarani, S., Ahmad, A., 2006, Viral strategies for evading antiviral cellular immune responses of the host. J Leukoc Biol 79, 16-35.

Imai, T., Koyanagi, N., Ogawa, R., Shindo, K., Suenaga, T., Sato, A., Arii, J., Kato, A., Kiyono, H., Arase, H., Kawaguchi, Y., 2013, Us3 kinase encoded by herpes simplex virus 1 mediates downregulation of cell surface major histocompatibility complex class I and evasion of CD8+ T cells. PLoS One 8, e72050.

Klupp, B.G., Altenschmidt, J., Granzow, H., Fuchs, W., Mettenleiter, T.C., 2005, Identification and characterization of the pseudorabies virus UL43 protein. Virology 334, 224-233.

Koppers-Lalic, D., Reits, E.A., Ressing, M.E., Lipinska, A.D., Abele, R., Koch, J., Marcondes Rezende, M., Admiraal, P., van Leeuwen, D., Bienkowska-Szewczyk, K., Mettenleiter, T.C., Rijsewijk, F.A., Tampe, R., Neefjes, J., Wiertz, E.J., 2005, Varicelloviruses avoid T cell recognition by UL49.5-mediated inactivation of the transporter associated with antigen processing. Proc Natl Acad Sci U S A 102, 5144-5149.

Koppers-Lalic, D., Verweij, M.C., Lipinska, A.D., Wang, Y., Quinten, E., Reits, E.A., Koch, J., Loch, S., Marcondes Rezende, M., Daus, F., Bienkowska-Szewczyk, K., Osterrieder, N., Mettenleiter, T.C., Heemskerk, M.H., Tampe, R., Neefjes, J.J., Chowdhury, S.I., Ressing, M.E., Rijsewijk, F.A., Wiertz, E.J., 2008, Varicellovirus UL 49.5 proteins differentially affect the function of the transporter associated with antigen processing, TAP. PLoS Pathog 4, e1000080.

Kydd, J.H., Townsend, H.G., Hannant, D., 2006, The equine immune response to equine herpesvirus-1: the virus and its vaccines. Vet Immunol Immunopathol 111, 15-30.

Levitskaya, J., Coram, M., Levitsky, V., Imreh, S., Steigerwald-Mullen, P.M., Klein, G., Kurilla, M.G., Masucci, M.G., 1995, Inhibition of antigen processing by the internal repeat region of the Epstein-Barr virus nuclear antigen-1. Nature 375, 685-688.

Liang, X., Chow, B., Babiuk, L.A., 1997, Study of immunogenicity and virulence of bovine

herpesvirus 1 mutants deficient in the UL49 homolog, UL49.5 homolog and dUTPase genes in cattle. Vaccine 15, 1057-1064.

Ma, G., Feineis, S., Osterrieder, N., Van de Walle, G.R., 2012, Identification and characterization of equine herpesvirus type 1 pUL56 and its role in virus-induced downregulation of major histocompatibility complex class I. J Virol 86, 3554-3563.

Nathan, J.A., Lehner, P.J., 2009, The trafficking and regulation of membrane receptors by the RING-CH ubiquitin E3 ligases. Exp Cell Res 315, 1593-1600.

Neefjes, J., Jongsma, M.L., Paul, P., Bakke, O., 2011, Towards a systems understanding of MHC class I and MHC class II antigen presentation. Nat Rev Immunol 11, 823-836.

Paludan, S.R., Bowie, A.G., Horan, K.A., Fitzgerald, K.A., 2011, Recognition of herpesviruses by the innate immune system. Nat Rev Immunol 11, 143-154.

Reusch, U., Muranyi, W., Lucin, P., Burgert, H.G., Hengel, H., Koszinowski, U.H., 1999, A cytomegalovirus glycoprotein re-routes MHC class I complexes to lysosomes for degradation. EMBO J 18, 1081-1091.

Roeth, J.F., Williams, M., Kasper, M.R., Filzen, T.M., Collins, K.L., 2004, HIV-1 Nef disrupts MHC-I trafficking by recruiting AP-1 to the MHC-I cytoplasmic tail. J Cell Biol 167, 903-913.

Rosas, C.T., Goodman, L.B., von Einem, J., Osterrieder, N., 2006, Equine herpesvirus type 1 modified live virus vaccines: quo vaditis? Expert Rev Vaccines 5, 119-131.

Said, A., Azab, W., Damiani, A., Osterrieder, N., 2012, Equine herpesvirus type 4 UL56 and UL49.5 proteins downregulate cell surface major histocompatibility complex class I expression independently of each other. J Virol 86, 8059-8071.

Smiley, J.R., 2004, Herpes simplex virus virion host shutoff protein: immune evasion mediated by a viral RNase? J Virol 78, 1063-1068.

Smiley, J.R., Elgadi, M.M., Saffran, H.A., 2001, Herpes simplex virus vhs protein. Methods Enzymol 342, 440-451.

Soboll Hussey, G., Ashton, L.V., Quintana, A.M., Van de Walle, G.R., Osterrieder, N., Lunn, D.P., 2014, Equine herpesvirus type 1 pUL56 modulates innate responses of airway epithelial cells. Virology 464-465, 76-86.

Soboll Hussey, G., Hussey, S.B., Wagner, B., Horohov, D.W., Van de Walle, G.R., Osterrieder, N., Goehring, L.S., Rao, S., Lunn, D.P., 2011, Evaluation of immune responses following infection of ponies with an EHV-1 ORF1/2 deletion mutant. Vet Res 42, 23.

Thomas, M., Boname, J.M., Field, S., Nejentsev, S., Salio, M., Cerundolo, V., Wills, M., Lehner, P.J., 2008, Down-regulation of NKG2D and NKp80 ligands by Kaposi's sarcoma-associated herpesvirus K5 protects against NK cell cytotoxicity. Proc Natl Acad Sci U S A 105, 1656-1661.

Tischer, B.K., von Einem, J., Kaufer, B., Osterrieder, N., 2006, Two-step red-mediated recombination for versatile high-efficiency markerless DNA manipulation in Escherichia coli. Biotechniques 40, 191-197.

Ushijima, Y., Goshima, F., Kimura, H., Nishiyama, Y., 2009, Herpes simplex virus type 2 tegument protein UL56 relocalizes ubiquitin ligase Nedd4 and has a role in transport and/or release of virions. Virol J 6, 168.

Ushijima, Y., Koshizuka, T., Goshima, F., Kimura, H., Nishiyama, Y., 2008, Herpes simplex virus type 2 UL56 interacts with the ubiquitin ligase Nedd4 and increases its ubiquitination. J Virol 82, 5220-5233.

Ushijima, Y., Luo, C., Kamakura, M., Goshima, F., Kimura, H., Nishiyama, Y., 2010, Herpes simplex virus UL56 interacts with and regulates the Nedd4-family ubiquitin ligase Itch. Virol J 7, 179.

Summary

Equine Herpesvirus Type 1 (EHV-1) pUL56 Promotes Dynamin-dependent Endocytosis and Cooperates with pUL43 for Downregulation of Cell Surface MHC class I

As a member of the *Alphaherpesvirinae*, Equine herpesvirus type 1 (EHV-1) is a prevalent pathogen that causes health risk to horse populations worldwide. To establish persistent infection, EHV-1 has evolved an elegant system to escape from recognition and elimination by host immune responses. Usually in mammalian cells, viral infection is a danger signal and activates antigen presentation mediated by major histocompatibility complex class I (MHC-I). On the cell surface, MHC-I molecules carrying viral antigenic peptides recruit cytotoxic T lymphocytes (CTLs), which in turn kill the virus-infected cells and thus restrain the systemic circulation of virus. However, we recently found that pUL56, a viral component of EHV-1, functions as a major player to effectively prevent MHC-I presentation on the cell surface *in vitro* and affect a broad range of immune responses *in vivo*. These facts invoke a question about the molecular basis of pUL56.

Using different pharmacological inhibitors, the endo-lysosomal pathway was determined to be responsible for internalization and degradation of cell surface MHC-I upon EHV-I infection, which concurred with the early expression of pUL56. Further study revealed that dynamin and tyrosine kinase were required for pUL56-induced MHC-I endocytosis, but this endocytic process was not affected by inhibition of clathrin or caveolin-1, which primarily constitutes clathrin- and raft/caveolae-mediated endocytosis pathway, respectively. Moreover, significant restoration of cell surface MHC-I was observed in the presence of the ubiquitin-activating enzyme E1 inhibitor PYR41, suggesting that ubiquitination plays a dominant role in induction of MHC-I downregulation. Apart from MHC-I, pUL56 also triggered reduced expression of other cell surface molecules, including CD46 and CD63.

It is noted that pUL56 by itself is unable to induce MHC-I downregulation in transfected cells, indicating that interaction of another viral protein with pUL56 might be required for this process. To search for the elusive pUL56 interactor, we screened a single gene knockout library of EHV-1 mutants and identified pUL43, encoded by *ORF17* gene, as a novel protein that modulates antigen presentation by MHC-I. Specifically, downregulation of cell surface MHC-I was significantly attenuated when cells were infected with the virus mutant containing a stop codon in place of *ORF17* gene, which highlights the important role of pUL43 in regulating presentation of MHC-I to the cell surface. pUL43 is evolutionarily conserved throughout the *Alphaherpesvirinae* subfamily and contains 10 putative transmembrane (TM) domains. Despite mild influence on cell-to-cell spread, EHV-1 pUL43 proved dispensable for

virus replication and release. Expression of pUL43 was detectable from 2 h post infection (h p.i.) and increased until 8 h p.i.; afterwards, the pUL43 protein was degraded in lysosomes. Indirect immunofluorescence analysis revealed that pUL43 co-localized with the Golgi apparatus and required the TM domains at the C-terminus to maintain the formation of vesicles. Furthermore, deletion of its hydrophilic region at the N-terminus (amino acid residues 3-40) compensated the low levels of surface MHC-I expression in infected cells. Intriguingly, co-transfection of pUL43 and pUL56 dramatically prevented surface retention of MHC-I, which depended on the PPxY motifs in the cytoplasmic domain of pUL56.

In summary, this dissertation addressed two major concerns: (i) The mechanism of pUL56, by which EHV-1 infection promotes the internalization of cell surface MHC-I molecules via the dynamin-dependent endocytic pathway; (ii) Identification and characterization of pUL43 as a novel MHC-I modulator that acts in concert with pUL56 for regulation of cell surface MHC-I expression. These findings advance our understanding of the intricate strategy that EHV-1 manipulates to circumvent the CTL-mediated immunity and meanwhile shed light on the possible optimization of vaccines against EHV-1 infection.

Zusammenfassung

pUL56 des Equinen Herpesvirus Typ 1 (EHV-1) führt zur Steigerung der Dynamin-abhängigen Endozytose und in Kooperation mit pUL43 zur Herabregulation von MHC-Klasse I Molekülen auf der Zelloberfläche

Das Equine Herpesvirus Typ 1 (EHV-1), ein Mitglied der *Alphaherpesvirinae*, ist ein weit verbreitetes Pathogen und stellt ein Risiko für Pferdepopulationen weltweit dar. Um eine persistierende Infektion zu etablieren, bedient sich das Virus eines raffinierten Systems zur Umgehung der zellulären Immunabwehr. Normalerweise lösen Virusinfektionen Gefahrensignale aus, welche zur Antigenpräsentation auf infizierten Zellen durch den Haupthistokompatibilitätskomplex Klasse I (major histocompatibility complex class I, MHC-I) führen. Durch die Präsentation antigener viraler Peptide durch MHC-I Moleküle auf der Zelloberfläche werden zytotoxische T-Zellen (cytotoxic T lymphocytes, CTL) rekrutiert. Diese töten Virus-infizierte Zellen ab und verhindern so eine systemische Virusausbreitung. Wie wir kürzlich zeigen konnten, ist das EHV-1-Protein pUL56 ein Hauptakteur in der effektiven Reduktion der MHC-I-Präsentation *in vitro* was weitreichende Folgen auf die Immunantwort *in vivo* hat. Diese Fakten werfen Fragen über den molekularen Wirkmechanismus von pUL56 auf.

Mit Hilfe von verschiedenen pharmakologischen Inhibitoren konnte die endo-lysosomale Maschinerie für die Internalisierung und den Abbau der MHC-I-Moleküle auf der Zelloberfläche nach einer EHV-1 Infektion verantwortlich gemacht werden, was auch mit der frühen Expression von pUL56 koinzident war. Weitere Experimente zeigten, dass Dynamin und Tyrosinkinasen für die Endozytose von MHC-I erforderlich sind und dass eine Inhibition von Clathrin (Clathrin-vermittelte Endozytose) oder Caveolin-1 (Caveolae-vermittelte Endozytose) keinen Einfluss auf die Endozytose des MHC-I hat. Außerdem konnte in Anwesenheit von PYR41, einem Inhibitor des Ubiquitin-aktivierenden Enzyms E1, beobachtet werden, dass die Anzahl der MHC-I-Moleküle auf der Zelloberfläche signifikant anstieg. Dies legte nahe, dass die Ubiquitinierung eine wichtige Rolle in der Verminderung von MHC-I auf der Zelloberfläche spielt. Neben MHC-I-Molekülen wurde durch pUL56 auch die Präsenz anderer Moleküle auf der Zelloberfläche reduziert (u.a. CD46, CD63).

Wie bereits bekannt ist, ruft pUL56 alleine in Transfektionsexperimenten keine MHC-I-Reduktion hervor, was darauf hindeutete, dass eine Interaktion von pUL56 mit einem anderen viralen Protein für diesen Prozess notwendig ist. Zur Identifizierung dieses unbekannten Interaktionspartners wurde eine EHV-1 Knockout-Bank erstellt und analysiert. Mit pUL43, das durch den offenen Leserahmen (open reading frame, ORF) 17 kodiert ist,

wurde ein neues Protein identifiziert, welches die MHC-I-Antigenpräsentation moduliert. Nach Infektion von Zellen mit einer *ORF17*-Stop-Virusmutante kam es zur signifikanten Abschwächung der Reduktion von MHC-I auf der Zelloberfläche. Dies weist auf eine zentrale Rolle von pUL43 in der Präsentation der MHC-I-Moleküle auf der Zelloberfläche hin. pUL43 ist in allen *Alphaherpesvirinae* konserviert und enthält 10 mutmaßliche Transmembrandomänen (TM). Obwohl EHV-1 pUL43 die Zell-zu-Zell-Virusausbreitung in geringem Maße beeinflusst, ist es weder essentiell für Virusreplikation noch für Virusfreisetzung. Die Expression von pUL43 war ab 2 Stunden nach Infektion nachweisbar und stieg bis 8 Stunden nach Infektion an. Danach wurde pUL43 durch lysosomale Aktivität degradiert. Mit Hilfe von indirekter Immunfluoreszenz konnte gezeigt werden, dass pUL43 mit dem Golgi-Apparat kolokalisert und die TM-Domänen am C-Terminus für eine Aufrechterhaltung der Golgi-Vesikel essentiell sind. Außerdem hatte eine Deletion der hydrophilen Region am N-Terminus (Aminosäuren 3 bis 40) eine Kompensation der geringerne Anzahl an MHC-I-Molekülen auf der Zelloberfläche zur Folge. Interessanterweise verhinderte eine Ko-Transfektion von pUL43 mit pUL56 die Aufrechterhaltung von MHC-I auf der Zelloberfläche größtenteils, bedingt durch die PPxY-Motive des zytoplasmatischen Teils von pUL56.

Zusammenfassend adressiert diese Arbeit zwei zentrale Komplexe: (i) den Mechanismus von pUL56, durch den eine EHV-1 Infektion die Internalisierung von MHC-I-Molekülen von der Zelloberfläche via Dynamin-abhängiger Endozytose hervorruft; (ii) die Identifikation und Charakterisierung von pUL43 als neuen MHC-I-Modulator, der zusammen mit pUL56 die MHC-I-Expression auf der Zelloberfläche reguliert. Diese Erkenntnisse führen zu einem besseren Verständnis, wie EHV-1 die durch CTL mediierte Immunantwort manipuliert und zeigen gleichzeitig Möglichkeiten zur Optimierung gängiger EHV-1-Impfstoffe auf.

Publications

1. **Huang T**, Lehmann MJ, Said A, Ma G, Osterrieder N. 2014. Major histocompatibility complex class I downregulation induced by equine herpesvirus type 1 pUL56 is through dynamin-dependent endocytosis. **J Virol** 88:12802-12815.

2. **Huang T,** Ma G, Osterrieder N. 2015. Equine herpesvirus 1 multiply inserted transmembrane protein pUL43 cooperates with pUL56 in downregulation of cell surface major histocompatibility complex class I. **J Virol** 89:6251-6263.

3. Hussey GS, Goehring LS, Lunn DP, Hussey SB, **Huang T,** Osterrieder N, Powell C, Hand J, Holz C, Slater J. 2013. Experimental infection with equine herpesvirus type 1 (EHV-1) induces chorioretinal lesions. **Vet Res** 44:118.

Acknowledgements

Transformation from a layman into a specialist of equine herpesvirus could not have been that smooth without the constant and generous help from my doctoral advisor Prof. Dr. Nikolaus Osterrieder, who always patiently waits for my experimental results and motivates my dedication to exploring the interplay between viral proteins and MHC-I, a fascinating story covered by this dissertation. I am often inspired by his insightful comments on experiment design and convincing interpretation of results. My professional career in the future will be enormously benefited from his strict requirements and critical thoughts. I'd like to express my heartfelt gratitude to his efforts in supervising my studies, editing and revising the manuscripts, and supporting me in other aspects. The institute provides the most vibrant and efficient research environment I have ever seen and will leave me with lifelong memories. I feel proud to be a member of this outstanding team and its alumni.

I am grateful to Prof. Dr. Benedikt Kaufer, who is always ready to help me solve difficulties in experiments. In particular, he showed me how to design the mutagenesis primers for my first BAC mutant. In BBQ parties and social gatherings, he always gave me a glass full of wine and encouraged me to eat more. I acknowledge Dr. Karsten Tischer for his important tips to increase the generation efficiency of BAC mutants and inspiration in swapping the location of a tag epitope, which finally overcame the intractable trouble in protein detection by Western blotting.

I feel glad to work with Dr. Guanggang Ma and would like to extend my appreciation to the precious friendship between us. Ma and I worked closely and created a handful of BAC mutants and plasmids. He taught me plenty of techniques, such as Western blotting, immunofluorescence and flow cytometry, etc., which are essentially related to data acquisition. Apart from collaboration in the lab, we travelled together and prepared dinners for celebrating the Chinese New Year, which added more joy to my daily life. Dr. Abdelrahman Said is really nice and often shares his distinct perspectives in virology and ideas about experiment optimization. He invited me to taste the original Arabic food and we spent a few pleasant days in Alpbach. Moreover, I deeply thank those who contributed materials and reagents for my research, they are: Dr. Walid Azab for his continued supply of equine cells and chemical inhibitors that helped me define the pathway selected by EHV-1 for MHC-I downregulation; Dr. Douglas F. Antczak who satisfied my large demand for the MHC-I MAb CZ3 and Dr. Volker Haucke for the Pitstop2 inhibitor that made our conclusion safer.

I am getting well with all my colleagues in the lab and friends across Berlin. They contributed a number of valuable suggestions, excellent technical assistance and helpful trouble-shootings.

Due to space limitation, I am sorry that not all of their names can be displayed in this list. I will remember Jichun Wang, Zhiyong Xu, Armando Damiani, Dusan Kunec, Timo Schippers, Bart Spiesschaert, Ahmed Osman, Maik Lehmann ……, particularly Luca Bertzbach and Nina Wallaschek who are kind enough to help edit the German summary (Zusammenfassung) of this thesis.

Many thanks should be presented to the China Scholarship Council (CSC) that offered the financial sponsorship over the past four years, which translated my dream of studying abroad into reality.

Last but not least, I am deeply indebted to my parents for their understanding and continuous encouragements over the years. This intangible but precious support fostered a great deal of confidence that plucked up my pursuit of advance and excellence.

Selbeständigkeitserklärung

Hiermit bestätige ich, dass ich die vorliegende Arbeit selbständig angefertigt habe. Ich versichere, dass ich ausschließlich die angegebenen Quellen und Hilfen Anspruch genommen habe.

Berlin, den 15.04.2015 Teng Huang